The Corneal Endothelium in Development, Disease and Surgery.

A Thesis Submitted to Cardiff University for the Degree of Doctorate of Philosophy

School of Optometry and Vision Sciences

2013

Frances E. Jones

Acknowledgements

Foremost, I would like to thank my supervisors Professor Andrew Quantock and Drs Rob Young and Jim Ralphs for their continuous support during my PhD and for their enthusiasm, advice and knowledge.

My sincere thanks also go to Professor Keith Meek and Drs Carlo Knupp, Barbara Palka and Julie Albon for their invaluable advice, guidance and help regarding my research.

I greatly appreciate the support I received from the collaborative work I undertook with Doshisha University, I would especially like to thank Professor Noriko Koizumi and Drs Naoki Okumura and Hiroki Hatanaka for their support in this research.

I am grateful to the staff and students of the Structural Biophysics Group, especially Elena Koudouna, Siân Morgan and Drs Erin Dooley and Leona Ho, my friends and family for all their encouragement and help during this challenging period.

Without this help this project would not have been possible, I am indebted to you all.

Abstract

Aims: The cornea is a tough, transparent tissue providing the primary refractive element of the eye. The stroma consists of specially arranged collagen required for corneal transparency. Correct stromal hydration is important in the maintenance of transparency, a feature controlled by the endothelial cells on the posterior surface of the cornea. The aims of this research were firstly to investigate the morphology of corneal endothelial cells and their expression of the sodium bicarbonate cotransporter during avian embryonic development and secondly, to clarify the effect of disease, surgery and drugs on the posterior cornea including in particular the corneal endothelium.

Methods: The corneal endothelial cell morphology and posterior stroma were examined using transmission electron microscopy to determine the ultrastructure of the cells and collagen fibril arrangement in the stroma in all results chapters. Immunohistochemistry and A-scan ultrasonography were employed to identify the presence of the $Na^{+}HCO_3^{-}$ cotransporter and to determine the thickness changes in embryonic chick cornea, respectively. Electron tomography was also used to determine the collagen arrangement in Descemet's membrane.

Results: The expression of the $Na^{+}HCO_3^{-}$ cotransporter was identified in the endothelial layer of the embryonic chicks at all stages imaged. Central corneal thickness increased in the initial stages of development before a plateau between the E12-E15 developmental period followed by a steady thickness decrease. The ultrastructure of Descemet's membrane was determined using electron tomography of transverse and en face resin embedded sections from which a model was produced. Polygonal and elongated structures were observed with proteoglycans present at the intermodal regions of the collagenous structures. The polygonal lattice visualised in en face sections appeared to be composed of stacked globular domains which were integrated into the collagen type VIII model. Predominant changes in the *Col8a2* knock-in mouse models were observed in the posterior cornea. Differences included increased proteoglycans at the Descemet's endothelial interface, dilated rough endoplasmic reticulum and focal posterior oedema. This animal model exhibits

features similar to those seen in the human form of early-onset Fuchs' endothelial corneal dystrophy, unlike previous models reported. The final chapter is concerned with regeneration of the corneal endothelial cells. Tissue from posterior corneal surgery examined using electron microscopy revealed the presence of the host endothelial cells and fibrous tissue at the interface in non-Descemet's membrane stripping automated endothelial keratoplasty and interface haze in Descemet's membrane stripping automated endothelial keratoplasty. However, these features did not appear to interfere with the adhesion of the graft nor the clarity.

Finally, ultrastructural analysis of Rho-kinase inhibited cells showed cells with typical morphology when compared with the untreated group

***Conclusions*:** 1) The $Na^{+}HCO_3^{-}$ cotransporter is present in the embryonic cornea. It is possible that the cotransporter is involved in the developmental stages and probably the thickness changes we observe during this period. 2) The ultrastructure of Descemet's membrane appears to be composed of stacked globular domains arranged in a polygonal lattice alongside more elongated structures interspersed with proteoglycans within the internodal regions. 3) Our studies have helped validate *Col4a2* mice as a promising Fuchs' endothelial corneal dystrophy model. 4) Our investigation into posterior corneal surgery revealed ultrastructural changes that occur post-surgery at the graft interface.

Table of Contents

List of Figures

List of Tables

List of Abbreviations

AE	Anion exchanger
C	Carboxyl
CHED	Congenital hereditary endothelial dystrophy
Cl	Chlorine
CO_2	Carbon dioxide
CS	Chondroitin sulphate
DALK	Deep anterior lamellar keratoplasty
DLEK	Deep lamellar endothelial keratoplasty
DS	Dermatan sulphate
DSAEK	Descemet's stripping automated endothelial keratoplasty
DSEK	Descemet's stripping endothelial keratoplasty
E	Embryonic day
EGF	Epidermal growth factor
EK	Endothelial keratoplasty
EM	Electron microscopy
FACIT	Fibril associated collagens with interrupted triple helices
FECD	Fuchs' endothelial corneal dystrophy
FGF	Fibroblast growth factor
G	Glycine
G1	Gap 1 phase
GAG	Glycosaminoglycan
H	Hydrogen
HCO_3^-	Bicarbonate ion
ICE	Iridocorneal endothelium syndrome
Ig	Immunoglobulin
JAMs	Junction adhesion molecules
K	Potassium
KS	Keratan sulphate
M	Molar
µm	Micrometre
µs	Microsecond

mg	Milligram
ml	Millilitre
mm	Millimetre
min	Minutes
mRNA	Messenger ribonucleic acid
mV	Millivolts
N	Amino
Na	Sodium
NaCl	Sodium chloride
NBC	Sodium bicarbonate cotransporter
nDSAEK	Non Descemet's stripping automated endothelial keratoplasty
nm	Nanometer
O.C.T.	Optimal cutting temperature
PBS	Phosphate buffered saline
PDGF	Platelet derived growth factor
pHi	Intracellular pH
PK	Penetrating keratoplasty
PLK	Posterior lamellar keratoplasty
PPD	Posterior polymorphous dystrophy
RER	Rough endoplasmic reticulum
ROCK	Rho kinase
SLRPs	Small leucine rich proteoglycans
TEM	Transmission electron microscopy
TER	Trans-endothelial resistance
TGF-β2	Transforming growth factor beta 2
ZO-1	Zona occluden-1

Chapter 1: Introduction

1.

The cornea is a transparent, tough, connective tissue providing the primary refractive element within the eye. This tissue is responsible for more than two thirds of the eye's dioptric power (42.4 Dioptres), the remainder of which is provided by the crystalline lens, controlled by the muscles of the ciliary body. Together with the sclera and limbus, the cornea forms a protective envelope enclosing the ocular tissue (Figure 1.1). Collagen fibrils constitute the principal components of the cornea and sclera, conferring rigidity and protection; however, these tissues are remarkably different in collagen organisation resulting in corneal transparency and scleral opaqueness.

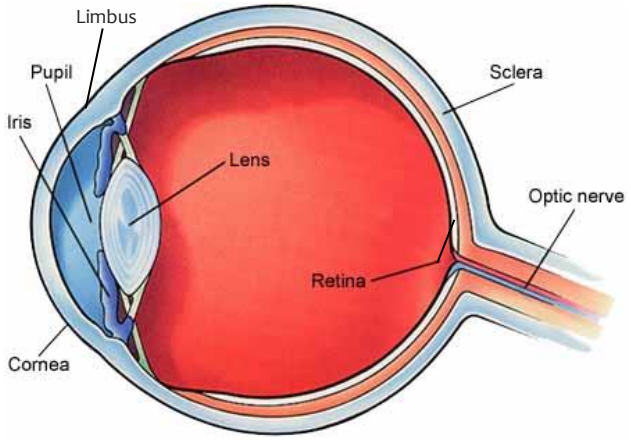

Figure 1.1 Cross section schematic of human eye. Adapted from http://www.royles-opticians.co.uk/glossary.shtml

1.1 The Cornea: Structure and Function

The cornea (Figure 1.2) is comprised of five main layers; an outer epithelium anterior to Bowman's layer, the corneal stroma, Descemet's membrane and most posterior, the corneal endothelium. Corneal avascularity and the regular arrangement of the collagen fibrils within the stroma are essential for corneal clarity. Oxygen is predominantly obtained from the tear film, whilst nutrients originate from the aqueous humour that bathes the endothelium. The tear film also plays a role in protection against microbes and pathogens that come into contact with the anterior surface by producing immunoglobulins and antimicrobials. It also provides a clear refractive interface for the cornea, filling depressions present in the epithelial layer.

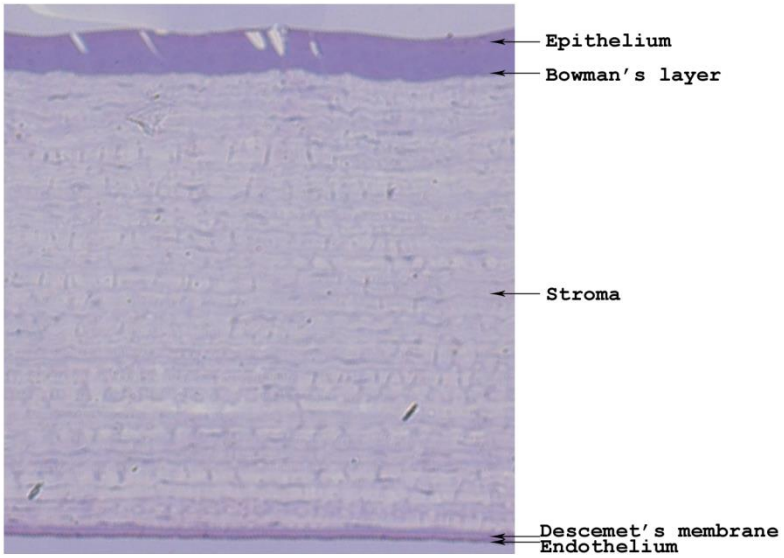

Figure 1.2 Cross-section of cornea.

1.2 Corneal Epithelium

The corneal epithelium is a stratified, non-keratinised layer between five and six cells thick that is continuous with the conjunctiva at the corneal limbus. The layer is composed of three cell types, the outermost superficial cells, wing cells and finally basal cells, the innermost layer in which mitosis occurs. Older epithelial cells move toward the surface of the cornea and are replaced by daughter cells that become more differentiated with time. Cells eventually degenerate and are shed from the corneal surface, a process resulting in replacement of the entire epithelium every seven days (Hanna et al, 1961) from limbal stem cells (Davanger and Evensen, 1971; Dua and Azuara-Blanco, 2000). These stem cells are located in the basal region of the limbus and divide to produce the daughter transit amplifying cells that migrate to populate the epithelium basal layer. These cells differentiate, eventually becoming post-mitotic terminally differentiated cells. In development the corneal epithelium is responsible for secreting the primary stroma (Hay and Dodson, 1973), a collagenous matrix comprising of collagen types I and II (Linsenmeyer et al, 1977; Von der Mark et al, 1977) that appears on embryonic day 3 (E3) in the avian cornea. (Hay and Revel, 1969). The basal cells of the epithelium lie on and produce a basement membrane, 40-60nm thick, anterior to Bowman's layer (Kenyon, 1969). The basal lamina is composed of collagen and glycoproteins, whilst short anchoring filaments attach it firmly to Bowman's membrane on its posterior surface.

1.3 Bowman's Layer

Bowman's layer is an acellular, 8-14μm thick zone posterior to the basal lamina. This layer is present in primates but absent in many species inluding cats, dogs, mice and other carnivores (Calmettes et al, 1956). The layer is composed of type I, III, V and VII collagen (Gordon et al, 1994; Nakayasu et al, 1986) of uniform size which become more ordered in the posterior region of Bowman's. These fibrils are thinner than those present in the stroma and their compact arrangement confers strength to this layer helping its resistance to trauma. Anterior Bowman's is smooth, whilst posteriorly it fuses indistinctly with collagen in the stroma.

1.4 Stroma

The stroma is a dense, regularly packed structure of collagen fibrils arranged as orthogonal layers or lamellae (200-300 centrally) that lie within a proteoglycan matrix interspersed with keratocytes. The stroma constitutes around 90% of the cornea's thickness, measuring around 500 μm in man. Lamellae consist of small diameter collagen fibrils (25-30 nm) whose arrangement allows minimal light scattering, permitting transparency. The stroma is made up of predominantly type I collagen, each layer between 1.5-2.5 μm thick. Keratocytes occupy 2.5-5% of the stroma (Smelser and Ozanics 1965), these are mesenchymal-derived cells responsible for the synthesis of stromal collagen and wound healing. Stromal repair involves activation of keratocytes and production of scar tissue.

1.4.1 Collagen

Collagen is the main component of connective tissue present in tendon, ligament, skin, cornea, cartilage, bone and blood vessels. Collagen has a unique structure composed of three polypeptide chains assembling into a triple-helical arrangement. Corneal collagen fibrils are organised into layers referred to as lamellae in which collagen fibrils tend to be aligned in the same direction, surrounded by proteoglycans. The three polypeptide chains (α-chains) are made up of a sequence of amino acids characterised by the repeating motif G-X-Y, where G represents glycine. The presence of glycine, the smallest amino acid, at every third position is important for

the formation of the triple helix. Biosynthesis of fibril-forming collagens begins when collagen polypeptide chains are synthesised on the ribosomes of the rough endoplasmic reticulum (RER) before being moved into its lumen. Here, they undergo triple helix formation before the procollagen molecule (precursor form) is secreted into the extracellular matrix (ECM) for enzyme modification. Specific proteases cleave the N- and C- propeptides on the globular ends (Kielty and Grant, 2003) (Figure 1.3) allowing the molecules to associate into fibrils (Kadler et al, 1987) that in turn assemble into collagen fibres. The presence of the globular ends prevents aggregation and fibril assembly occurring intracellularly.

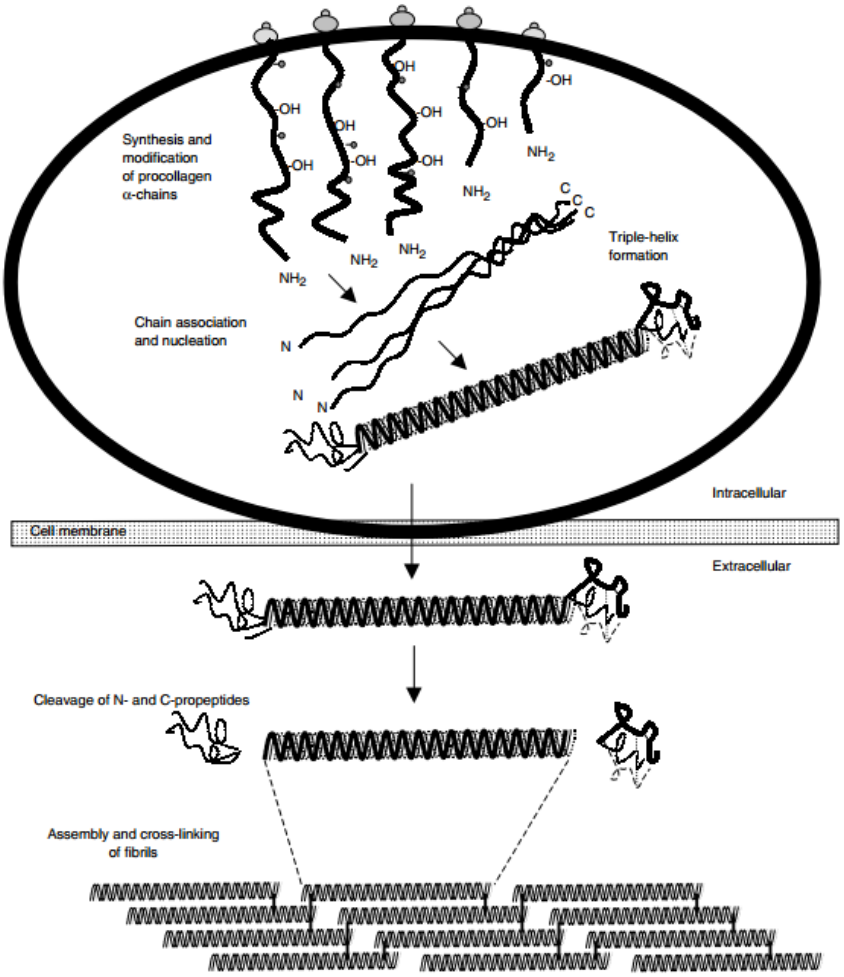

Figure 1.3 Schematic of the steps involved in collagen biosynthesis. Collagen polypeptide synthesis and triple helix formation occurs in the RER prior to secretion of the procollagen into secretory vesicles. Once in the ECM, proteases cleave the N and C propeptides before fibril formation (Taken from Kielty and Grant, 2003)

Corneal transparency is due primarily to the uniformly small diameter (25 nm) of collagen fibrils and their regular interspacing. Collagen types I, III, and V assemble into cross striated fibrils whose molecules have staggered ends at one-quarter of their

length referred to as the 'quarter staggered array'. D periodicity (Chapman et al, 1990) results from molecules in a quarter staggered assembly. The D period has a value of 67 nm (65 nm in cornea) and is comprised of a gap (4 molecules) and an overlap (5 molecules) region. Staining with a heavy metal under transmission electron microscopy (TEM) shows the banding pattern present in the D period, displaying five staining zones labelled a-e (Figure 1.4).

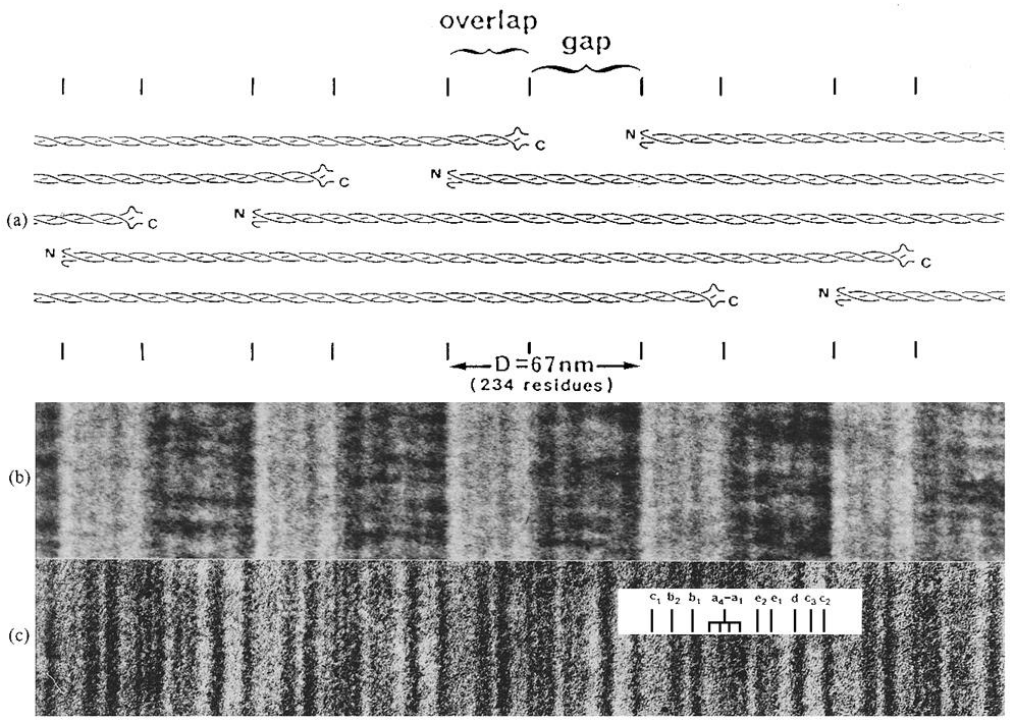

Figure 1.4 Collagen fibril structure. (a) Collagen arrangement includes gap and overlap regions that represent the D period. The light and dark regions observed in (b) indicate the preferential stain penetration. (c) Darkly stained areas are the result of the uptake of electron-dense heavy metal ions from the stain (Chapman et al, 1990).

1.4.1.1 Fibril Forming Collagens

Fibril-forming collagens consist of an uninterrupted triple helix synthesised as procollagen molecules that undergo processing to assemble into collagen fibrils. The major fibrillar collagens are long, unbranched and have a periodicity of between 60-70 nm.

Type I collagen is an abundant heterotrimeric fibrillar collagen composed of two α1 chains and one α2 chain (Piez et al, 1963). It is not only found in primary (Linsenmayer et al, 1977) and secondary cornea but also in many other adult connective tissues. Type I collagen molecules are 300 nm long with a diameter of 1.5

nm. Type I collagen is essential for corneal tensile strength and for the establishment of normal stromal organisation, this is demonstrated by Mov13 mutant mice where a lack of collagen type I results in thin fibrils with no orthogonal arrangement (Bard and Kratochwil, 1987). In the avian cornea there is strong evidence that collagen type I forms heterotypic fibrils with collagen type II during development and with type V collagen in mature stroma (Hendrix et al, 1982).

Type II is a homotrimeric collagen consisting of three identical α1(II) chains, present in the primary stroma of embryonic chick (Linsenmayer et al, 1977). Type II collagen is converted into fibrils within the primary stroma (Chen et al, 1993). Type II collagen mRNA was also detected after cell invasion, thought to function as a template for corneal growth (Linsenmayer et al, 1990). Synthesis of type II is superseded by collagen type I synthesis by mesenchymal cells post E10.

One of the most heterogeneous collagens is type V, the most common isoform comprising of $\alpha1(V)_2$ α2(V) is present in the cornea (Birk et al, 1988). The appearance of type V collagen has been shown to coincide with mesenchyme invasion (Linsenmayer et al, 1984) and is coassembled with type I collagen. Types I and V form heterotypic structures (Fitch et al, 1984; Birk et al, 1988) that help to regulate fibril diameter within the cornea (Birk et al 1990).

1.4.1.2 Non-Fibrillar Collagens

1.4.1.2.1 FACIT Collagens

Fibril associated collagens with interrupted triple helices (FACIT) are a family of collagens including type IX, XII, XIV, XVI, XIX and XX (Gordon et al 1989). FACIT collagens are capable of interacting with fibrillar collagens, characterised by short triple helices interrupted by non-collagenous sequences (Kielty and Grant, 2003).

Type IX is a major FACIT collagen present in the early developing chick cornea (Fitch et al, 1988; Svoboda et al, 1988). There is a decrease in type IX collagen prior to stromal invasion by mesenchymal cells (Fitch et al, 1988; Cai et al, 1994) and by

E11 it is undetectable. Type IX is thought to act as a stabilising factor concerned with keeping the primary stroma in a compact form. As a result, when type IX collagen is removed mesenchymal cells are able to invade the tissue and construct the secondary stroma (Cai et al, 1994).

1.4.1.2.2 Short Chain Collagens

Type VI is a short chain collagen comprised of short triple helical domains (105 nm) which come together to form tetramers. Dimers are formed by lateral aggregation of anti-parallel monomers; these align to form tetramers whose structures aggregate end-to-end resulting in long, thin, beaded filamentous structures (Kielty and Grant, 2003).

Type VIII collagen is a non-fibrillar short chain collagen originally identified as a product of endothelial cells from bovine aorta and rabbit cornea (Sage et al, 1983). It is a major component of Descemet's membrane, made up of two distinct α-chains forming heterotrimers ($\alpha1(VIII)_2$ α2(VIII)). A collagen type VIII hexagonal lattice is observed in Descemet's (Sawada et al, 1990) which is arranged in stacks parallel to the surface of the membrane (Figure 1.5). Rotary shadowing images show a 132.5 nm long, rod shaped structure with large and small domains at either end. These globular regions are the non-collagenous domains, whilst the filamentous structures represent the triple helices (Shuttleworth, 1997).

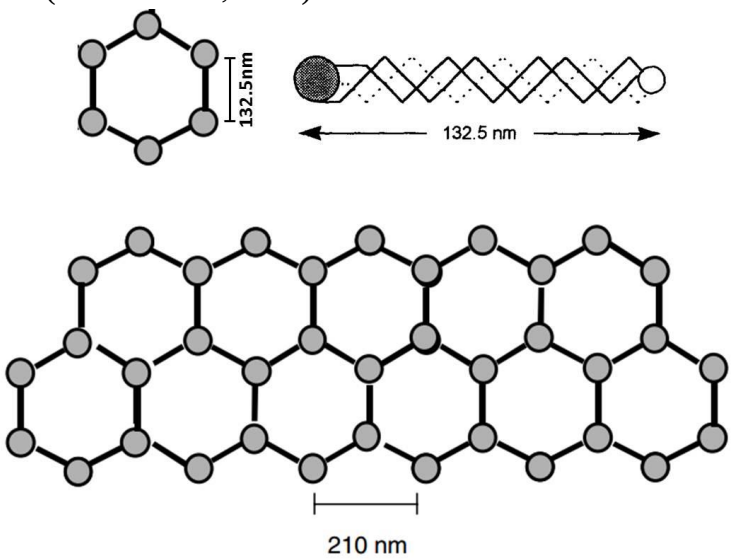

Figure 1.5 Hexagonal lattice present in Descemet's membrane. Type VIII collagen forms open hexagonal arrays that are stacked in parallel to the surface of the membrane. Rotary shadowing imaging shows a rod like structure measuring 132.5 nm Taken from Shuttleworth, 1997; Kielty and Grant, 2003.

1.4.2 Proteoglycans

Proteoglycans have been implicated in cell motility, adhesion, differentiation and morphogenesis. They are present in connective tissue, on cell surfaces and in extracellular matrices. Proteoglycans are also present within the stroma. They are small in size (approx. 50kDa) allowing them to fit into the spaces between the collagen fibrils which helps to regulate spacing (Cintron et al, 1978; Hassell et al, 1983). Proteoglycans consist of a core protein (25-450kDa) with one or more covalently attached glycosaminoglycan (GAG) chains, by which they are named and grouped.

Proteoglycans present in the stroma belong to the small leucine-rich proteoglycan (SLRP) family that interact with fibrillar collagens to achieve correct collagen spacing. The leucine-rich repeats make up the central part of each protein flanked by cysteine-rich regions. Another dimension is the attachment of one or more GAG chains. The current theory suggests that the core proteins of the proteoglycans bind to the surface of collagen fibrils to help modulate interfibrillar spacing (Scott, 1996). Proteoglycan synthesis involves precursor protein release into the RER before being processed in the Golgi, involving the addition of the GAG chains. The fate of the proteoglycan is then dependent on the tissue and the proteoglycan itself. For example, some proteoglycans will be secreted into the extracellular matrix where they become structural components, others can be deposited on the cell surface as a membrane component (Hassell et al, 1986).

1.4.3 Glycosaminoglycans

GAGs are a class of biological macromolecules that are major structural components of proteoglycans. GAGs are linear polysaccharides composed of repeating disaccharide units in which the disaccharide building blocks consist of an amino sugar and a uronic acid or galactose. The predominant corneal GAG side chains are chondroitin sulphate/dermatan sulphate (CS/DS), keratan sulphate (KS) and smaller amounts of heparan sulphate (Hassell et al, 1986). Sulphate groups present on GAG chains bind water. At the correct hydration present in normal cornea, CS/DS chains are fully hydrated whilst KS chains are not. These may act as a reserve for hydration

(Bettelheim and Plessy, 1975). GAGs carry a very high negative charge density provided by the sulphate and uronic acid at physiological pH (Gandhi and Mancera, 2008). The negative charge on the sulphate group allows proteoglycans to make ionic interactions with arginines, lysines and histidines on the surface of proteins.

1.4.3.1 Keratan Sulphate

KS is the major GAG in the corneal stroma regulating matrix architecture (Anseth, 1961; Funderburgh et al, 1986). In the cornea, KS is present on three SLRPs, lumican (Blochberger et al, 1992), keratocan, and mimecan (Corpuz et al, 1996). Electron microscopy on bovine cornea revealed KS proteoglycans are 40 nm long (Scott, 1992) and capable of fitting in between (Hassell et al, 1983) and interacting with collagen fibrils (Scott and Haigh, 1985). Corneal KS consists of repeating N-acetylglucosamine and galactose units, linked to an asparagine residue in the core protein (Figure 1.6). KS is only partially hydrated, suggesting it plays a role in buffering corneal hydration. Lumican is one of the major corneal KS proteoglycans with an abundant amount of mRNA (Blochberger et al, 1992), suggesting it has an important role. The leucine rich repeat region allows lumican to interact with collagen fibrils to modulate fibril formation whilst the GAG chains extend out to regulate interfibrillar spacing (Weber at al, 1996). The importance of KS is seen in homogenous lumican knockouts that show altered collagenous matrix characteristics including disorganised collagen spacing and larger fibril diameter (Chakravarti et al, 1998). However, keratocan knockouts result in thinner corneas but show no significant alteration of stromal collagenous matrix (Kao and Liu, 2003).

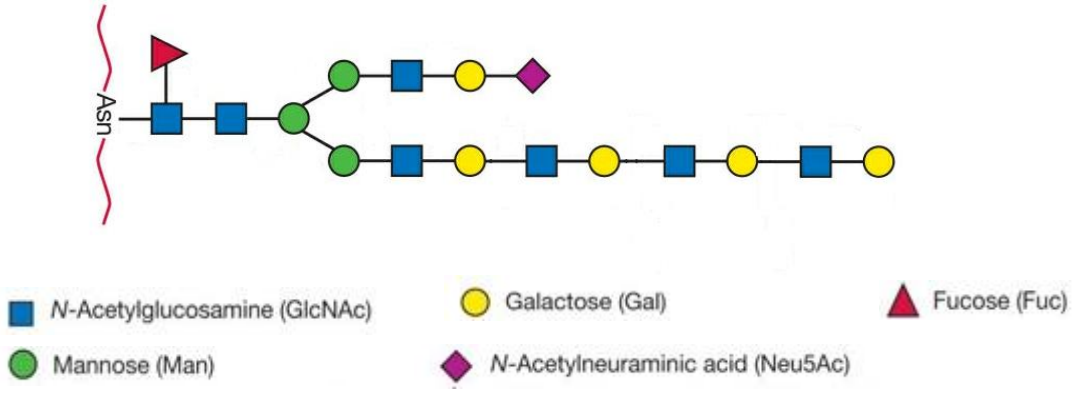

Figure 1.6 Simplified schematic of the repeating units in KS. Linear polymer of N-acetylglucosamine and galactose. Adapted from Esko et al, 2009.

1.4.3.2 Chondroitin Sulphate/Dermatan Sulphate

CS is composed of alternating N-acetylgalactosamine and glucuronic acid whilst DS is distinguished by the presence of iduronic acid in place of glucuronic acid (Figure 1.7). Electron microscopy on bovine corneas revealed CS/DS proteoglycan filaments are 70 nm long (Scott, 1992) and attach to the protein core via a serine residue. Decorin, the other main proteoglycan present in cornea (Li et al, 1992), has a GAG chain composed of a CS/DS hybrid linked to serine residues in the core protein. Mutations in decorin have been linked to congenital stromal dystrophy, a disease characterised by corneal opacity demonstrating its importance within this tissue (Bredrup et al, 2005). Decorin is responsible for collagen organisation within the stroma (Scott, 1992) as well as influencing the activity of growth factors including transforming growth factor β (Iozzo et al, 1999).

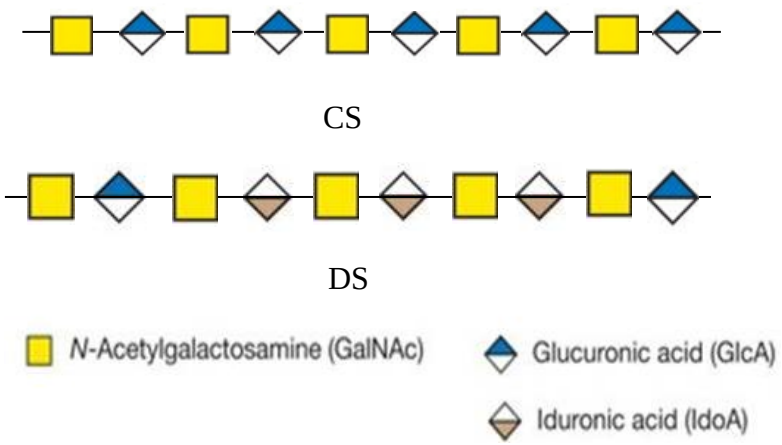

Figure 1.7 Simplified versions of CS and DS. Repeating units of N-acetylgalactosamine and glucuronic acid are present in CS whereas glucuronic acid is substituted for iduronic acid in DS. Modified from Esko et al, 2009.

1.4.4 Collagen-Proteoglycan Interactions

Evidence suggests that there is direct contact between collagen fibrils and the proteoglycan protein core. Two-dimensional electron microscopy used to measure Cuprolinic blue-stained tissue has shown that CS/DS proteoglycans are 70 nm long, whereas KS proteoglycans are 40 nm long (Scott, 1992). Various models have been proposed for the collagen organisation within the stroma. Farrell and Hart considered models where GAG chains formed bridges between collagen fibrils. For example, six GAG chains from one collagen fibril would connect six neighbouring fibrils (Farrell

and Hart, 1969). All of the models have one thing in common, that being, they all have a sixfold symmetry of the collagen-proteoglycan interaction. Muller offered a theory similar to Farrell's which included six proteoglycan bridges extending from one collagen fibril. In this model the bridges do not interact with the nearest or adjacent collagen fibril but with the next nearest neighbouring fibril (Muller et al, 2004). This would result in a sixfold symmetry. Nevertheless, transverse views of the stroma show it does not have a perfect sixfold symmetry and that this is not a requirement for transparency. A more recent study proposed a model whereby proteoglycan protein cores attach to the collagen fibril leaving their GAG chains to interact with other GAG chains. No sixfold arrangement was observed in this three dimensional tomography study but it did show bridges connecting fibrils (Lewis et al, 2010). The three-dimensional reconstructions using bovine cornea found that CS/DS proteoglycans form long chains that extend between several collagen fibrils whereas KS proteoglycans, being shorter, connect only adjacent fibrils. In the model proposed by Lewis, the GAG chains, if long enough, can make noncovalent antiparallel connections between the same proteoglycan, or a mix (i.e. KS and CS/DS chain). This study also describes how opposite forces are present between collagen fibrils, an attractive and repulsive force. The attractive force is produced by the thermal motion between the GAG chains arising between the fibrils due to the chain vibrations that pull the core proteins together. The repulsive force is caused by the Donnan potential, positively charged ions are drawn in by the charges on the GAG chains creating a local gradient within the stroma that attracts water molecules by osmosis (Elliott and Hodson, 1998). The water molecules occupy the space between the fibrils causing a repulsive force between them. It is thought that these two forces are equal, hence, the space between the collagen fibrils is maintained (Lewis et al, 2010) (Figure 1.8).

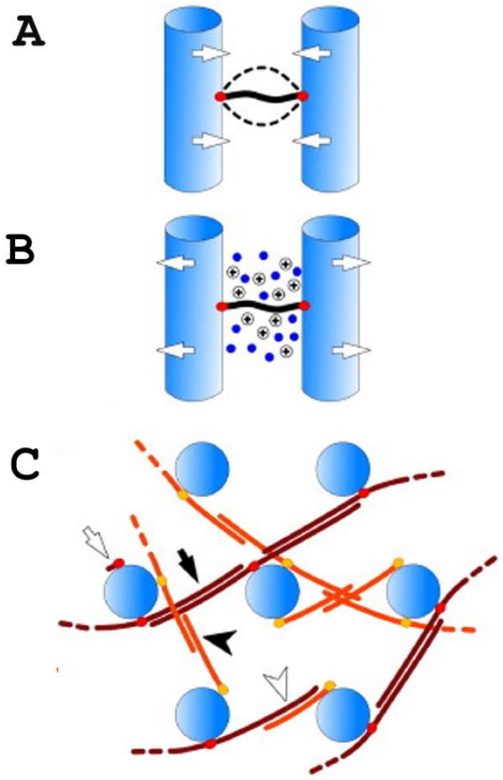

Figure 1.8 Proposed models for proteoglycan controlling mechanisms and collagen-proteoglycan interactions. Two opposite forces exist between collagen fibrils, an attractive force caused by the thermal motion of the proteoglycan/GAG complex (A) and a repulsive force due to the Donnan effect (B). (C) Black arrows indicate the antiparallel interactions between CS/DS GAG chains, whereas the black arrowheads represent the interaction between KS GAG chains. White arrowhead shows the hybrid KS-CS/DS antiparallel interaction. Taken from Lewis et al, 2010.

1.5 Transparency Theories

Several transparency theories exist within the literature but there is still debate about which one represents best the cornea itself. A lattice or interference model suggesting that the cornea is made of a hexagonal lattice of regularly arranged collagen fibrils with equal spacing was proposed by Maurice (1957). Maurice recognised a regular hexagonal lattice would result in secondary radiation emanating from the fibrils to interfere either constructively or destructively. If the size of the components within this lattice is less than that of the wavelength of the incoming light, crests would sum to troughs in every direction except forward. In simpler terms, all of the secondary light would be cancelled out except for that moving in the forward direction resulting in transparency (Maurice, 1957).

EM studies do not show a regular packing of collagen and some believe that a less ordered structure would also allow transparency (Hart and Farrell, 1969; Cox et al, 1970). It is thought that the narrow distance between adjacent fibrils is of more importance i.e. this distance must be similar and less than half the wavelength of the incoming light. As long as the degree of order is sufficient to warrant constructive interference of waves only in the forward direction and destruction of scattered light, corneal transparency will prevail (Hart and Farrell, 1969). Proteoglycans are also thought to be implicated in the onset of corneal transparency during development. Variations in the nature of the proteoglycans are thought to be important in the regulation of cell migration and differentiation during corneal development (Quantock and Young, 2008).

1.6 Descemet's Membrane

Descemet's membrane, the basal lamina of the endothelium, is predominately composed of type IV (Kefalides et al, 1976) and type VIII collagen (Tamura et al, 1991). This membrane was first described by Descemet in 1758, a membrane produced by the endothelium (Hay and Revel, 1969; Perlman and Baum, 1974) with a more detailed structure than most. In adults the membrane is divided into two zones, anterior and posterior. The anterior third of Descemet's is approximately 3.5µm thick, produced during development and viewed as an irregular banded pattern. The remaining two thirds of the membrane is the posterior non-banded zone. This zone increases with age, reaching up to 20µm in some elderly patients (Murphy et al, 1984). Descemet's membrane is attached to the endothelium by a transitional zone known as the 'interfacial matrix', an area where type IV collagen is observed (Fitch et al, 1990). Fibronectin and laminin (Gordon, 1988) are also present within the membrane. Fibronectin adheres the endothelial cells to the membrane (Gospodarowicz et al, 1979), however, its exact location is yet to be determined. Some studies report its presence on the stromal side of the membrane (Tervo et al, 1986; Sramek et al, 1987) or in a bilayered distribution (Morton et al, 1989).

1.7 The Corneal Endothelium

The posterior surface of the cornea is lined by a single layer of hexagonal cells known as the endothelium. Hay and Revel (1969) concluded this layer was derived from a

mesodermal origin in the avian cornea. Johnston's findings contradicted these conclusions suggesting that corneal endothelial cells are derived from neuroectodermal origin rather than mesodermal as originally thought (Johnston et al, 1979). Mitosis occurs in young human endothelium, but is infrequent in the adult (Joyce et al, 1996), with an average cell density of 2000cells/mm^2. The corneal endothelium measures 4-6µm thick. The number of endothelial cells declines through life, however, the number of cells present at birth is enough to last a lifetime (over 100 years). The minimum density required to maintain the functions of the cell monolayer is 400-700cells/mm^2 (Bourne and Kaufman, 1976). Cell-cell contact prevents cell proliferation (Wulle and Lerche, 1969), a process known as contact inhibition. The benefit of a non-proliferating endothelial layer is unclear. Typically active endothelial cells are identified as having large nuclei, numerous mitochondria, prominent endoplasmic reticulum and Golgi apparatus. A healthy endothelial layer has cells of uniform size with between 70-80% of cells having a hexagonal shape.

In chicks interdigitations are present on the lateral and basal membranes of the corneal endothelium during development (Figure 1.9) but decrease by 13 days post hatch as the cells have spread, this could act as a mechanism for reserving the cell membrane (Materson et al, 1977).

Figure 1.9 Interdigitations present in the endothelial cell membrane at stage 36. Interdigitations (arrowheads) are thought to act as a reserve/store of the cell membrane (Materson et al, 1977).

Endothelial wound healing occurs by enlargement and migration of remaining cells resulting in an age related cell size increase (Figure 1.10) (Svedbergh and Bill, 1972; Laing et al, 1976; Murphy et al, 1984; Landshman et al, 1988). Cells surrounding the wound enlarge and elongate into the damaged area without losing contact with

neighbouring cells. This mechanism is known as monolayer spreading (Kaufman and Katz, 1977; Joyce et al, 1990).

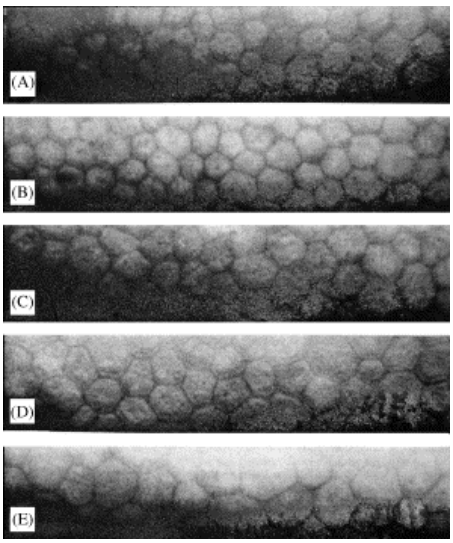

Figure 1.10 Age related changes in endothelium cells. (A)20 years (B)44 years (C)59 years (D)69 years (E)83 years. Decreased cell density and increased cell size are observed (Laing et al, 1976).

1.7.1 Proliferation

Studies have found a higher cell density of cells in the periphery compared to the centre of the endothelial layer in normal human corneas (Schimmelpfennig, 1984). The peripheral regions also have a reduced rate of cell density reduction suggesting that this could be a regenerative zone. Telomerase activity was found in peripheral regions in both young and old donors, with younger donors having increased telomerase activity compared to the older group. However, the same study found no telomerase activity in central cornea (Whikehart et al, 2002). These findings suggest that the peripheral regions of the endothelium may act as a source of cell renewal. Endothelial cells are capable of cell proliferation but remain arrested in the G1-phase of the cell cycle, a theory supported by Joyce, who found no Ki67 expression (a marker of actively cycling cells) (Joyce et al, 1996). Studies comparing old and young endothelium showed significantly lower numbers of older donor endothelial cells entering the cell cycle compared to younger cells (Senoo and Joyce, 2000). This signifies that age related changes exist within endothelial cells, decreasing their proliferative capacity. There is also strong evidence that cell-cell contact is an anti-proliferative factor and a predominant cause of total cessation of endothelial proliferation in vivo (Senoo et al, 2000).

1.7.2 Growth Factors

Growth factors act by binding to cell-surface receptors, resulting in a range of intracellular signals that are important for a variety of cellular processes. Many of the growth factors are produced by the endothelial cells themselves or are present in the aqueous humor and help to regulate the monolayer. Growth factors may be beneficial not only for endothelial proliferation in wound healing but also as a component of corneal preservation media for human donor corneas. A proliferative additive in preservation medium may result in less endothelial cell loss and improved graft results.

Epidermal growth factor (EGF) has many biological activities throughout the body including cell growth and proliferation via the EGF receptor. In the corneal endothelium EGF stimulates cell division, migration and elongation of cells in cell culture systems in bovine (Gospodarowicz et al, 1977; Crow et al, 1994), human (Fabricant et al, 1982; Samples et al, 1991) and rabbit models (Raymond et al, 1986; Hongo et al, 1992). Interestingly, in one study, EGF increased cell cycle entry in older cells with relatively little effect on younger cells (Senoo and Joyce, 2000) which may be beneficial in endothelium regeneration in elderly patients. Platelet derived growth factor (PDGF) promotes wound healing in human (Hoppenreijs et al, 1994) and also stimulates mitosis of endothelial cells in bovine and rabbit (Hoppenreijs et al, 1993; Hecquet et al, 1990). Fibroblast growth factor (FGF) changes corneal endothelial cell shape and stimulates mitosis in bovine (Feldman et al, 1992, Woost et al, 1992), rabbit (Raymond et al, 1986; Kay et al, 1993) and human (Engelmann et al, 1988; Nayak and Binder, 1984). There is still much work to do in this area of endothelial regeneration, for example the effect of these agents on older endothelial cells and the side effects. However, they could be beneficial in endothelial wound healing and repair. There are also features that negatively regulate proliferation such as transforming growth factor-β2 (TGF-β2) present in the aqueous humor. Contact inhibition can also stop endothelial cell proliferation, leaving the monolayer in a contact-inhibited state (Joyce et al, 2002). Other external factors reducing cell counts include trauma, ultraviolet radiation, intraocular surgery, dystrophies and contact lens wear.

1.7.3 Tight Junctions

Tight junctions (*maculae occludens*) are located on the apical surface of the basolateral membrane (Hirsch et al, 1977; Stiemke et al, 1991). Trans-membrane molecules in tight junctions include occludins, claudins, and junction adhesion molecules (JAMs) that interact with their homophilic counterparts on neighbouring endothelial cells (Mehta and Malik, 2006) (Figure 1.11). Tight junctions in the endothelial layer offer a weak resistance to the paracellular movement of water and solutes, this is apparent by the low trans-endothelial resistance of between 15-25Ω.cm (Edelhauser, 2006; Srinivas et al, 2004). However, if this barrier breaks down, stromal swelling will result (Edelhauser, 2006), demonstrating the importance of tight junctions in the maintenance of stromal hydration. TEM has shown electron dense regions between rabbit endothelial cells very early in gestation (Hirsch et al, 1976), these were interpreted as tight junctions. A more complicated junctional network is built as more strands are formed and a more complex tight junction results in decreased endothelial permeability (Stiemke et al, 1991). This was tested using carboxyfluorescein, a hydrophobic dye measuring intracellular permeability (Grimes et al, 1982). Peroxidase injection fills intercellular spaces either side of the junctions which suggests incomplete zona occludens exist in the endothelial layer (Kaye et al, 1973; Hirsch et al, 1976). Tight junctions could also influence the endothelial pump by helping maintain the osmotic gradient that promotes trans-endothelial fluid movement and assisting apical-basal polarity of proteins including those transported via the pump. If tight junction breakdown occurs polarity and pump rate would become affected.

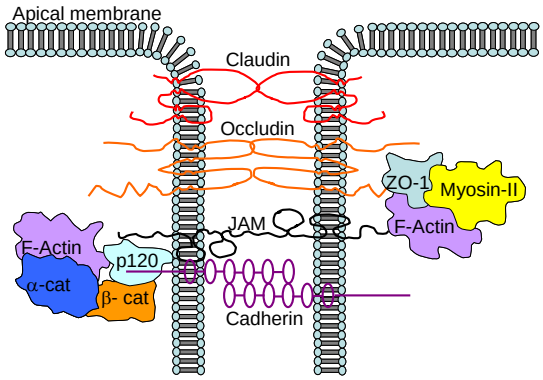

Figure 1.11 Apical junctions present in the endothelial monolayer. Schematic of the apical junction complex. Tight junctions are made up of several trans-membrane and cytoplasmic components including occludin, claudin, and JAM that maintain homophilic interactions with their counterparts in the neighbouring cells. They are also linked to the actin cytoskeleton via adapter proteins such as ZO-1 (Adapted from Srinivas 2010).

Gap junctions are also present in the endothelial layer although they diminish in number with age, suggesting they are present for increased intercellular communication when the endothelium is organising itself (Stiemke et al, 1991). One study found no change in endothelial permeability despite the loss of gap junctions which reveals these junctions may not be of primary importance in the maintenance of the corneal endothelial barrier (Watsky et al, 1990).

1.7.4 Membrane Potential

The resting membrane potential of any cell is the result of ionic conductance properties that arise from transporters and channels present in the cell membrane. The resting membrane potential will have an important role in the cells transport functions. Different studies have been carried out aiming to measure resting membrane potentials of the corneal endothelium, potentials ranged from +2.2(±1.0) to -61.6(±4) mV. Most studies found mean values ranging between -30 to -50mV, measured between 22 and 37°C in intact and cultured cells (Wiederholt and Koch, 1978; Jumblatt, 1981; Jentsch et al, 1984).

1.7.5 Pump

The epithelium and endothelium are important layers in the cornea which were first recognised to behave as semi-permeable membranes by Kinsey and Cogan (1942). The endothelial layer has as a leaky membrane (Hirsch et al, 1977) due to the low resistance junctions between the cells, this enables a leak of solutes and fluid across the endothelial barrier into the stroma. The layer's primary role in corneal hydration is maintained by a pump function; this has been demonstrated by a study measuring the corneal thickness in vitro with removal of the epithelium. The results show that corneal thickness was maintained for more than 6 hours casting doubt on the role of the epithelial layer in regulating corneal hydration (Doane and Dohlman, 1970). Riley concluded that the epithelium is a semi-permeable layer but acts primarily as a barrier and therefore the endothelium must control corneal hydration (Riley, 1971).

1.7.5.1 Sodium Bicarbonate Cotransporter

Ion-coupled fluid transport is important for corneal hydration and transparency. Studies have shown that hydration and intracellular pH (Bonanno and Giasson, 1992; Bonanno et al, 1999) are dependent on the transport of bicarbonate and are sensitive to carbonic anhydrase inhibitors (Fischbarg and Lim, 1974; Hodson, 1971; Hodson, 1974: Hodson and Miller, 1976: Kuang et al, 1990). Bicarbonate is now recognised to be one of the important ions involved in the endothelial pump system (Hodson and Miller, 1976; Jentsch et al, 1984; Riley et al, 1995; Bonanno, 2003) and results in a small apical side negative transepithelial potential (Fischbarg and Lim, 1974; Hodson and Miller, 1976). Two thirds of the substrate is derived from exogenous bicarbonate, the remaining third is supplied by the conversion of exogenous carbon dioxide by intracellular carbonic anhydrase (Hodson and Miller, 1976).

Evidence suggests that an electrogenic bicarbonate sodium cotransporter exists and is responsible for mediating bicarbonate exit via the endothelial apical membrane (Jentsch et al, 1985). Further studies carried out on bovine tissue have shown there is an uptake of bicarbonate by a sodium (Na^+) dependent, 4,4'-Diisothiocyano-2,2'-stilbenedisulfonic acid sensitive electrogenic transporter (Bonanno and Giasson, 1992; Bonanno et al, 1999; Jenstch et al, 1984). Rationale behind this cotransporter participating in bicarbonate uptake was indicated by three findings 1) steady-state pH was higher in the presence of bicarbonate 2) 4,4'-Diisothiocyano-2,2'-stilbenedisulfonic acid added to the basolateral membrane reduced pHi and 3) intracellular Na^+ concentration was higher in the presence of bicarbonate ions (Bonanno and Giasson, 1992).

As well as the basolateral $Na^+/2HCO_3^-$ cotransporter (NBC) (Bonanno and Giasson, 1992; Bonanno et al, 1999; Sun & Bonanno, 2003) the endothelial transport system requires the presence of the $Na^+/K^+/2Cl^-$ cotransporter, the $2Cl^-/2HCO_3^-$ exchanger, Na^+/H^+ exchange and apical anion channels permeable to both chloride (Cl^-) and bicarbonate. It is thought that together these channels and transporters move bicarbonate from the stroma into the aqueous humor. There is now a consensus that the NBC is present on the basolateral membrane. Movement of bicarbonate requires energy (Green, 1991; Hodson and Miller, 1976) provided by the Na^+/K^+ ATPase

located on the basolateral membrane (Green, 1991; Hodson and Hodson, 1988). The location of the Na^+/K^+ ATPase on the basolateral membrane suggests that the cotransporter is probably located here to obtain the energy necessary for bicarbonate transport (Wigham et al, 1994). Studies have also localised the cotransporter to the basolateral cell membrane in bovine corneal endothelium (Sun et al, 2000). Basolateral NBC loads endothelial cells with bicarbonate from the stromal side, once inside the cell there is a net conversion of bicarbonate to carbon dioxide by carbonic anhydrase II. There are three possible modes of bicarbonate efflux into the aqueous humor, 1) Cl^-/HCO_3^- exchange, 2) CO_2 efflux and conversion to bicarbonate via membrane bound carbonic anhydrase IV (Bonanno et al, 1999) and finally 3) conductive flux through anion channels (Sun et al, 2000). A 1:2 stoichiometry results in an influx of bicarbonate ions, thus, this is thought to exist in endothelial cells (Bonanno and Giasson, 1992). Two isoforms of NBC have been cloned, kidney (kNBC) and pancreatic (pNBC), the difference between the two lies in the NH_2 terminus. The stoichiometry of both kNBC and pNBC can change depending on the cell type (Gross et al, 2001) and location, respectively. The pancreatic isoform is present in bovine (Sun et al, 2000) and human (Sun and Bonanno, 2003) corneal endothelial cells. One study suggests that both the kNBC and pNBC isoforms are present in cultured and fresh human corneal endothelial cells (Usui et al, 1999), however, a later study contradicted these findings detecting only pNBC in fresh human corneal endothelial cells (Sun and Bonanno, 2003). Studies have found that apical permeability to bicarbonate is significantly lower than the basolateral permeability (Bonanno et al, 1999), consequently this could be the rate-limiting step in the transendothelial transport of bicarbonate.

1.7.5.2 Na^+/H^+ Exchange

There is also evidence for sodium hydrogen (Na^+/H^+) exchange in endothelial cells. When an acid load is counteracted to recover the pHi in the absence of bicarbonate ions, the Na^+H^+ exchanger becomes inhibited by amiloride (a Na^+/H^+ exchanger inhibitor) (Bonanno and Giasson, 1999). The predominant alkalinising mechanism, Na^+/H^+ exchange, is thought to be present but not active in the presence of bicarbonate. Previous studies on the Na^+/H^+ exchanger show that the activity is reduced as pHi increases and activated when pH decreases (Aronson, 1985). This

occurs in all cell types including the corneal endothelium suggesting pH sensitivity with activity ceasing at pH 7.2-7.3). The exchange becomes active when intracellular pH is reduced leading to alkalinisation of endothelial cells which is the equivalent of introducing bicarbonate ions. However, this transport mechanism acts purely as a housekeeping mechanism in response to pH challenges.

1.7.5.3 Cl^-/HCO_3^- Exchange

Bonanno et al found expression of an anion exchanger (AE)2 in fresh bovine corneal endothelial cells present on the lateral membranes (Bonanno et al, 1998). The exchange is responsible for Cl^- influx and bicarbonate efflux which is thought to modulate intracellular bicarbonate or load endothelial cells with Cl^-. When Cl^- is removed from ringers solution, pHi increases (Bonanno and Giasson, 1992), this alkalisation is inhibited by 4,4'-Diisothiocyano-2,2'-stilbenedisulfonic acid. When Cl^- is present with bicarbonate, its influx and efflux is slowed by 4,4'-Diisothiocyano-2,2'-stilbenedisulfonic acid suggesting the presence of a Cl^-/HCO_3^- exchange. When Cl^- is removed/replaced from solution the membrane significantly depolarises, thought to result in bicarbonate influx through the NBC.

1.7.6 pH

Bicarbonate and Na^+ movement are both influenced by the pH of the bathing solution (Fischbarg and Lim, 1974) and the intracellular level of bicarbonate is related to the intracellular pH. It is thought the main regulators of intracellular pH are the Na^+/H^+ exchanger, NBC and Cl^-/HCO_3^- exchange. The movement of CO_2 into cells causes a small acidification followed by a slower, larger alkalinisation due to bicarbonate influx via the NBC cotransporter. A peak pHi is reached which is followed by a small, slow acidification to restore steady state pH. This drop in pHi may be due to bicarbonate efflux from the cell. The removal of bicarbonate/CO_2 from the cell reverses the pHi changes. When no bicarbonate is present in solution, Na^+ is required to recover the cells from acid load and maintain its steady state pH via a Na^+ dependent proton efflux in a bicarbonate free environment.

1.7.7 Corneal Development

1.7.7.1 Primate Cornea

The optic cup and lens placode have formed by the fifth week of development. The cornea begins its development when the lens detaches from the overlying ectoderm. Prior to endothelial development on embryonic day 40 (E40), a narrow corneal stroma containing disorganised fibrils is present between the corneal epithelium and the lens at E38 (Ewer, 1970). Two waves of mesenchymal cells form the corneal endothelium and corneal keratocytes (Dublin, 1970; Ewer, 1970). Corneal swelling precedes invasion of the second mesenchymal cells in primate (Ozanics et al, 1977) which are destined to become the corneal fibroblasts. Descemet's and Bowmans membrane are formed between the third and eighth month.

1.7.7.2 Avian Corneal Development

Development of the avian eye begins with the appearance of the optic vesicle which induces lens placode development. Extracellular matrix is first observed at E3 as a 1µm layer of collagen fibrils, termed the 'primary stroma', which triples in thickness between E3 and E3.5 (Hay and Revel, 1969). The presumptive epithelium is two cells thick at E3. Meanwhile, mesenchymal cells present at the lip of the optic cup at E3.5 are destined to become the corneal endothelium (Hay and Revel, 1969). These cells flatten in preparation for their migration along the posterior face of the cornea at E4, covering the entire posterior surface in 1.5 days. By E5 the primary stroma is 10µm thick, composed of at least 20 layers, it then doubles in thickness by E5.5 to between 30µm and 50µm. This event simultaneously occurs with a second invasion of mesenchymal cells destined to become the corneal keratocytes on E6; cells responsible for producing the secondary stroma. Keratocan mRNA is expressed by all keratocytes as soon as they migrate into the stroma on E6 (Conrad and Conrad, 2003). Hyaluronate reaches its highest point at stage 27/28 (Toole and Trelstad, 1971), a GAG that is thought to be important in early developmental events because of its appearance in multiple embryonic tissues. Some studies have shown increased levels of hyaluronate during mesenchymal cell migration suggesting it influences mesenchymal cell behaviour (Toole and Gross, 1971). By E6 the endothelium has begun to produce a basement membrane that thickens to form Descemet's membrane.

KS proteoglycans are then synthesised between E5-E7 (Hart, 1976; Funderburgh et al, 1986) becoming highly sulphated by E14 (Hart, 1976), whilst the lumican core protein increases three-fold between E7 and E9 (Cornuet, et al, 1994). The accumulation of KS proteoglycans between the E12-E18 developmental period may influence matrix hydration and collagen fibril spacing (Liles et al, 2010). Keratocan mRNA steadily declines from E9-E18 whilst lumican levels remain high (Dunlevy et al, 2000). Hyaluronate is removed by hyaluronidase between E9-12 resulting in decreased water binding affinity in the stroma. The secondary stroma undergoes structural modifications from E9 through to hatching at E21; these include stromal compaction (Hay and Revel, 1969; Quantock et al, 1998; Siegler and Quantock, 2002) and proteoglycan alterations, previously mentioned (Anseth, 1961; Toole and Trelstad, 1971). The cornea reaches its maximum thickness of 220µm at E9 soon after the mesenchymal cell invasion is complete on E10 (Hay and Revel, 1969), probably as a result of secreted type I/V collagen fibrils (Linsenmeyer et al, 1984; Birk et al, 1986) and stromal oedema. Descemet's membrane is complete by E12 whilst hyaluronidase activity decreases. Rapid removal of water from the cornea occurs due to decreased water binding affinity and an increased pumping mechanism within the endothelium, dehydrating and thinning the stroma. The secondary stroma becomes complete at this stage with a thickness of approximately 200µm, invaded throughout by mesenchymal cells (Hay and Revel, 1969). Light transmission increases from 40% at E14 to 96% by E19 (Coulombre and Coulombre, 1958) due to the increase in collagen fibril packing (Quantock et al, 1998) and reorganisation of the collagen.

1.7.7.3 Endothelial Development

Endothelial cells are derived from mesenchyme and associated with the vascular uveal tract. The mesenchyme destined to form the endothelium is present on E2 in the avian cornea before moving towards the lip of the optic cup where it stalls for a day. At E4 the cells migrate into place, pushing their way through the subectodermal stroma that has begun to swell by this point (Coulombre and Coulombre, 1958). The cells and stroma are pushed away from the lens by the fibrous matrix that fills the now anterior chamber (Bard et al, 1975). Endothelial cells are capable of moving by extending cell processes forward at a rate of approximately 1µm/minute (Bard et al, 1975). A confluent sheet is formed by E6; subsequently, junctions occur between the

cells whilst cilia extend into the anterior chamber (Hay and Revel, 1969). Soon after the formation of the endothelium, hyaluronic acid is produced by the cornea, some studies suggesting it is produced by the endothelial layer itself (Treslstad et al. 1974). Corneal hydration increases on E6, probably as a result of the cells leaky quality, a feature that will eventually be counteracted by its pumping mechanism. Descemet's membrane appears as a narrow band of extracellular matrix, produced by the endothelium.

1.7.8 Endothelial Dysfunction

Posterior corneal dystrophies are characterised by abnormalities in the endothelium and Descemet's membrane. Defects in the endothelial layer can result in an oedematous stroma due to a defective or decreased fluid transport mechanism. The primary corneal endotheliopathies are presented in the table below (Table 1.1).

Corneal endotheliopathy	Features	References
Fuchs endothelial corneal dystrophy	Bilateral Posterior guttae Thickened Descemet's membrane Altered endothelium pump rate Endothelial cell apoptosis	Wilson et al, 1988 Adamis et al, 1993
Posterior polymorphous dystrophy	Bilateral Epithelial-like cells Abnormal endothelium Thickened Descemet's	Richardson and Hettinger, 1985; Boruchoff and Kuwabara, 1971; Cribs et al 1977
Congenital hereditary endothelial dystrophy	Corneal clouding Thickened Descemet's membrane Posterior collagenous secretion	Callaghan et al, 1998 Kenyon and Maumenee, 1973
Iridocorneal endothelial syndrome	Cobblestone endothelium	Levy et al, 1995

Table 1.1 Primary corneal endotheliopathies. Disorders affecting the corneal endothelium and the features they display.

1.7.8.1 Fuchs' Endothelial Corneal Dystrophy

Ernst Fuchs, an Austrian Ophthalmologist, is best known for his work on dystrophia epithelialis corneae (Fuchs', 1910). This is now more commonly known as Fuchs' endothelial corneal dystrophy (FECD), the most common indication for corneal transplantation (Adamis et al, 1993). FECD is a bilateral disease leading to corneal clouding as a result of dysfunctional endothelial cells. There are two forms of FECD, a rare early-onset form (Biswas et al, 2001) and the more common late-onset form

which affects approximately 4% of the population. Early-onset FECD results in endothelial decompensation in the third or fourth decade of life whilst the late-onset form develops into advanced stages by the sixth to ninth decade of life. A major hallmark of the disease are the endothelial excrescences or guttae that appear as indentations or drops on the posterior surface of Descemet's membrane (Figure 1.12). Guttae eventually become confluent, starting centrally before spreading peripherally so that the endothelium attains a beaten metal appearance. The guttae are accumulations of collagen posterior to Descemet's membrane. When the central guttae lead to corneal hydration, FECD can be identified as the cause.

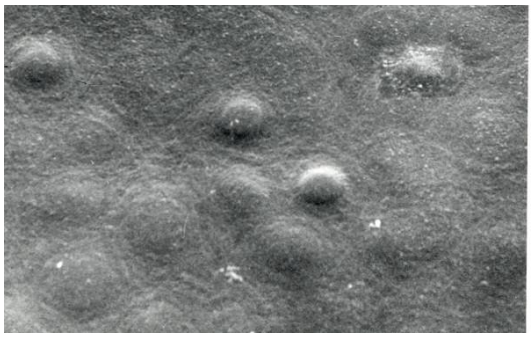

Figure 1.12 Features of FECD dystrophy in patients. Scanning electron micrograph of guttae present on the corneal endothelium (Klintworth, 2009).

Descemet's membrane is also significantly thickened in FECD (Wilson and Bourne, 1988), this thickening occurs in the posterior nonbanded zone (Iwamoto and DeVoe, 1971). FECD can be broken down into three stages. Stage I is characteristically asymptomatic with thickened Descemet's membrane and corneal guttae which appear as small, centrally located black dots on the endothelium under specular reflection. Endothelial cell loss occurs at this early stage but is compensated for by cell spreading and polymegethism; as a result there is a lack of symptoms. The disease progresses causing a slight loss of sight due to stromal oedema, a feature establishing the patient as stage II. Stromal oedema creates a ground-glass area studded with water clefts whilst corneal thickness increases twofold. Large lakes of fluid appear within and under the epithelium which can burst leaving epithelial defects. Stage III is diagnosed by bullae that occasionally rupture causing intense pain alongside subepithelial and stromal scar tissue, this leads to vascularisation of the cornea and decreased transparency (Table 1.2).

Stage	Symptoms	Clinical Features	Visual acuity
I	None	Few guttae Endothelial cells loss	20/20
II	Slight loss of vision	Moderate guttae Mild edema Increased corneal thickness	20/20 to 20/80
III	Moderate/severe vision loss Pain	Confluent guttae Severe edema Subepithelial scars Ruptured bullae Stromal scar tissue Vascularisation	20/100 to 20/400

Table 1.2 Documented stages of FECD dystrophy. Three separate stages of the disease are recognised by the advancing clinical features.

For treatment, hypertonic agents such as 5% NaCl are used to raise the hyperosmolarity of the tear film as well as a warm hair dryer to aid corneal dehydration. In the final stage of the disease, a loose fitting soft contact lens can help decrease irritation and some of the pain caused by the epithelial bullae. Intraocular pressure, thought to be linked to stromal oedema, can be reduced to help control swelling. A final measure, usually required for those patients in stage III, is surgical intervention in the form of penetrating keratoplasty.

Disease pathogenesis is not yet fully understood in FECD, however, recent studies have linked mutations in collagen VIII as a possible cause in the early-onset form of the disease (Biswas et al, 2001; Gottsch et al, 2005; Jun et al, 2012). Further investigation into the pathogenesis of the disease will help determine its cause and in defining appropriate treatments which are currently lacking in FECD.

1.7.8.2 Additional Corneal Endotheliopathies

Posterior polymorphous corneal dystrophy is an autosomal dominant corneal dystrophy with a range of clinical features including endothelial vesicles (Waring et al, 1978; Krachmer, 1985). The endothelial cells appear epithelial like including multiple layers and can extend over the iris and trabecular meshwork. Some studies

suggest that the normally non-mitotic cells of the endothelium do divide in this disorder, taking on epithelial like properties (Blair et al, 1992).

Congenital hereditary endothelial dystrophy is a rare disorder characterised by bilateral corneal oedema occurring soon after birth. Patients have thickened Descemet's membrane (Chan et al, 1982) and deteriorated corneal endothelium (Ehlers et al, 1998), which is likely to cause stromal swelling.

Iridocorneal endothelial dystrophy comprises of Chandler's syndrome, essential iris atrophy and iris nevus syndrome. The features of these dystrophies include corneal oedema, glaucoma and iris changes (Chandler, 1955).

1.7.9 Corneal Surgery

The predominant treatment for corneal endothelial dysfunction, until recently, was penetrating keratoplasty (PK), a surgical intervention replacing the entire cornea (Figure 1.13). PK has come to be very popular and successful in most patients suffering from corneal dystrophies and trauma, however, this surgery does carry risks including prolonged visual recovery, induced astigmatism and globe fragility.

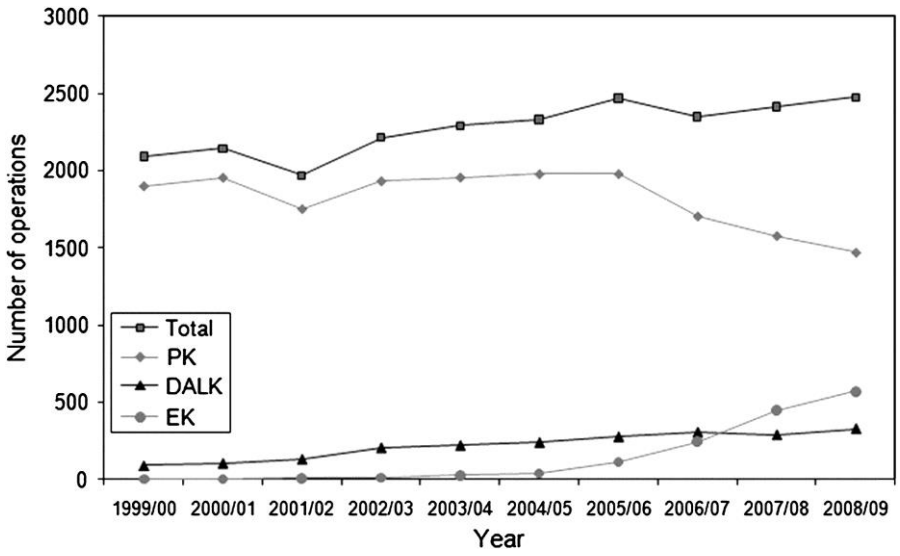

Figure 1.13 Total number of keratoplasties carried out from 1999 to 2009 under the Corneal Transplant Service (UK). All keratoplasties (Total), Deep anterior lamellar keratoplasty (DALK), Endothelial Keratoplasty (EK) in the 1999/2000 till 2008/2009 period. (Keenan et al, 2010).

Replacement of only the damaged layers of the cornea is now becoming a more popular choice for surgeons and patients. Deep anterior lamellar keratoplasty (DALK) removes the diseased/damaged anterior layers preserving the healthy posterior

Descemet's membrane whilst posterior lamellar keratoplasty (PLK) removes the damaged/diseased posterior stroma and Descemet's membrane preserving the healthy anterior layers. During PLK recipient stroma is dissected at 80-90% of its depth along with Descemet's membrane and endothelium before replacement with donor stroma, Descemet's membrane and endothelium (approximately 10-20% of corneal thickness). The procedure results in faster recovery, reduced astigmatism, fewer sutures, whilst also maintaining globe integrity. This overcomes some of those problems associated with PK (Melles et al, 2000, Gorovoy, 2006, Price & Price, 2007). A 9.0mm scleral incision is created before donor insertion (Melles et al, 1998, 1999; Terry and Ousley, 2003), a practice that was further modified by decreasing the incision to 5.0mm, combined with donor tissue folding prior to insertion (Melles et al, 2002). PLK was later referred to as deep lamellar endothelial keratoplasty (DLEK), a technique using the same procedure with modified instruments (Terry and Ousley, 2003).

1.7.9.1 DSEK

DLEK was advanced further by removing Descemet's membrane from the host cornea without the posterior stroma, a procedure termed descemetorhexis (Melles et al, 2004). The donor tissue, consisting of posterior stroma, endothelium and Descemet's membrane, is transplanted onto the recipient posterior surface. This procedure was later named Descemet's stripping endothelial keratoplasty (DSEK) (Price and Price, 2005). DSEK showed a lower rate of graft rejection (7.5%) compared to PK (13%) within the first 2 years of the surgery in a study by the Swedish Corneal Graft Registry for those patients suffering from FECD (Allan et al, 2007). A microkeratome has allowed this technique to have a greater degree of precision and a smoother graft-host interface. The use of the microkeratome resulted in a procedure now known as Descemet's stripping automated keratoplasty (DSAEK) (Gorovoy, 2006). This technique is now favoured by many corneal surgeons for correcting endothelial related problems.

1.7.9.2 Non Descemet's Stripping Automated Endothelial Keratoplasty (nDSAEK)

Non-Descemet's stripping automated endothelial keratoplasty (nDSAEK) involves a similar method to DSAEK but instead leaves the host cornea fully intact (Price and Price, 2006; Kobayashi et al, 2008) (Figure 1.14). This method was introduced for the treatment of failed PKs (Price and Price, 2006) and endothelial dysfunction not associated with guttae. nDSAEK is not beneficial in FECD as the pathologic endothelial layer needs to be removed, a step not involved in nDSAEK (Kobayashi et al, 2008). In relevant circumstances, such as extensive endothelial cells loss and failed PK, Kobayashi has shown positive results for this surgery, with superior visual acuity and little induced astigmatism. It also diminishes the need to remove Descemet's membrane resulting in a simpler procedure. As well as failed PK surgery and endothelial dysfunction not associated with FECD, nDSAEK may also be beneficial for aphakic aniridic eyes. DSEK/DSAEK can be challenging in an eye where both the iris and lens are missing as Descemet's membrane stripping can lead to fragments of recipient Descemet's membrane falling back onto the retina. nDSAEK, however, does carry complications, one of which includes graft dislocation after surgery (Kobayashi et al, 2008).

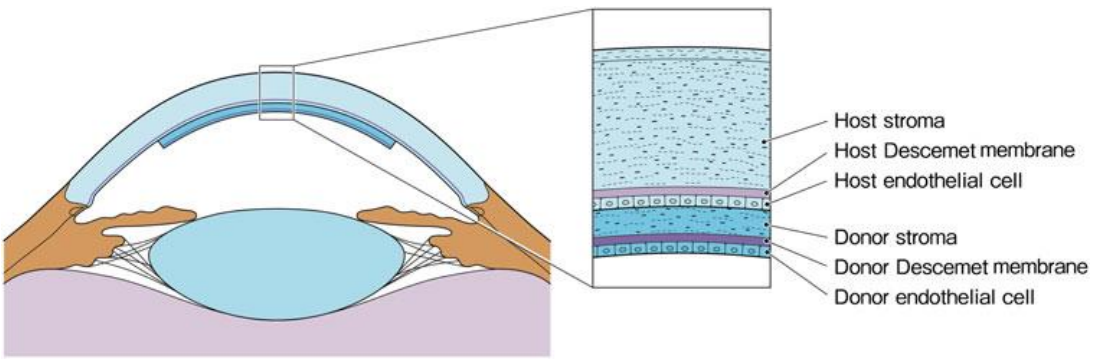

Figure 1.14 Schematic of the corneal components post nDSAEK surgery. Host cornea remains fully intact anterior to donor stroma, donor Descemet's membrane and endothelium. Taken from Masaki et al, 2012.

1.8 Summary and Objectives

The structure and composition of the corneal stromal collagen is important and needs to be kept at a consistent hydration for corneal transparency to prevail. This, in part, is controlled by a pump mechanism present in the corneal endothelium, an essential monolayer of cells present on the posterior of the cornea. It is already known that the NBC plays an essential role in the endothelial pump, however, when this cotransporter is present in the developing cornea and if it correlates with stromal compaction and thinning is still unknown. The importance of this posterior layer is reiterated in corneal endotheliopathies whereby damaged or decreased endothelial cells results in stromal oedema and consequently, visual impairment. In circumstances where the endothelial cells are depleted or damaged beyond recovery, corneal surgery is the only remaining treatment at this time. Posterior corneal surgeries are becoming increasingly popular as they do not carry the same side effects as full PK. Pharmaceutical agents are now being brought to the market to maintain or increase endothelial cell survival. Both surgical and drug intervention have shown positive outcomes on visual acuity, however, the effects on the stroma and endothelial cells is unknown.

The aims of this research were firstly to investigate the morphology of corneal endothelial cells and their expression of the NBC during avian embryonic development and secondly, to determine the effects of an early-onset FECD murine model on the posterior cornea. The final aim was to determine how the stroma and endothelium changes in response to DSAEK and nDSAEK surgery and after the addition of a Rho kinase (ROCK) inhibitor.

Alterations in corneal thickness and protein expression in the endothelium, together with endothelial cell morphological changes will help us better understand the relationship between these factors. Determining the ultrastructural changes in the posterior stroma in disease models will help us realise the similarities to the human disease, and consequently, whether or not they are beneficial in defining the genetic changes and disease pathogenesis. Finally, observing corneal structure after surgery

and drug intervention will help clarify the positive and negative aspects of the individual treatments and the overall tissue alterations that occur.

Chapter 2: Materials and methods

2.

This chapter outlines the experimental procedures used throughout the project, including tissue from developmental, diseased, surgical and pharmacologically targeted corneas.

2.1 Experimental Models

2.1.1 Corneal Endothelial Development

Fertilised White Leghorn chicken eggs (Henry Stewart, Lincolnshire, UK) were incubated at 37.5°C in a humidified chamber (Brinsea products Ltd) for chicks aged between E8 and 18. All animals were killed in accordance with the Association for Research in Vision and Ophthalmology statement for use of animals for Ophthalmic and Vision Research and local ethical regulations. Embryonic chicks were used for general TEM, immunohistochemistry and A-sound ultrasonography for studies observing the corneal endothelium and corneal thickness in development. Corneas used for immunohistochemistry and TEM were excised by an incision around the limbus of the eye and immediately placed in either O.C.T. (optimal cutting temperature) or fixative solution, respectively.

2.1.2 Pathology

Knock-in mice were generated by Jun and colleagues (2012). Targeting vectors containing the *Col8a2*$^{Q455K/Q455K}$ and *Col8a2*$^{L450W/L450W}$ mutations were generated prior to incorporation into the mouse genome establishing an early-onset FECD murine model (see chapter 4 for more details). Following euthanasia by inhaled isoflurane followed by cervical dislocation, one eye of each animal was examined by clinical confocal microscopy using a Confoscan 3 microscope (Nidek, Fremont, CA). 5-month-old mouse corneas with *Col8a2*$^{L450W/L450W}$ or *Col8a2*$^{Q455K/Q455K}$ homozygous knock-in gene mutations were stained with Cuprolinic blue to image sulphated proteoglycans before resin embedding and examination with TEM, alongside age-

matched controls. Prior to processing tissue underwent digestion in specific glycosaminoglycan-degrading enzymes (see later).

2.1.3 Surgery

Posterior corneal surgery is becoming an increasingly popular alternative to PK because of the fewer complications that occur post-surgery. Japanese white rabbits that had undergone DSAEK and nDSAEK surgery were used to study the posterior ultrastructure of the cornea post-surgery. Surgeries were conducted by Dr. Hiroki Hatanaka (Kyoto Prefecture University of Medicine) and tissue was examined two weeks post-surgery.

2.1.4 Non-Surgical Treatment

ROCK inhibition is a novel treatment for endothelial disease revealing that it may prevent apoptosis and increase cell adhesion and proliferation in corneal endothelial cells. Studies have reported that the specific ROCK inhibitor, Y-27632, promotes adhesion and proliferation of monkey corneal endothelial cells, and decreases apoptosis (Okumura et al, 2009). Y-27632 has also been shown effective when applied topically in wound healing *in vitro* and *in vivo* (Okumura et al, 2012). These studies signify that ROCK inhibition with Y-27632 has the potential to regenerate the corneal endothelium where the number of cells is inadequate to maintain stromal deturgescence and in wound healing. ROCK-inhibitor-treated rabbit and human tissue obtained from Dr Naoki Okumura (Doshisha University, Kyoto) was prepared for conventional TEM to examine endothelial morphology.

2.2 Experimental Protocols

2.2.1 General Preparation for TEM

Samples were fixed for 2-3 hours at 4°C in appropriate fixative in buffer solution (Table 2.1). Samples were trimmed and fixed in 1% osmium tetroxide (Sigma Aldrich, UK) in buffer (Table 2.1) for 1 hour before being contrasted in 0.5% aqueous uranyl acetate (Sigma Aldrich, UK) for 1 hour. Specimens were then dehydrated

through a graded ethanol series (70%, 90% and 100% [x2]) for 15 min each. Immersion into propylene oxide was conducted for 15 min before insertion into a 1:1 propylene oxide: Araldite resin mixture for 1 hour prior to infiltration with fresh resin (see Appendix I). Embedding was carried out over 2 days with 3 changes per day. Tissue was embedded in moulds late on the second day and left to polymerise at 60°C for 72 hours.

Study	Buffer	Fixative	pH	Section stain
Chick development	0.1M sodium cacodylate	2.5% Glut 2% PF	7.2-7.4	UA Lead citrate
Fuchs'	25mM sodium acetate (0.1M $MgCl_2$, 0.05% Cuprolinic blue	2.5% Glut	5.7	UA PTA
DSAEK/nDSAEK	0.1M Sørensen	2.5% Glut 2% PF	7.2-7.4	UA Lead citrate
ROCK-Inhibitor	0.1M sodium cacodylate	2.5% Glut 2% PF	7.2-7.4	UA Lead citrate

Table 2.1 Buffer, Fixative and stains used in TEM studies. Glut-Glutaraldehyde, PF-Paraformaldehyde, UA-Uranyl acetate and PTA-Phosphotungstic acid. See Appendix I for buffer components.

2.2.2 TEM Enzyme Treatment of Tissue

Corneas undergoing proteoglycan localisation were prefixed in 4% paraformaldehyde in Tris acetate for 10 minutes prior to enzyme treatment. Original working stock for each enzyme was 5U, which was rehydrated in distilled water and added to Tris acetate buffer (Table 2.2).

Enzyme	Enzyme activity	Buffer	Unit/ml
1000µl Chondroitinase ABC (5U)	Digestion of chondroitin sulphate proteoglycans	1000µl 2x Tris acetate buffer+BSA (pH 8) + protease inhibitors	2.5
1000µl Keratanase (5U)	Digestion of keratan sulphate proteoglycans	1000µl 2x Tris acetate buffer+BSA (pH 7.5) + protease inhibitors	2.5
500µl Chondroitinase ABC (2.5) + 500µl keratanase (2.5)	Digestion of chondroitin and keratan sulphate proteoglycans	1000µl 2x Tris acetate buffer+BSA (pH 7.5) + protease inhibitors	1.25 (of each enzyme)

Table 2.2 Chondroitinase ABC and keratanase enzyme solutions. Enzymes were rehydrated in distilled water and Tris acetate buffer to obtain the above units. BSA-bovine serum albumin. See Appendix I for buffer components.

Corneas were rinsed in 1x Tris acetate buffer prior to incubation in the above enzyme solutions for 4 hours at 37°C with protease inhibitors to decrease protein degradation. Wild type and mutant corneas for the experiments investigating endothelial pathology each went through i) chondroitinase ABC digestion ii) keratanase digestion iii) buffer only treatment and iv) Cuprolinic blue only. Post enzyme treatment, corneas were rinsed in sodium acetate/0.1M magnesium chloride buffer prior to fixation overnight in 2.5% glutaraldehyde in 25mM sodium acetate buffer (pH 5.7) containing 0.1M $MgCl_2$ and 0.05% Cuprolinic blue. Staining of GAGs was developed by Scott and Haigh (1985) using Cuprolinic blue. This stain allows observation of GAG chains on proteoglycan molecules helping determine how proteoglycans interact with collagen fibrils. After rinsing three times in sodium acetate buffer, samples were washed a further three times in 0.5% aqueous sodium tungstate (Sigma Aldrich, UK). Samples were dehydrated in 0.5% sodium tungstate in 50% ethanol for 15 minutes, before further dehydration in a graded ethanol series (70%, 90% and 100% [x2]) for 15 minutes in each. Resin infiltration was carried out as discussed above. Blocks were stored at room temperature until required. Semi (0.5 µm) and ultra-thin (100 nm) sections were cut and collected on glass slides and uncoated copper grids, respectively, before being stained in appropriate solutions (Table 2.1).

2.2.3 Staining

Contrast observed in the electron microscope is produced by the differential scattering of electrons by the tissue embedded within the resin. Darker areas are due to the denser areas of the tissue, whereas the lighter areas correspond to those with less density. However, sometimes it is difficult to distinguish between different components of the tissue as well as between the resin and the tissue itself due to the section thickness. Thus, stains employing heavy metal salts are used to increase the contrast.

A number of staining techniques are used in TEM which fall into two categories, positive staining and negative staining. Positive staining is visualised when the density of the biological structure is increased as opposed to the background. The heavy metal salts bind to parts of the tissue, increasing their density and subsequently, their contrast, whilst unbound stain is removed. Osmium tetroxide is used to increase

density; additional staining (post embedding with uranyl acetate and lead citrate) will increase the contrast further. The positive stains used in this thesis were uranyl acetate and lead citrate. Uranyl acetate, used before and after embedding, binds with phosphate and amino groups resulting in highly stained nucleic acids (Hayat, 2000). Lead ions are thought to bind to negatively charged components of the tissue, for example, those areas that have reacted with osmium and hydroxyl groups (Bozzola and Russell, 1999). In negative staining the macromolecule is unstained surrounded by a dark background, this type of staining has a minimal effect on the specimen itself. The substructure of the individual organelle is contrasted by stain penetration into the voids present within the specimen which is responsible for the dark background. Phosphotungstic acid is a commonly used negative stain, used alongside uranyl acetate.

Additionally, Cuprolinic blue was also used in the experimental pathology experiments of FECD mouse models (Chapter 4). Cuprolinic blue was first introduced as a cationic RNA specific dye. Cuprolinic blue can be used to stain proteoglycans associated with collagen fibres and combined with enzymatic digestion can help determine the location of certain proteoglycans within the tissue (Scott, 1975). Cuprolinic blue was used in this study to determine if proteoglycans were altered in the FECD model and they're placement in Descemet's membrane.

Grids were stained with either:

i) Phosphotungstic acid (2%), and uranyl acetate-2min and 12 min respectively

ii) Uranyl acetate (saturated) followed by lead citrate-12 min and 5min respectively.

Grids were viewed using an electron microscope (JEOL 1010 transmission electron microscope with Gatan ORIUS SC100 CCD camera).

For buffer and general TEM components see Appendix I.

2.2.4 Electron Tomography

Electron tomography is employed to obtain a three-dimensional image of a sample which has been tilted around a single axis. Each face of the ultra-thin corneal sections (120 nm) undergoing tomography was exposed to a colloidal gold solution (10 nm-

BBl, Cardiff, UK). Thicker sections were used to help prevent tissue destruction, a problem that can occur due to the extensive amount of time the tissue is exposed to the electron beam. Colloidal gold was placed on both sides of the grid and served as a fiducial marker, facilitating alignment of the tilt micrographs. A −60° to +60° single axis tilt series of long-spacing collagen and proteoglycans present in Descemet's membrane was captured in one and two degree increments at x20k magnification using a JEOL 1010 transmission electron microscope with Gatan ORIUS SC199 CCD camera. Reconstruction and segmentation was carried out on sections for a three-dimensional insight into the structure of the long-spacing collagen present in Descemet's membrane. The reconstructed image is created from projections of the structure of interest. Each of the images was returned to the same co-ordinates using centrally located fiducials to ensure each image was aligned with the previous.

2.2.4.1 Alignment of the Tilt Series

An important part of electron tomography is to align the collected images using the fiducials (gold particles). The tiff images that composed the tilt series were converted into a .mrc file and .st image stack. The .st file was then opened in the eTOMO software programme (University of Colorado, USA) to align the fiducials in each tilt image taken. Once the coarse and fine alignment of the fiducials is complete, eTOMO uses a backprojection to generate a three-dimensional reconstruction from the two-dimensional micrographs. A tomograph is created by merging the aligned images to create an image that can be used to pass through the thickness of the image stack.

2.2.4.2 Segmentation of Three-Dimensional Reconstruction

EM3D software (Stanford University, USA) (Ress et al, 2004) was used to segment the final tomogram. Objects of interest were manually outlined in each image of the image stack. The stack with the traced objects was rendered producing a three-dimensional reconstruction of the object of interest (Figure 2.1). Full methods used can be found in Electron Tomography (2006).

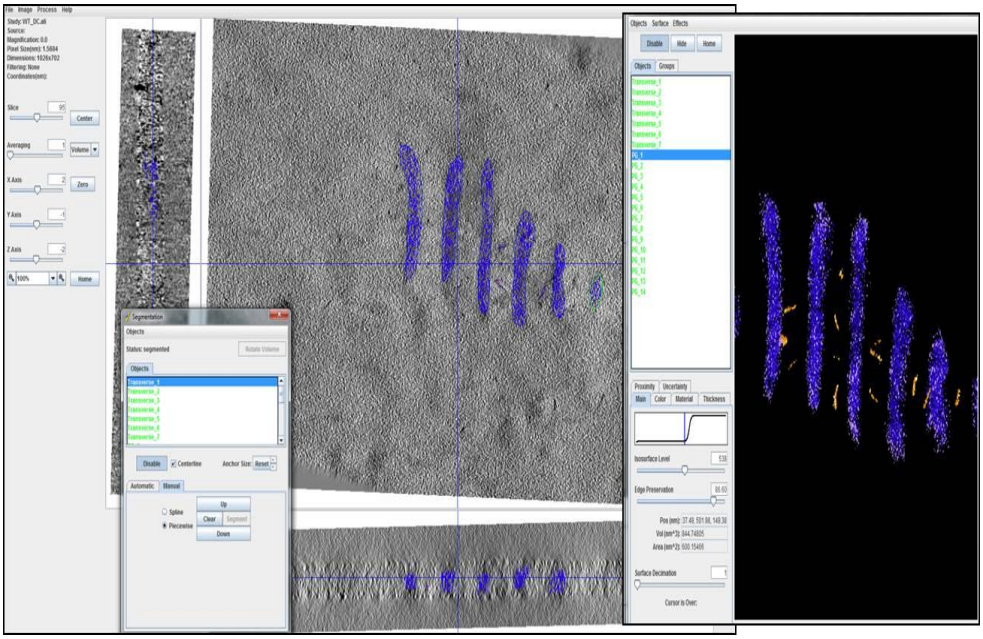

Figure 2.1 Screenshot of the segmentation and rendering process using EM3D. Segmentation step (left) followed by rendering process (right) to obtain the three-dimensional reconstruction.

Light microscopy was also used to view DSAEK/nDSAEK samples at lower magnification so the entire corneal depth could be examined. Semi-thin sections of 500 nm were cut and placed onto glass slides. Sections were stained with 1% toluidine blue and washed with distilled water before being analysed using a Leica DM RA2 photomicroscope with Leica DC 500 camera.

2.3 Immunohistochemistry

Immunohistochemistry was undertaken to pinpoint specific antigens (i.e. NBC) present in the developing avian cornea.

Corneas were dissected from embryonic chicks (E8-14), placed into moulds containing O.C.T. compound (optimal cutting temperature) and rapidly submerged into isopentane cooled by liquid nitrogen and stored until required. O.C.T. embedded samples were mounted onto a chuck before cooling in the cryostat chamber (Bright,

OTF5000). 10μm frozen O.C.T. sections were cut and placed onto glass slides (Fisher scientific), left briefly to dry and stored at -20°C until required. Cryosections were drawn around using an ImmEdge (PAP) pen (Vector laboratories, UK) before rehydrating in PBST (0.05M phosphate buffered saline with 0.1% Tween-20). Tissue was fixed in cold (-20°C) ethanol (75%) for 1 minute and washed in PBST (5 min (x3)). Sections were pre-blocked with 5% normal goat serum before staining with either primary antibody or non-specific rabbit IgG for 1 hour at room temperature. Rabbit anti-Na^+/HCO_3^- cotransporter polyclonal antibody (Merck Millipore, UK) was diluted (1:200) as suggested by manufacturer before being added to the tissue. Negative controls included primary antibody omission (PBS) or substitution with a non-immune rabbit immunoglobulins (5mg/ml).

Slides were washed with PBST (5 min) prior to incubation with the secondary antibody, Alexa Fluor 488 goat anti-rabbit IgG (Invitrogen, UK), for 1 hour at room temperature. Further washing with PBST was carried out before mounting in Vectashield mounting medium containing DAPI, used as a nuclear counterstain (Vectashield, Vector Laboratories, Burlingame, CA). Results were analysed using fluorescence microscopy (BX61; Olympus, Tokyo, Japan).

After examination using the fluorescence microscope, it appeared the 5% chick serum was adequate to reduce the non-specific binding; as a result, this step was incorporated in the protocol.

2.4 A-Scan Ultrasonography

A-scan ultrasonography was used to measure corneal thickness in the eyes of embryonic chicks. The system comprised a panametrics model 5073PR pulser-receiver and a 20MHz transducer fitted with a 15mm saline stand-off perfused at 0.05ml/min which was placed onto the fresh cornea. Readings were taken once five peaks were visible representing cornea, lens and retina. Readings were obtained in triplicate, with re-alignment between readings and recorded as they were taken. Ultrasound velocities were assumed to be 1.534 mm/μs in the cornea. Calibration of the equipment was carried out daily using a water filled cuvette with known internal dimensions. The schematic shows the peaks present before a reading was taken

(Figure 2.2). One way analysis of variance and Tukey-Kramer multiple comparisons post-hoc test were used to determine differences between embryonic days. Two-way analysis of variance was used to examine the influence of two independent variables (left/right cornea and developmental day) on the corneal thickness.

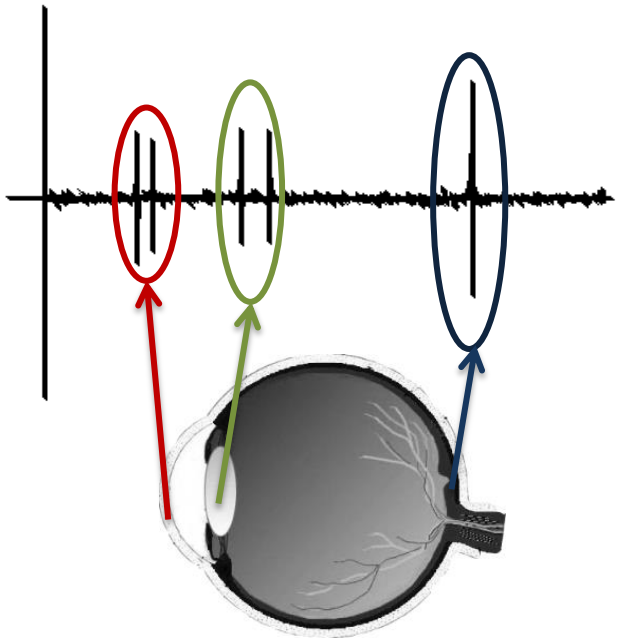

Figure 2.2 Schematic showing the peaks observed during ultrasonography. Red-corneal peak, green-lens and blue-retina. Identification of all five peaks was ensured before the reading was taken to ensure accurate measurement. Adapted from http:/webvision.med.utah.edu/book/part-i-foundations/simple-anatomy-of-the-retina/.

Chapter 3: Endothelial development in avian cornea

3.

3.1 Introduction

3.1.1 The Corneal Endothelium Pump Mechanism

The corneal endothelium is a leaky cell layer as a result of the discontinuous zonula occludens that allow nutrients into the avascular stroma. The leak is counteracted by the removal of fluid out of the stroma to prevent oedema. In healthy cornea there is no net fluid transport, as fluid is actively secreted out of the cornea counterbalancing the leak of fluid into the cornea. This process is referred to as the 'pump-leak' mechanism, a feature required to keep the cornea at the appropriate hydration for transparency. The pump mechanism ceases in the absence of bicarbonate ions and is significantly diminished in the presence of carbonic anhydrase inhibitors (CAIs) (Hodson, 1974; Hodson and Miller, 1976). Numerous studies have shown a net basolateral-to-apical flux of bicarbonate (Hodson and Miller, 1976; Huff and Green, 1983; Wigham and Hodson 1985), a result that has highlighted bicarbonate as the main ion involved in endothelial fluid transport. There is also a negative trans-endothelial potential on the apical side of the endothelium, suggesting that there is a net transport of anions from the stroma to the anterior chamber.

Bonanno and Giasson concluded that a novel Na^+ dependent Cl^- independent $Na^+/2HCO_3^-$ cotransporter (NBC1) was present in the corneal endothelium (Bonanno and Giasson, 1992). Na^+ HCO_3 transport is now identifiable in numerous cell types (Romero and Boron, 1999). In the corneal endothelium the NBC is located on the basolateral membrane which has a 3x higher bicarbonate permeability than the apical membrane based on studies in cow (Sun at al, 2000) and human corneas (Usui et al, 1999). This has led to the conclusion that NBC loads endothelial cells with bicarbonate on the basolateral surface. Sodium is also thought to be transported via the endothelial layer, from the basolateral to apical side of the membrane (Hodson, 1974; Huff and Green, 1981; Lim and Fischbarg 1981), and is likely to be the counterion (Figure 3.1).

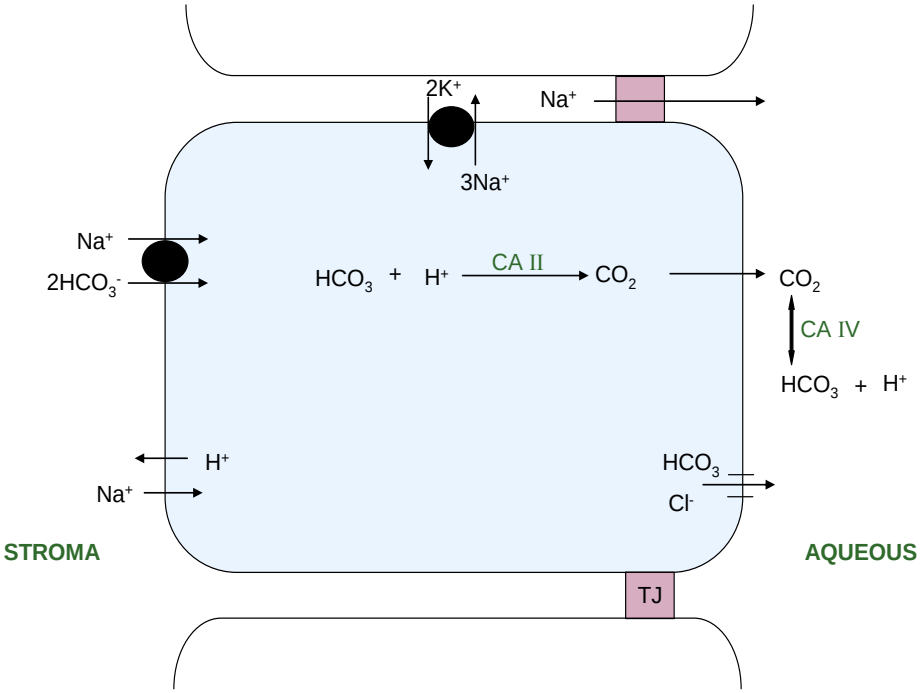

Figure 3.1 Model for endothelial ion transport. NBC loads corneal endothelial cells with HCO_3^- from the basolateral (stromal) side of the membrane. HCO_3^- entry drives the formation of carbon dioxide within the endothelial cell, this is catalysed by carbonic anhydrase II and inhibited by carbonic anhydrase inhibitors (Hodson, 1971). The carbon dioxide is transported across the apical membrane quickly due to its high permeability, then immediately converted to HCO_3^- and hydrogen by membrane bound carbonic anhydrase IV.

There are two isoforms of NBC-1, kidney (kNBC) (Romero et al, 1998) and pancreatic (pNBC) (Abuladze et al, 1998), the differences between these lie within the NH_2 terminal sequences. kNBC has a $1Na^+:3HCO_3^-$ stoichiometry favouring bicarbonate efflux from the cell, whilst pNBC has a $1Na^+:2HCO_3^-$ stoichiometry favouring HCO_3^- influx. However, the stoichiometry of pNBC and kNBC can change depending on location and cell type, respectively. Studies have shown that the pNBC isoform is expressed in the corneal endothelium with a 1:2 stoichiometry. A cotransporter with a 1:2 stoichiometry would have to exist for bicarbonate influx (Bonanno and Giasson, 1992).

There are three possible modes of bicarbonate efflux into the aqueous humor, 1) Cl^-/HCO_3^- exchange 2) CO_2 efflux and conversion to bicarbonate via membrane bound carbonic anhydrase IV on the apical membrane (Bonanno et al, 1999) and finally 3) via a conductive flux through anion channels (Sun et al, 2000).

3.1.2 Embryonic Corneal Thickness

A series of events occur during avian corneal development that affects the thickness of the cornea. On E5 a rapid increase in thickness correlates with the second migration of mesenchymal cells resulting in a corneal thickness between 30 and 50µm. These mesenchymal cells are destined to become corneal fibroblasts. The trigger for cellular invasion is thought to be expansion of the matrix (Fitch et al, 2005) and possibly the removal of collagen type XI which acts as a stabilising factor, keeping the stroma in a compact state (Cai et al, 1994). Hyaluronate, a GAG produced on E4 (Toole and Trelstad, 1971), is also thought to be involved in stromal swelling post endothelial migration. By E6 the thickness of the stroma has increased to 100µm, the posterior of which invaded by mesenchyme. Fibroblasts occupying the stroma are responsible for the synthesis of the secondary stroma on E7 (Hay and Revel, 1969). Histology indicates that the stroma reaches a maximum thickness by E10, prior to a dramatic compaction between the E14 and E19 developmental period when water is lost. This loss increases transparency as demonstrated by spectrophotometry studies reporting an increase from 40% to over 95% in light transmission in the adult cornea (Coulombre and Coulombre, 1958; 1961; Hay and Revel, 1969). Some studies see corneal compaction after E9 (Coulombre and Coulombre, 1958; Hay and Revel, 1969), whilst x-ray diffraction studies suggest compaction after E12. Water is lost initially from envisaged collagen-free spaces in the corneal stroma followed by homogenous compaction of collagen fibrils throughout the tissue after E14 (Siegler and Quantock, 2002). Factors suggested for this compaction include changes in water binding components within the stroma (proteoglycans), increased hyaluronidase (Toole and Trelstad, 1971) and the activation of the NBC in the corneal endothelium.

This study was carried out to determine when the NBC appeared in developmental chick corneal endothelium to help determine when the pump becomes activated and stromal dehydration occurs. This will be discussed in relation to new in situ measurement of corneal thickness determined using A-scan ultrasonography. Finally, TEM analysis was carried out to detect changes in endothelial morphology during the developmental period with focus on organelles likely to be associated with the pump.

3.2 Methods

3.2.1 A-Scan Ultrasonography

A-scan ultrasonography was used to measure corneal thickness in the eyes of embryonic chicks. Chicks aged between E9 and E18 were killed and immediately analysed ensuring the head and eyes were left fully intact before mounting and measuring using the method described in Chapter 2. Three separate experiments were carried out to improve the data set. The first measured the thickness of the cornea from E10 to E18, recorded on separate days requiring separate calibrations on each (data not shown). The second experiment measured corneal thickness in embryonic chicks aged between E9 to E18 on one day requiring one calibration. The second experiment was repeated with an increased n number and only measured thickness in the left corneas after a small difference was seen between left and right corneas in the previous experiments. The rationale behind these experiments was to obtain a more accurate measurement of the thickness changes that occur during corneal development. Previous thickness measurements have been carried out using histology (Hay and Revel, 1969), a method not so reliable because of artefacts inherent within the chemical fixation involved. One and two-way ANOVAs with Tukey's multiple comparison analysis was carried out using GraphPad (Prism version 6.00 for Windows, GraphPad Software, La Jolla California USA, www.graphpad.com) (Appendix I). The one-way ANOVA was used to compare the thickness means over the developmental period i.e. to determine if there was a significant difference in corneal thickness between difference developmental days (E9-E18). The two-way ANOVA was used to examine the effect of two independent variables on corneal thickness i.e. to determine if developmental day or cornea (left or right) had an effect on the corneal thickness.

3.2.2 Immunohistochemistry

Immunohistochemistry was carried out to pinpoint specific antigens present in the developing avian cornea. Fully intact corneas were embedded in O.C.T. prior to cryostat sectioning. Immunohistochemistry was carried out as described in Chapter 2, with a rabbit anti-Na^+/HCO_3^- cotransporter polyclonal antibody (Merck Millipore, UK). Developmental days E10-E14 were examined (n=4).

Control sections containing rabbit non-immune IgG showed positive staining so the technique was altered to determine why the non-immune rabbit IgG was binding the tissue.

1. The primary antibody and controls were pre-absorbed with 5% normal chick serum at room temperature for 1 hour (Invitrogen, UK) in an attempt to prevent non-specific binding in the chick tissue.
2. Secondly, the primary antibody was diluted 1:2000 and 1:8000 to determine if the fluorescence intensity was the same as in 1:100 dilution previously used (to determine if the primary is binding ubiquitously and thus indicating no specificity for the endothelium).

3.2.3 TEM

Fertilised white leghorn eggs (Henry Stewart & Co. Ltd) were incubated at 37.5°C in a humidified rotating chamber. At E6, 8, 10, 12, 14, 16 and 18, embryos were killed in accordance with the Association for Research in Vision and Ophthalmology statement for use of animals for ophthalmic and vision research and in agreement with local ethical rules ($n \geq 3$). Corneas were excised immediately and fixed before undergoing TEM as described in Chapter 2. Several sections were collected, examined and stained on each grid from peripheral to central cornea.

3.3 Results

3.3.1 Corneal Thickness

Histology has been used in previous experiments to determine corneal thickness changes in development where the tissue is dehydrated and embedded. This study measured corneal thickness in fresh corneal tissue using A-scan ultrasonography. A-scan ultrasonography is capable of measuring corneal thickness *in vivo*, and therefore does not require the invasive fixation processes. Three separate experiments were carried out to determine the changes in embryonic chick corneal thickness. Experiments were altered each time to improve the data set (see Appendix I for raw data).

Measurements from the second experiment, carried out on one day, show a thickness increase up to E14 and a decrease immediately after (Figure 3.2A). The data was split to compare left and right corneas (Figure 3.2B). This highlighted differences between the data sets that led to the final experiment measuring left cornea only (Figure 3.3). It is speculated that the difference in thickness between left and right corneas was probably as a result of the time they were measured after death (left corneas were measured first). Thickness increased progressively from E9 until E12 before reaching a plateau between the E12 and E15 developmental period, prior to a steady decrease until E18, the latest time point measured.

A feature observed in all graphs was the plateau in thickness observed between E13-E15. The left cornea was thicker in the majority of time-points measured, some differences between left and right corneas were significant (E9, E10, E13, E14 and E18). This difference was confirmed using two-way ANOVA. The final experiment measuring left cornea only was carried out as a result of this difference. The n number at each developmental day was increased ensuring a minimum of six eyes were measured at each time point (Figure 3.3)

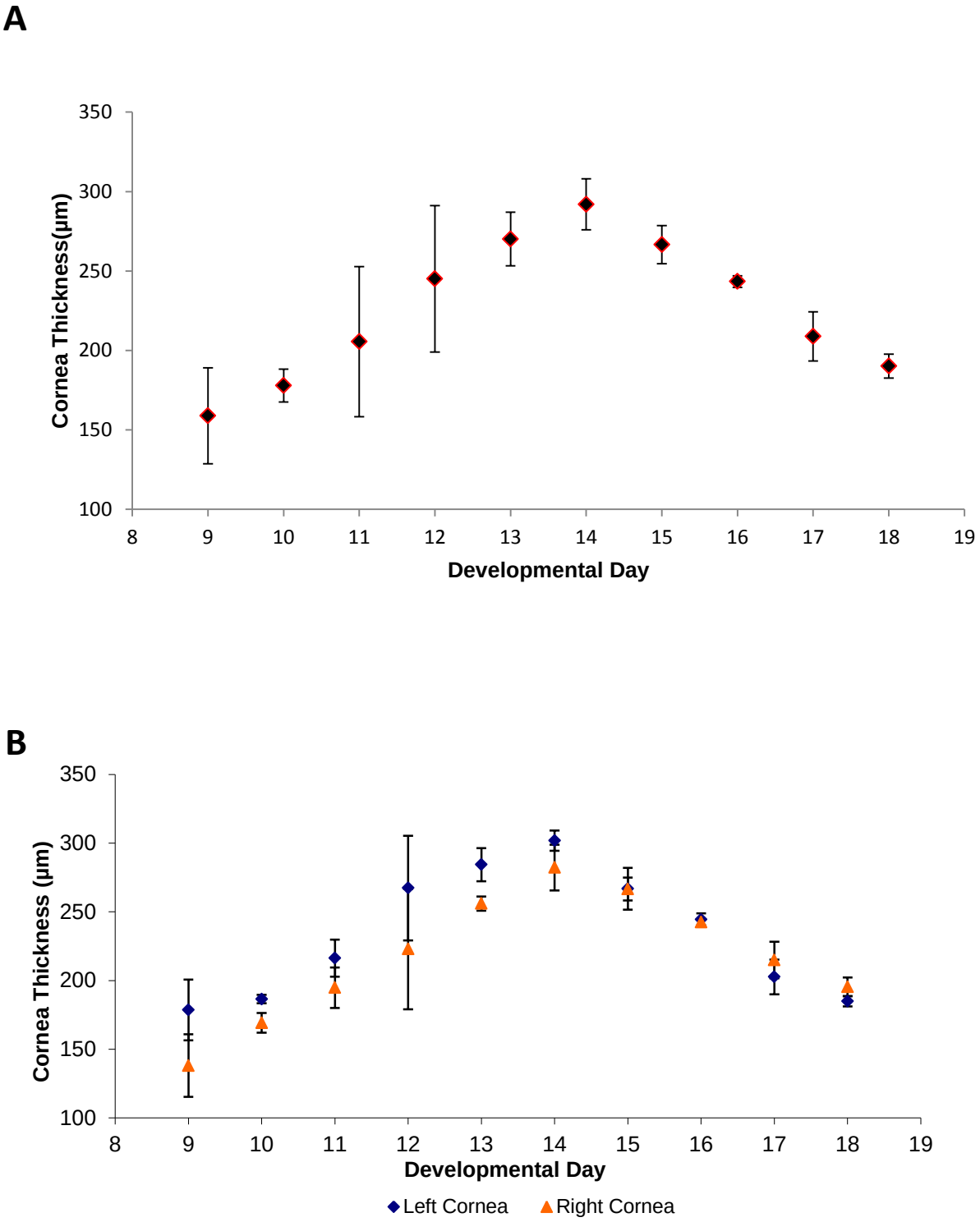

Figure 3.2 Corneal thickness measured on one day in left and right corneas. A) Average thickness of left and right corneal data for each embryonic day (n≥6). Significant differences were present between all consecutive days except E9-E10 and E17-E18 (p≤0.01). B) Thickness differences between left and right corneas (n≥3). Left cornea was consistently thicker than right and some of these differences were significant (E9, 10, 13, 14, and 18, p≤0.01). The difference between the thicknesses decreased as the chick aged. Error bars denote standard deviation. Two way ANOVA suggests that both age and cornea (left/right) affects the result (p≤0.01) (See appendix I).

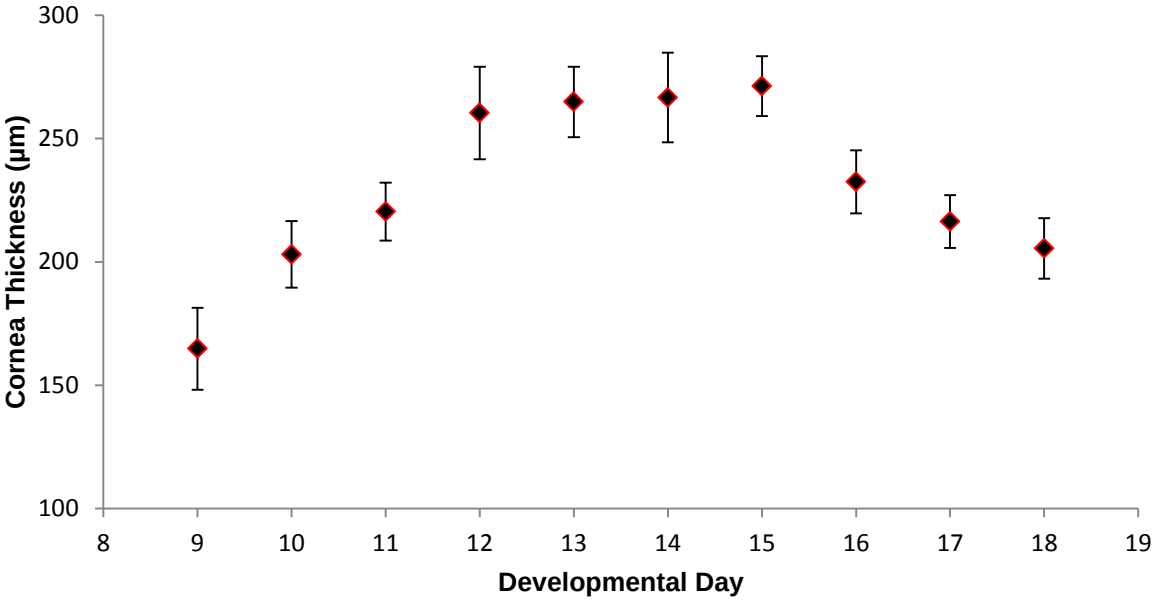

Figure 3.3 Cornea thickness taken from left eye only in the final experiment with increased n number (n≥6). Significant differences between consecutive days include E9-E10, E10-E11, E11-E12, E15-E16 and E16-E17 ($p \leq 0.01$). Error bars denote standard deviation. See Appendix I for statistical test.

3.3.2 Immunohistochemical Analysis

Results from immunolocalisation show the presence of the NBC within the endothelial cells from E10-E14 (Figure 3.4). The addition of chick serum prevented non-specific binding observed in initial control samples. The initial analysis showed non-immune rabbit immunoglobulin binding to the chick cornea in endothelial cells and parts of the stroma where it should not be detected. This indicated non-specific binding of control rabbit IgG which could indicate the fluorescence observed in the test samples is as a result of non-specific binding, a false positive result. The method was altered to include chick serum (5%) to the test and control samples to reduce what was thought to be non-specific binding. The results clearly indicate the presence of this transporter in chick endothelium which presumably becomes involved in the management of corneal deturgescence at this early stage of development.

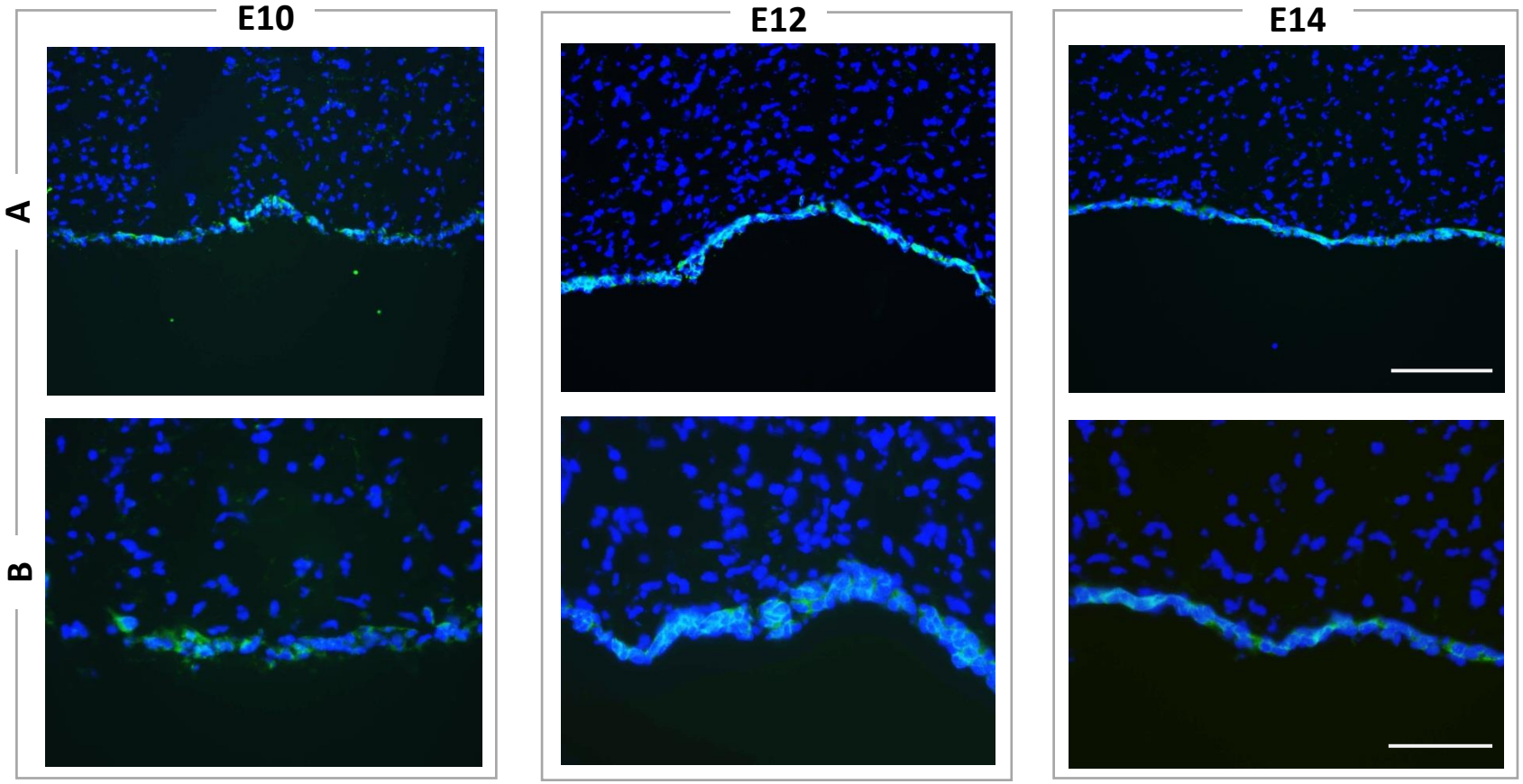

Figure 3.4 Immunolocalisation of the NBC and nuclear stained cells using rabbit anti-NBC antibody and DAPI, respectively. Immunolocalisation revealed the NBC was present at all developmental stages tested A) Low and B) high magnification. n= 4.Dapi=blue, NBC=green.Scale bar=100 µm (A) and 50 µm (B), respectively.

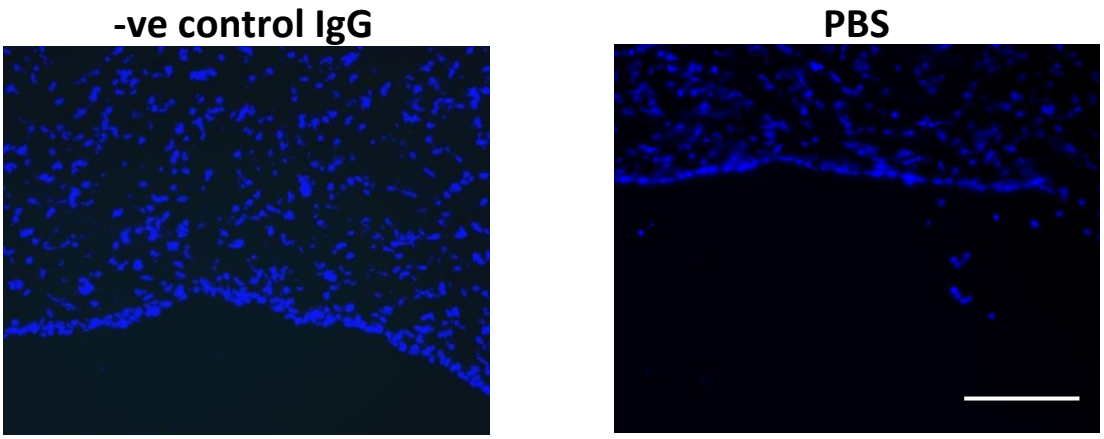

Figure 3.5 Negative controls for immunolocalisation of NBC in developmental cornea. Controls show negative staining to the primary antibody and non-random binding of secondary antibody. Scale bar= 100 µm

3.3.3 TEM Analysis of Developing Corneal Endothelium

Figures 3.6 and 3.7 show TEM images from developing chick corneal endothelium from E6-18. Images show the differences in the cells and the changes that occur within the posterior stroma and Descemet's membrane. The cells had interesting features throughout development, including a large population of mitochondria, the presence of vacuoles and interdigitations. Descemet's membrane becomes thicker as development progresses. A sparse stroma visualised on E6 becomes more compact as the embryo ages. Sections from peripheral and central cornea were visualised for each developmental day in order to obtain a detailed picture of the posterior cornea (n=3).

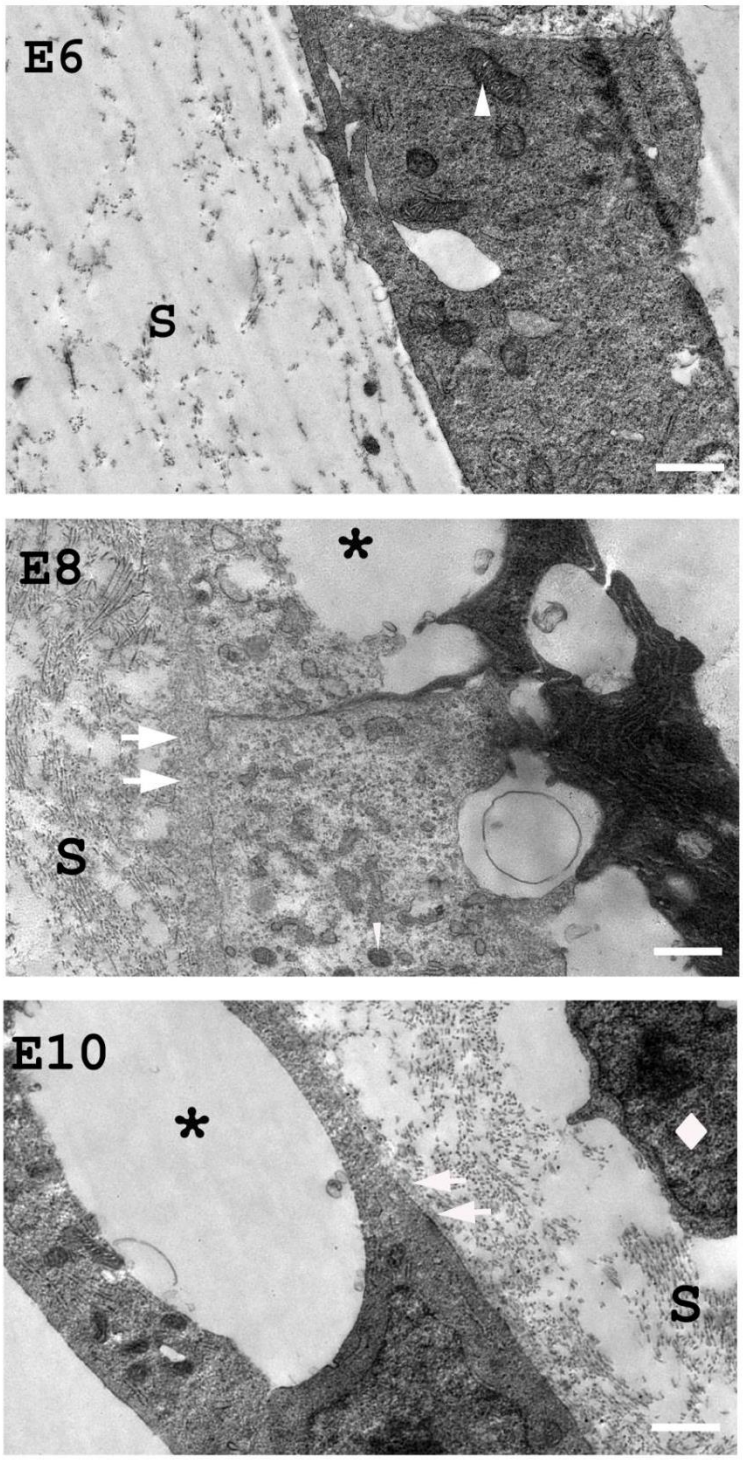

Figure 3.6 Prominent features observed in developing chick corneal endothelium (E6-E10). Descemet's membrane accumulation (arrows) and stroma (S) are highlighted. Vacuoles (*) and mitochondria (arrowheads) were also a common feature in the cell layer, together with keratocytes (◊). Scale bars=500 nm, n=3.

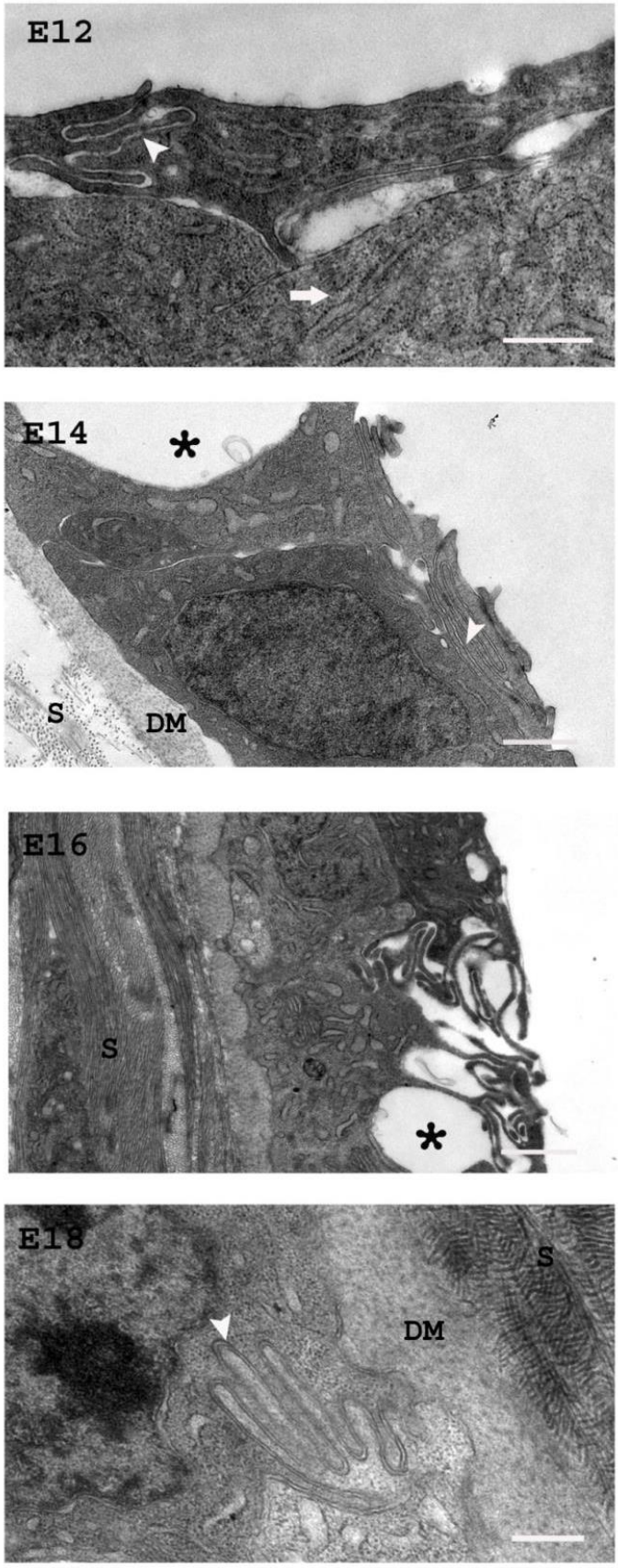

Figure 3.7 Prominent features observed in developing chick corneal endothelium. Membrane interdigitations were present at all stages of development (arrowheads). Vacuoles (*) were also a common feature in the cell layer, together with rough endoplasmic reticulum (arrow). S-stroma, DM-Descemet's membrane. Scale bars=500 nm, n=3.

3.4 Discussion

3.4.1 Thickness Changes during Avian Corneal Development

After the initial thickness experiment a second was carried out in one day to decrease possible experimental error caused by multiple calibrations. Significant differences between consecutive days were seen at every stage with the exception of E9-10 and E17-18. The data was split to determine if there was a difference between left and right corneas (Figure 3.2B). A number of significant differences were observed between the left and right corneas in this experiment. One reason for this difference may be experimental; the left cornea was always measured first, a procedure that may have resulted in the drying out of the right cornea. There may be developmental differences between the two eyes at this stage, however, it would seem that corneal drying would likely be the predominant effect. The difference was more noticeable in younger embryos, a result probably due to the absence of eyelids and therefore decreased protection against drying. Due to this difference, the experiment was modified once more measuring only left corneas, removing external factors. The n number at each developmental day was increased so a minimum of 6 chicks were used at each stage. Three areas of interest were observed in these experiments, an initial increase, followed by a plateau and finally a decrease in thickness. There were 5 significant differences observed between consecutive days in this final experiment. These differences present were between E9-E10, E10-E11, E11-E12, E15-E16 and E16-E17 ($p \leq 0.01$). Significant differences occurred in the early and late stages of development where the thickness changed most dramatically. There were no significant differences between the E12-E15 developmental period, the thickness plateaued during this stage before decreasing again, probably due to the loss of water and homogenous compaction of collagen fibrils (Siegler and Quantock, 2002).

In all experiments standard deviation was higher in the early embryonic stages due to the difficulty in obtaining measurements in the smaller eyes. Thickness measurements were similar to those measured in the final experiment.

The increase in thickness from E9-E12 is thought to occur as a result of the swelling period that occurs on E5 in preparation for the invasion of mesenchymal cells destined to become

the corneal keratocytes (Hay and Revel, 1969). These data correlates with studies by Siegler and Quantock (2002) showing changes in the interfibrillar spacing and hydration within the cornea throughout the developmental period. Interfibrillar Bragg spacing was significantly reduced between E16-E17. A sharp, rather than a gradual, decrease in spacing was observed, E16 (66.8 nm) and E17 (61.2 nm). A decrease in thickness post E15, thought to be as a result of dehydration and compaction, could be responsible for the increase in transmission (Coulombre and Coulombre, 1958). Hydration was also measured in Siegler's study, decreasing between E12 and E18 as the matrix becomes more compact. Siegler proposed a two stage dehydration, firstly between E13-E14 and secondly between E16-E17. The first dehydration was not accommodated by any change in centre-to-centre collagen fibril Bragg spacing so a different method of matrix compaction must occur. They concluded that this was a loss of water from non-collagenous regions, or regions of irregular collagen, such as stromal lakes. The second dehydration observed between E16-E17 correlated with a reduction in interfibrillar Bragg spacing. Therefore, the drop in hydration was attributed to the homogenous reduction in average spacing between the regularly arranged collagen fibrils which contribute to the matrix compaction (Siegler and Quantock, 2002). The hydration change which had the predominant effect on thickness was perhaps when interfibrillar spacing was reduced between E16-E17.

These data not only correlates with interfibrillar collagen spacing but also with transmission data collected by a colleague previous to this set of experiments (Figure 3.8). Data showed a steady increase in transmission post E14, this increase corresponds to the decrease in thickness we observe post E15. The plateau in thickness during the E12-E15 developmental period is possibly a sign of stromal reorganisation where the collagen fibrils are arranged in their specific locations ready for the onset of transparency.

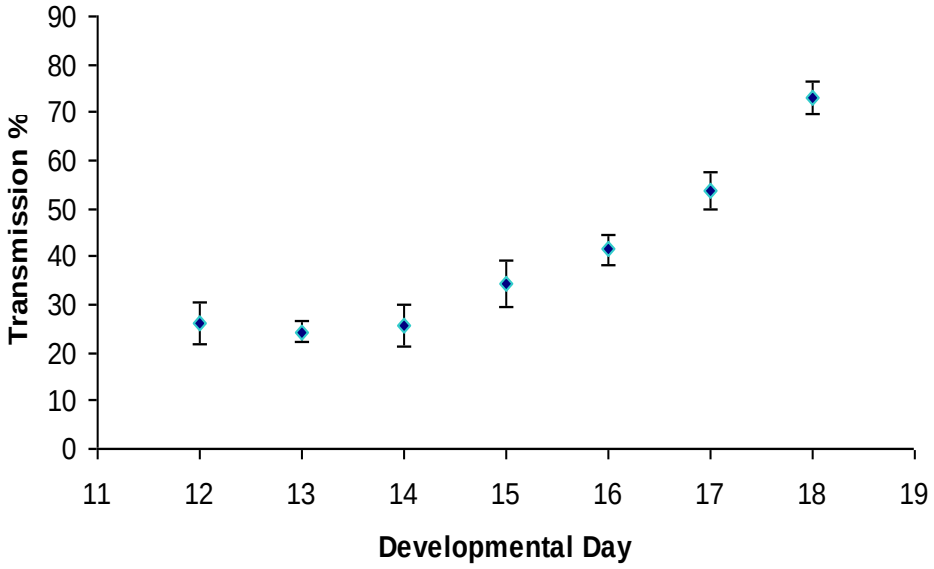

Figure 3.8 Light transmission at 550nm wavelength during the E12-E18 developmental period showing an increase post E14. Error bars illustrate standard deviation. Data obtained from Dr. Barbara Palka.

The most likely reason for the dehydration after this period is to attain optimal water content and interfibrillar spacing, discussed previously, required for transparency in the latter stages of development. This feature coincides with increased transmission (Coulombre and Coulombre, 1958), an outcome that is probably due to the combined effect of dehydration and the increased regularity of stromal collagen.

New methods measuring CCT are available, including Optical Low-Coherence Reflectometry (OLCR). OLCR measures corneal thickness on the basis of temporal separation of a low-coherent infrared laser beam reflected from the anterior and posterior surfaces of the cornea. Some studies have found significant differences between ultrasound pachymetry and OLCR measurements whilst others report similar measurements in both (Airiani et al, 2006). Most would agree that ultrasonography is an accurate technique with good reproducibility (Rainer et al, 2002), however, techniques including OLCR offer a non-contact method alongside rapid measurements. These additional features were not of primary importance in our experiments. The chicks were dispatched immediately so contact of the saline with the cornea was not a major concern. The main objective in this study was to obtain a more accurate picture of the thickness changes that occur during development, a feature that has only been measured previously by histology (Hay and Revel, 1969). Since ultrasonic pachymetry is the most commonly used method in patients and data exists using this method on hatched chicks (Montiani-Ferreira et al, 2004) this system seemed appropriate.

Results obtained using histology showed a maximum thickness at E9 (220 μm) and a decrease thereafter due to dehydration so that by E14 the thickness reached 150 μm (Hay and Revel, 1969). The study carried out by Hay and Revel showed considerable variation on E14 which was concluded to be as a result of variations in fixation or differences in water content at this developmental stage (Hay and Revel, 1969). Histological measurement of thickness can be inconsistent as the stroma has a tendency to compress and stretch during cutting. A true reading of the thickness can also be hindered by the fixation and dehydration processes.

The fluctuations in corneal thickness in our results imply there is a factor playing a role in stromal hydration/collagen organisation during embryonic development. The localisation of the NBC in the corneal endothelium (discussed later) supports the hypothesis that this cotransporter is influencing thickness at these early stages, especially during thickness decrease. As mentioned above, compaction and dehydration do occur in the embryonic cornea, thus, may be regulated by the NBC.

3.4.2 NBC Localisation during Avian Development

The bicarbonate ion is now agreed to be the main ion involved in endothelial fluid transport (Hodson and Miller, 1976; Jentsch et al, 1985; Bonanno and Giasson, 1992; Riley et al, 1995; Bonanno, 2003). Bicarbonate is transported through the NBC present in the basolateral membrane of the corneal endothelium (Sun and Bonanno, 2003). Immunolocalisation revealed the presence of NBC at all stages tested (E10-E14) (Figure 3.4), however, functional studies would have to be carried out to determine activity. It is already known that this transporter is important for corneal transparency later in life but it may also be involved in corneal compaction and dehydration in development. The results obtained support these claims, together with previously reported data on the expression of multiple genes, including NBC, in the developing avian cornea (Conrad et al, 2006). Conrad found that the NBC gene increased 10-fold through development into adult corneas in the chick model. mRNA expression was determined using real-time PCR using CDNA produced whole-cell RNA (Figure 3.9) (Conrad et al, 2006).

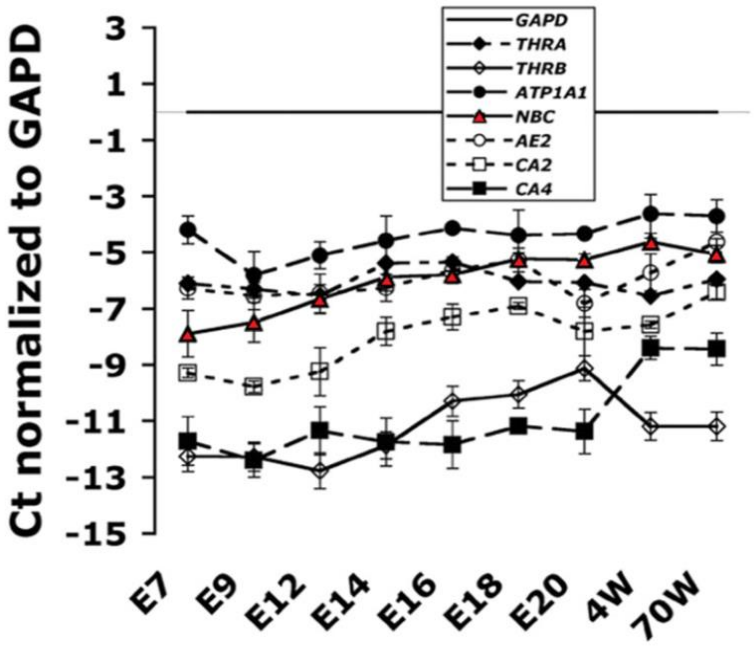

Figure 3.9 Expression of genes involved in endothelial cell transport using real-time PCR. NBC (red triangles) increased steadily during the developmental period before plateauing post E18. Results normalised to GAPD expression. Adapted from Conrad et al, 2006.

They found the largest increase in the NBC gene was between E7 and E14 (Figure 3.9), however, a difference in fluorescence was not observed in our data. A quantifiable technique is necessary to determine at what point the total amount of protein that is required is being expressed in the endothelium. The data suggests the NBC gene present, at the latest E7 (Conrad et al, 2006), has produced the cotransporter by at least E10 according to our data. Together, these data suggest that the NBC gene expression increases steadily during development and, based on our analysis, is localised within the endothelial cells. Both studies provide evidence that the NBC may be important in the developmental period. Gene expression increased until 4 weeks post hatching in Conrads study, the gene may increase into the adult cornea to produce more of the NBC required for transparency, however, light transmission is thought to reach 96% by E19 (Coulombre and Coulombre, 1958). Perhaps is it further unregulated to supply the growing demands and increase in size that occurs in the adult cornea, nevertheless, the change is minimal compared to that in the developmental period which is of more interest to us. The evidence presented here together with Conrad's study suggests that NBC has the potential to drive corneal dehydration during development.

3.4.3 TEM of Developing Endothelium

Several findings were observed in the embryonic chick cornea including high volumes of mitochondria, interdigitations within the endothelial cell membranes and thickening of the adjacent Descemet's membrane. Descemet's membrane is secreted by the endothelial cells once they have formed a complete monolayer on E5. The membrane begins to form on the endothelium's anterior surface on E6, thickening during development and throughout adulthood. Golgi bodies are also seen in many of the micrographs, an organelle responsible for manufacturing the proteins that comprise Descemet's membrane. Together with the RER (Figure 3.7), these organelles have important roles within the cell and in the formation of the primary stroma and Descemet's membrane via protein synthesis and migration. Interdigitations (Figure 3.7) are foldings of the endothelial cell surface, a feature thought to preserve excess cell membrane which can be used later in development and post hatching. The surface of endothelial cells increases as the eye grows and this is associated with cell spreading and as a result, fewer interdigitations (Materson et al, 1977). Vacuoles are also predominant in endothelial cells at all developmental stages. Whilst they are an organelle that can represent a manifestation of cellular activities, including the uptake of fluid, they may also represent post-mortem bleb formation (Speakman, 1959). It is thought that normal cell function would be difficult if the cell were so severely vacuolated. Other noticeable organelles are the mitochondria which are abundant in endothelial cells. They are responsible for the energy supply, the majority of which is directed towards the pumping mechanism in endothelial cell membrane. In addition to endothelial and Descemet's membrane changes, the stroma undergoes alterations as development progresses. The posterior stroma is sparse (Figure 3.6 [E6]) in the early developmental period, fewer fibrils are present, arranged in a disorganised manner compared to those seen later in development. By E18 the stroma is dense with regularly arranged collagen fibrils required for transparency (Figure 3.6 [E18]).

This chapter outlines significant changes that occur within the cornea during the developmental period and the potential mechanisms behind these alterations. The NBC is recognised to be one of the key components of the endothelial pump mechanism, this chapter further validates this component and discusses the possibility that it may play a role in the developmental context.

Chapter 4: The ultrastructure of Descemet's membrane and the structural changes in the cornea of *Col8a2* transgenic knock-in mice

4.

4.1 Ultrastructural Analysis of Descemet's Membrane

Descemet's membrane is the corneal endothelium's basement membrane which in the healthy cornea consists of an anterior banded layer and posterior non-banded layer (Figure 4.1). The anterior banded zone is composed of thin collagens fibrils with a periodicity of 110 nm produced during fetal life. The posterior non-banded zone is an amorphous assembly of extracellular matrix located between the anterior banded zone and the corneal endothelium. Descemet's membrane has been shown to contain hexagonal lattices aligned in parallel to the membrane surface (Jakus, 1956). The lattice is composed of electron dense nodes and rod-like structures measuring 132 nm in length which are now recognised to be type VIII collagen (Sawada et al, 1990). Type VIII collagen is a non-fibrillar short-chain collagen originally identified as a product of endothelial cells from bovine aorta (Sage et al, 1983) and rabbit corneal endothelial cells (Benya, 1980), and initially called endothelial collagen (Sage et al, 1983).

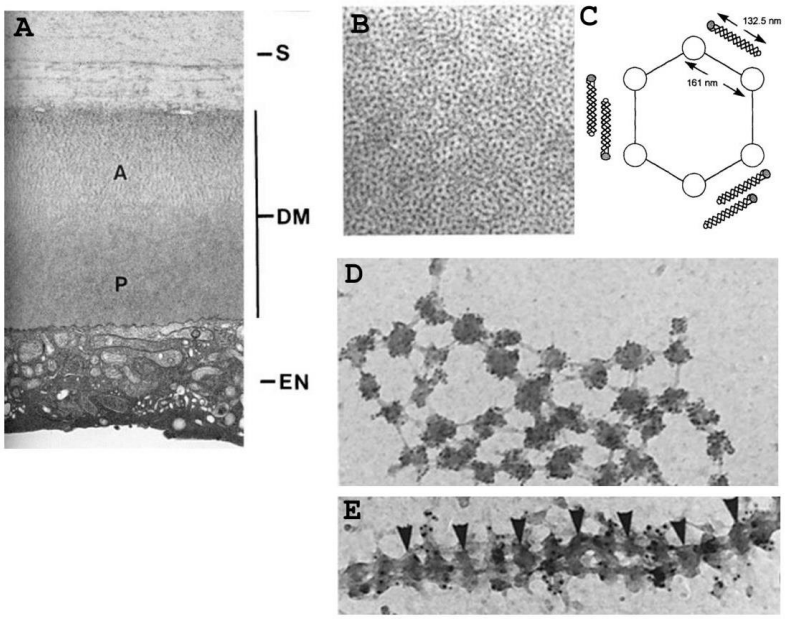

Figure 4.1 Schematic of Descemet's membrane alongside a type VIII hexagonal lattice. (A) Descemet's membrane is composed of an anterior banded layer (A) adjacent to a posterior non-banded layer (P). (B) The posterior layer is arranged as a lattice whereby collagenous filaments forma polygonal network (Bron et al, 1997). (C)Descemet's membrane is recognised to be composed of hexagonal lattices consisting of collagenous (132 nm) and non-collagenous regions. Possible type VIII constructs are presented including parallel and anti-parallel conformations. (D,E) Immunoelectron labelling of the lattice network produced by cultured bovine corneal endothelial cells (Sawada et al, 1990). S-stroma, DM-Descemet's membrane, EN-endothelium. (Taken from DelMonte and Kim, 2011; Shuttleworth, 1997).

Two distinct chains exist for type VIII collagen; α1(VIII) and α2(VIII). A heterotrimeric form of type VIII collagen is present in Descemet's membrane with a chain composition of [α1(VIII)2 α2(VIII)1] (Mann et al, 1990). The triple helix of collagen type VIII is flanked by non-helical N (NC2) and C (NC1)-terminal domains. The construction of type VIII is thought to help in maintaining an open structure, which consequently stabilises basement membranes (Yamaguchi et al, 1989). This is an important property in Descemet's membrane which has to be able to allow the movement of fluid, whilst being able to handle compression.

The main techniques used to visualise collagen type VIII have been two-dimensional, hence, little is known about the way in which it is packed and how it arranges itself through the depth of the Descemet's membrane. Whilst studying the corneal endothelium noticeable elongated structures were observed in Descemet's membrane. The first part of this chapter investigates the ultrastructure of Descemet's membrane in mice using electron tomography to gain a greater understanding of these elongated structures and the general arrangement of Descemet's membrane. The second part focuses on the ultrastructure of Descemet's membrane in murine corneas with collagen type VIII mutations.

4.1.1 Methods

5-month old mouse corneas were fixed for 2-3 hours at 4°C prior to general TEM embedding as described in Chapter 2. Ultrathin sections of embedded corneal tissue were cut at 100 nm and 120 nm thickness for transmission electron microscopy and electron tomography, respectively, and collected on uncoated copper grids. 1% phosphotungstic acid and a saturated uranyl acetate solution were used to stain the grids for 2 and 12 minutes, respectively, prior to examination in an electron microscope (JEOL 1010 transmission electron microscope with Gatan ORIUS SC100 CCD camera). Samples undergoing electron tomography (n=3) were also exposed to colloidal gold solution (10 nm-BBL, Cardiff, UK) which was applied to each face of the sections to serve as fiducial markers for later image alignment (details in chapter 2).

4.1.2 Results

Electron tomography was carried out on transverse and en face orientations of Descemet's membrane. Analysis revealed elongated structures in transverse sections, whilst polygonal and elongated structures appeared when en face orientated sections were examined (Figure 4.2) Figure 4.3 displays the structures present in Descemet's membrane with an annotated micrograph highlighting what are believed to be the collagenous and globular regions. The supplementary material attached to this thesis shows ImageJ movies of elongated and pentagonal structures (see CD). Initial analysis used transverse sections of Descemet's membrane where elongated structures with a periodicity of 100 nm were identified. On closer inspection these structures had a weaker intermediate band located centrally between the distinct elongated bands, (Figure 4.4). Globular domains of the same polygonal structure are thought to be responsible for this band, but are likely to be in a different plane.

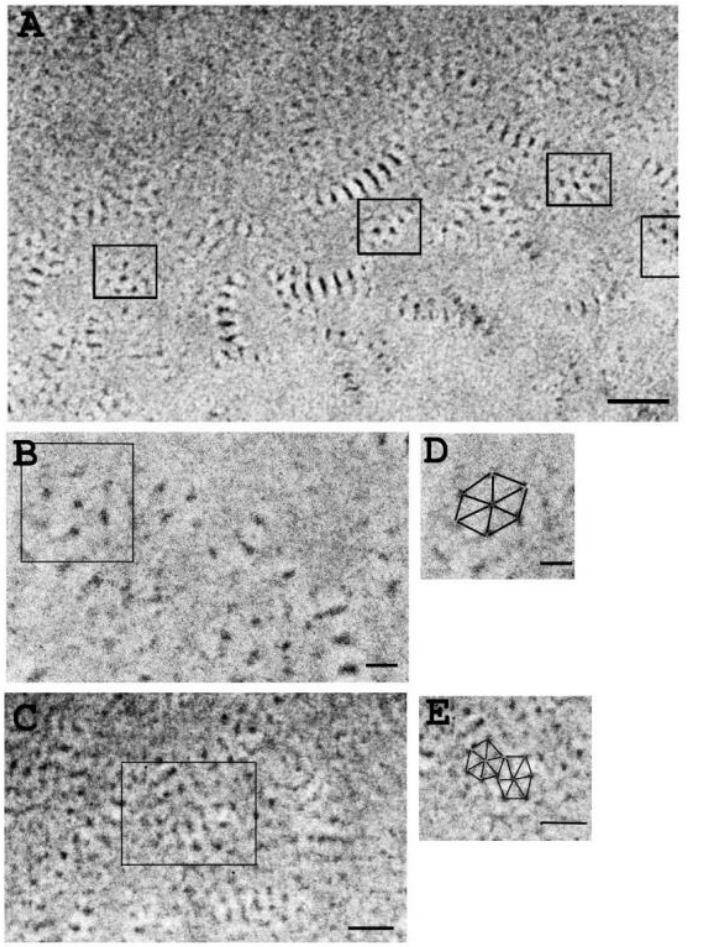

Figure 4.2 En face micrographs of Descemet's membrane. (A) Low mag image of the membrane where polygonal structures have been boxed (scale bar=500 nm). (B)(C) High mag images of polygonal structures (scale bar=100 nm and 500 nm, respectively) where black lines represent collagen in (D) (E) (scale bars=100 nm and 500 nm, respectively).

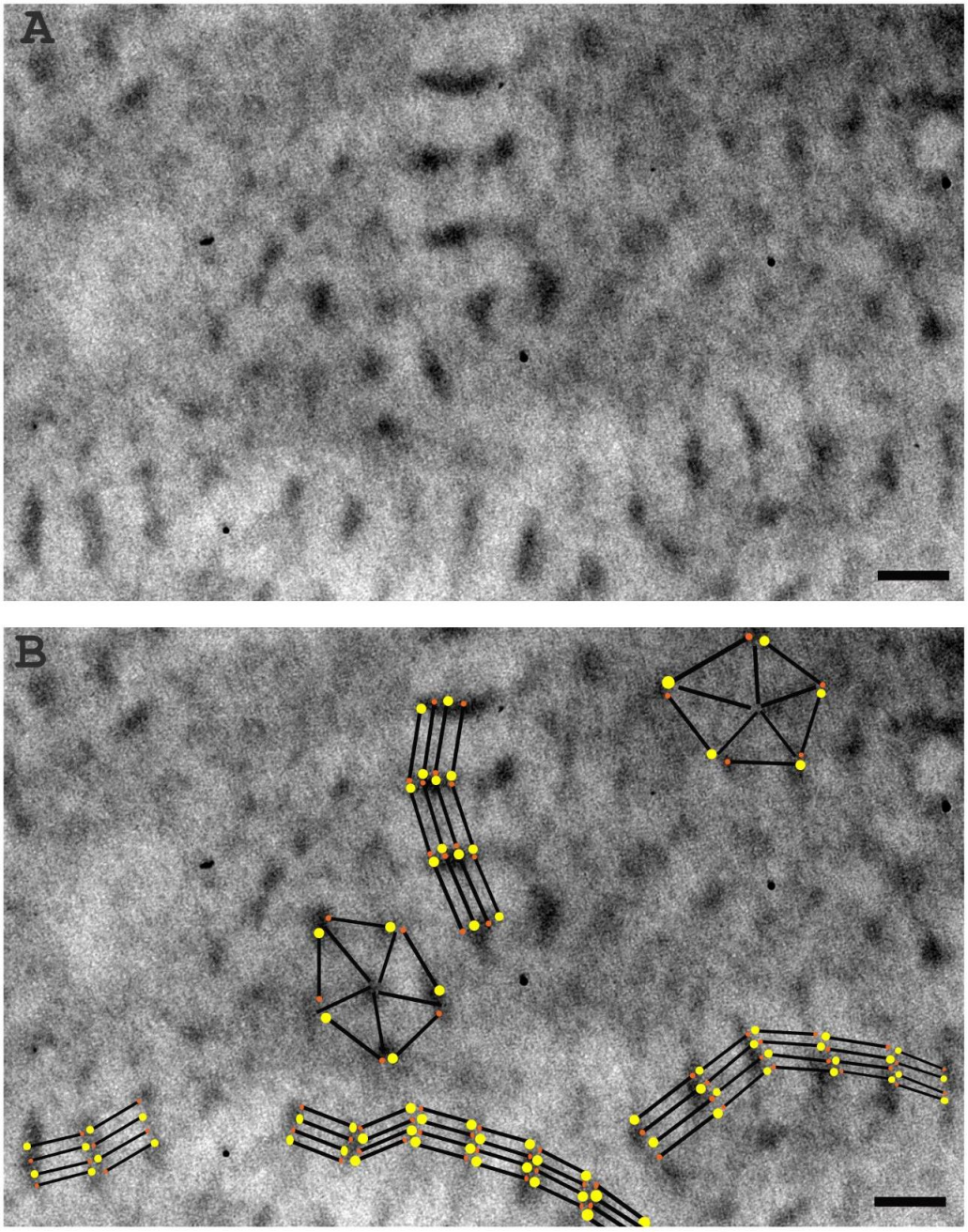

Figure 4.3 The morphology of Descemet's membrane in en face sections. Original (A) and annotated (B) micrographs of the structures observed in Descemet's membrane. Black lines represent the collagenous regions whilst yellow and orange circles signify the globular domains. Scale bar=100 nm.

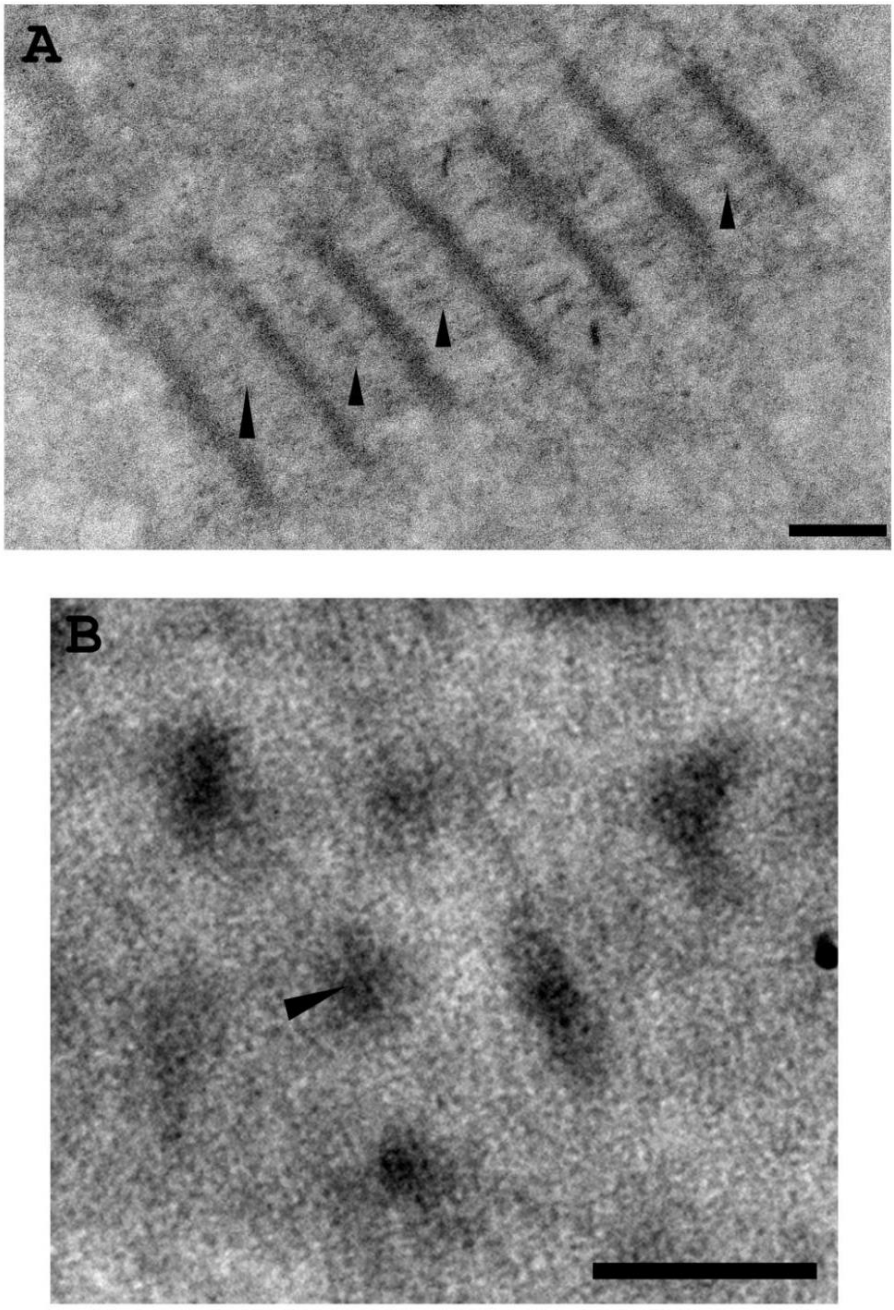

Figure 4.4 Presence of an intermediate band in Descemet's membrane. Elongated structures (A) imaged in transverse sections of Descemet's membrane had less distinct intermediate band (arrowheads). Based on the polygonal formations in en face sections (B) it is likely that the elongated structures observed in the transverse plane are stacked globular domains. This is also true of the less distinct intermediate band, produced from a globular domain in a different plane i.e. central globular domain (arrowhead). Scale bar=100 nm

A three-dimensional reconstruction was used to obtain a more detailed view of Descemet's membrane (Figure 4.5). This allowed a model of Descemet's membrane to be developed (Figure 4.6) which illustrates possible constructs of collagen type VIII.

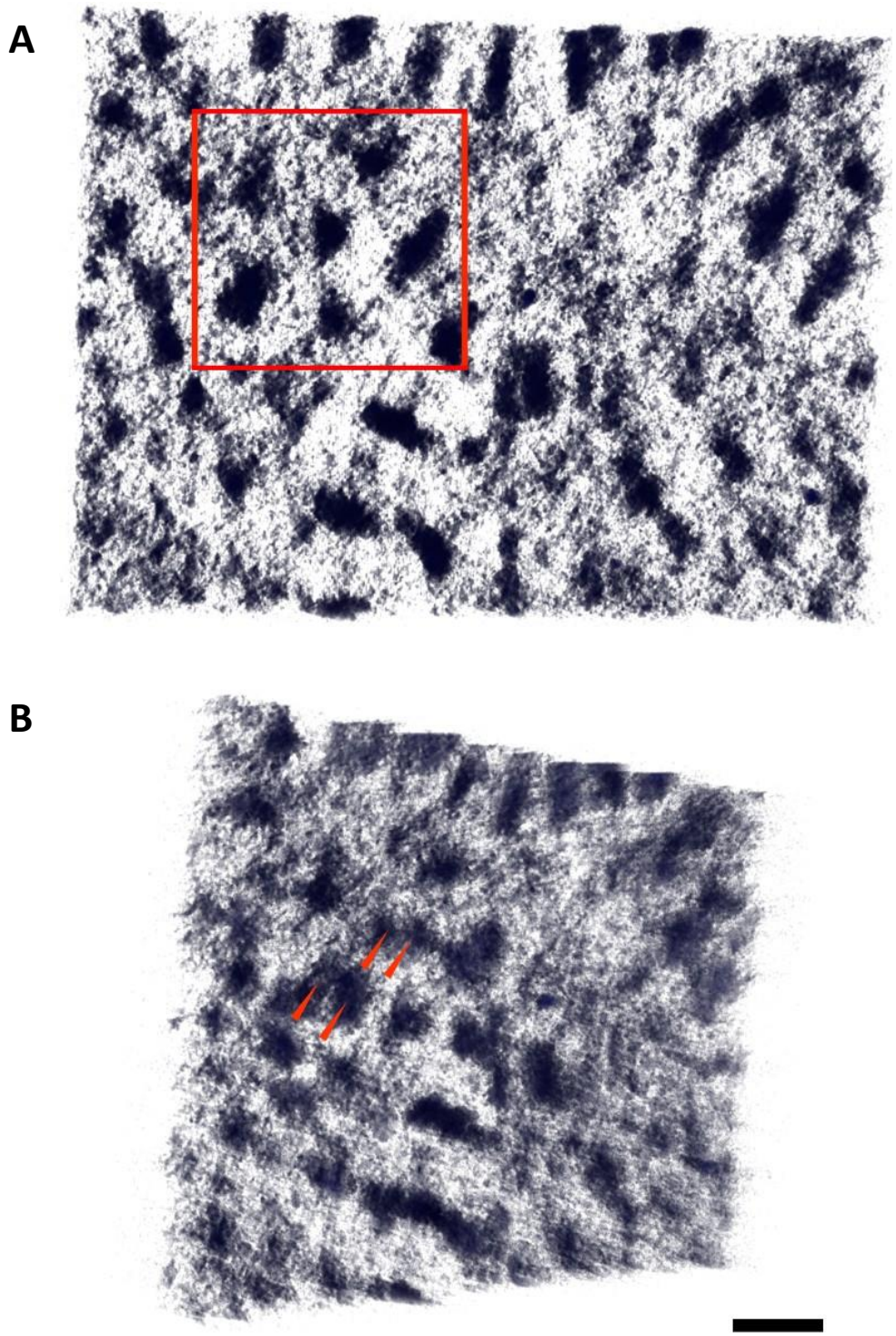

Figure 4.5 Reconstructed images of type VIII collagen arranged in its polygonal lattice in Descemet's membrane. En face sections show the polygonal lattice (squared) in Descemet's membrane (A) and the appearance of the lattice when tilted (B). The arrowheads (B) point to the separate globular domains which are not visible in (A). Scale bar=100 nm.

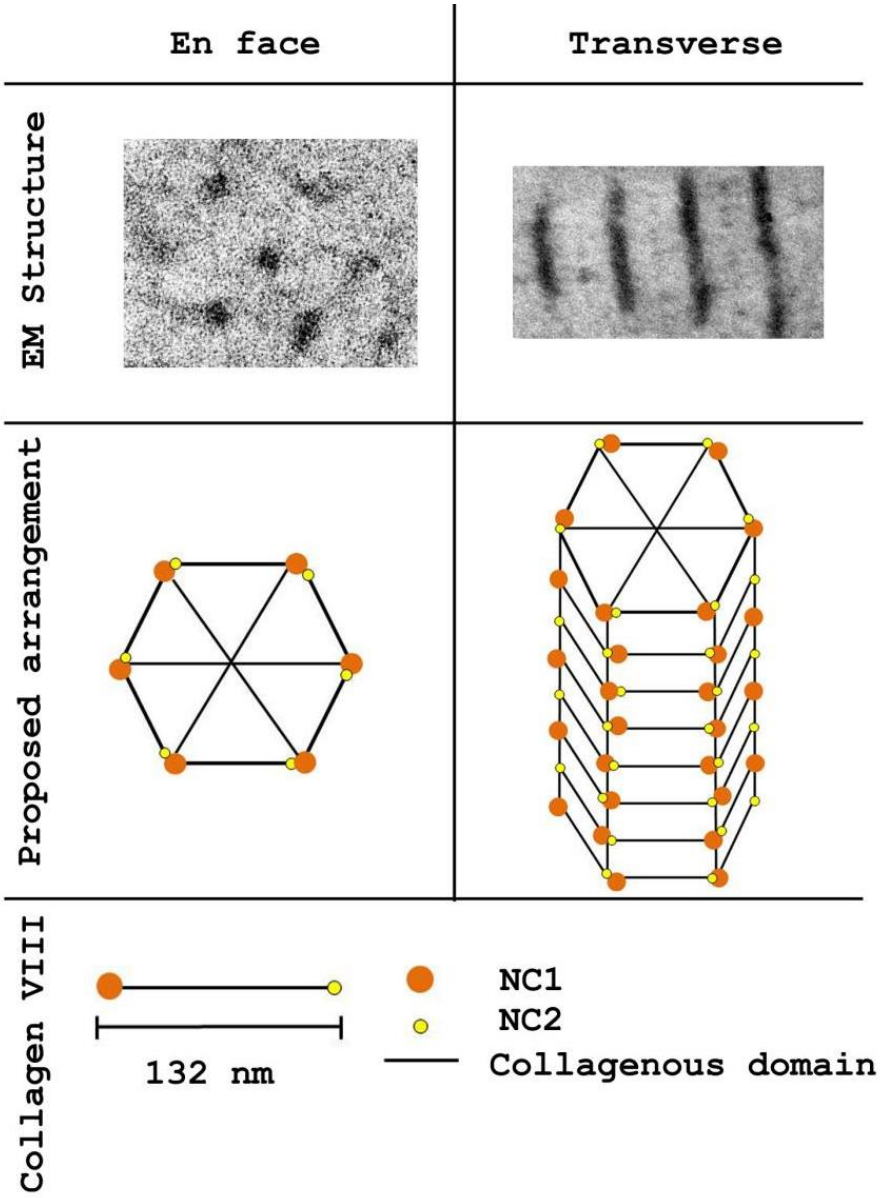

Figure 4.6 Schematic representation of type VIII collagen arrangement in Descemet's membrane. Type VIII collagen forms polygonal lattice structures that lie parallel to the surface of the membrane. The schematic relates the two-dimensional micrographs to the three-dimensional reconstruction of type VIII. Electron micrographs (EM) show polygonal and longitudinal structures viewed in en face and transverse orientation, respectively. Schematic representation of these structures are displayed directly below. The bottom schematic outlines collagen VIII composition. NC1 and NC2 domains (orange and yellow circles) are flanked by a collagenous domain (black).

Cuprolinic blue stained corneas revealed that proteoglycans were present in Descemet's membrane and more specifically the internodal regions of collagen type VIII. A -60˚ to +60˚ single-axis tilt series was captured every two degrees to examine if the proteoglycans interact with type VIII collagen (Figure 4.7).

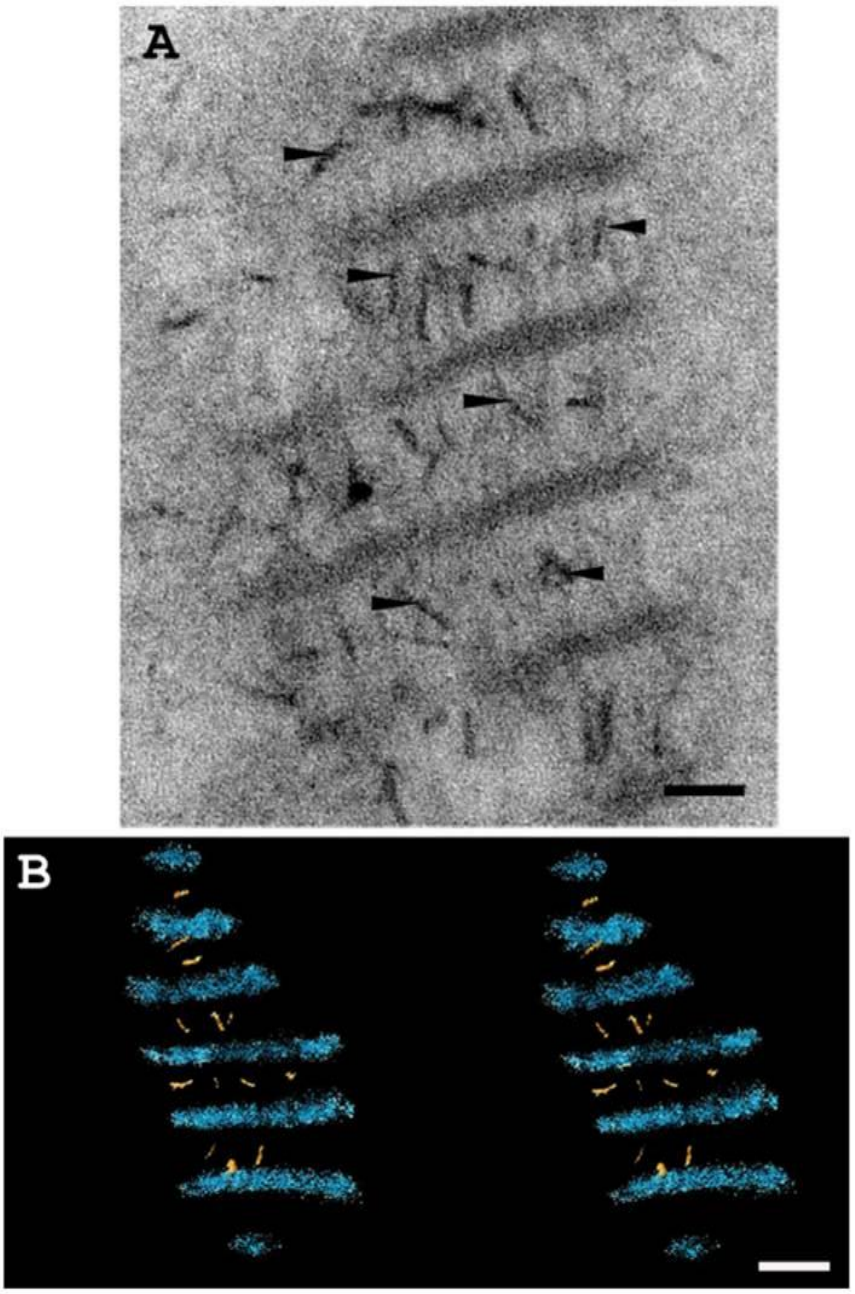

Figure 4.7 Proteoglycans present in Descemet's membrane. A) Cuprolinic blue stained corneas revealed proteoglycans were present in Descemet's membrane and appeared to bind to collagen type VIII. B) Stereo pairs of type VIII collagen in Descemet's membrane. Blue=globular domains, yellow=proteoglycans. Scale bars=50 nm and 100 nm, respectively.

4.1.3 Discussion

Transverse sections observed using electron tomography revealed long-spacing structures present in Descemet's membrane. The structures had a periodicity of 100 nm and therefore were initially assumed to be collagen type VI. However, after re-orientating the block face polygonal formations were observed implying the structure was more likely type VIII collagen, in agreement with previous literature (Sawada et al, 1990; Akimoto et al, 2008). As well as polygonal formations, the long-spacing structures were still visible (Figure 4.2 & 4.3). This suggests that type VIII collagen forms polygonal and linear structures. The proposed model involves a polygonal lattice with a linear component based on three-dimensional analysis with ImageJ (Figure 4.6). When viewed in transverse, globular domains stack perpendicularly to the membrane, but were viewed more frequently lying in parallel to the membrane surface. The elongated structures observed are thought to be components of the polygonal lattice. This was the case in some instances when the samples were tilted. However, other samples remained elongated and no visible lattice formation was observed. The presence of elongated structures would still allow the movement of fluid through the membrane in and out of the stroma whilst assisting in resisting compression. There are various studies who suggest a hexagonal type VIII construct exists in Descemet's membrane. Sawada and colleagues employed antibodies that bound to the nodal regions of both a hexagonal and long spacing linear structures produced by cultured endothelial cells in an immunogold labelling study (Yamaguchi et al, 1989; Sawada et al, 1990). There is also clear evidence that type X collagen, the other non-fibrillar, short chain collagen, forms hexagonal structures within cartilage extracellular matrix (Kwan et al, 1991). Type X and VIII collagen share striking structural similarities at nucleotide and amino acid level implying that their constructs are likely to be similar together with several studies reporting the type VIII hexagonal lattice that exists in Descemet's membrane (Sawada et al, 1984; Kapoor et al, 1988; Sawada et al, 1990).

Occasionally, interbands were present within the elongated transverse forms of the type VIII collagen molecule (Figure 4.4). After imaging en face sections it was concluded that these interbands are probably formed by the central globular domain observed in the polygonal formations. As mentioned previously, stacked globular domains are thought to form the dominant bands, this is likely to be true for the intermediate bands one observes in transverse

sections of Descemet's membrane. However, the less distinct banding is probably due to globular domains not being in the same plane as the distinct bands, hence, a weaker structure. The presence of proteoglycans within Descemet's membrane was also observed. Cuprolinic blue-stained corneas revealed that proteoglycans were distributed throughout the membrane, and in particular in association with type VIII collagen (Figure 4.7). Proteoglycans appeared in the internodal regions of the type VIII collagen in two-dimensional micrographs. Three-dimensional reconstruction confirmed the presence of proteoglycans at the internodal regions suggesting that they are likely to bind to the helical part of type VIII collagen. However, previous studies have speculated that it is the non-collagenous domains (NC1 and NC2 of α1(VIII) collagen) that are most likely to bind negatively charged components of the extracellular matrix due to their high isoelectric point (Rosenblum et al, 1993). The binding of proteoglycans to this collagen, whether to the collagenous or non-collagenous region, may assist in maintaining the arrangement of type VIII in either the polygonal lattice or the linear structures observed via the collagenous regions of the molecule.

These results support previously reported literature on the structure of Descemet's membrane. The three-dimensional reconstruction suggests that there is also a linear arrangement of type VIII collagen within Descemet's membrane. Proteoglycan labelling in Descemet's membrane has been previously reported (Bairaktaris et al, 1998; Davies et al, 1999), however, this is the first data that shows proteoglycans associating with internodal regions of type VIII collagen in Descemet's membrane. This may imply they have a role in maintaining the unique structure of type VIII collagen in membranes such as Descemet's.

4.2 Fuchs' Endothelial Corneal Dystrophy

The posterior corneal endothelium is an important cell layer and its main role is to maintain stromal deturgescence. Disruptions in this cell layer, as a result of endothelial dystrophies, trauma, infection or surgery, result in corneal swelling and consequently vision loss. Fuchs' endothelial corneal dystrophy (FECD) is an inherited progressive disorder that leads to visual disability and is one of the most common indications for penetrating keratoplasty (PK) (Adamis et al, 1993). Symptoms are revealed between the fifth and seventh decade of life in the late-onset form of the disease. These include Descemet's membrane thickening, a decrease in endothelial pump sites and stromal edema (Waring, 1982). A rare early-onset form of FECD arises between the third and fourth decade of life with the progressive development of corneal decompensation similar to that present in late-onset FECD.

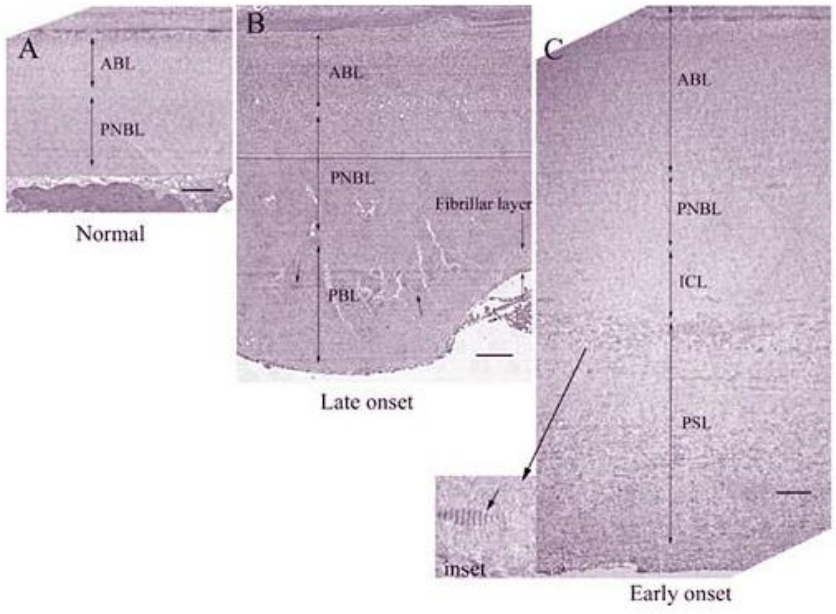

Figure 4.8 TEM of Descemet's membrane in normal and Fuchs' (COL8A2$^{L450W/L450W}$) patients. A) Normal B) Late-onset C) Early-onset Descemet's membrane. ABL-anterior banded layer, PNBL-posterior non-banded layer, PBL-posterior banded layer, ICL-internal collagenous layer PSL-posterior striated layer. (Gottsch et al, 2005).

In late-onset FECD, the anterior banded layer, and posterior non-banded layer are anterior to a pathologic posterior banded layer which is not ordinarily present. Whilst the posterior non-

banded layer is normal in the early-onset mutant, the anterior banded layer is thicker. There is also an internal collagenous layer, and a posterior striated layer (Figure 4.7).

Collagen VIII is a short-chain collagen, highly expressed in normal Descemet's membrane (Kapoor et al, 1988) and its quaternary structure has been elucidated in the first part of this chapter. Recently, a disorganised form of collagen type VIII has been associated with early-onset FECD (Gottsch et al, 2005). In Descemet's membrane, type VIII collagen is a heterotrimer composed of $\alpha1(VIII)_2$ and $\alpha2(VIII)$ (Shuttleworth, 1997). These form stacked polygonal lattice-like structures arranged in parallel to Descemet's membrane surface, thought to be important in resisting compression.

FECD models have recently been developed to investigate the α2 collagen VIII gene (COL8A2) responsible for encoding the α2 chain of type VIII collagen (Biswas et al, 2001; Gottsch et al, 2005). Collagen VIII accumulation in FECD, and the identification of a COL8A2 gene mutation in an early-onset FECD family (Biswas et al, 2001; Gottsch et al, 2005) has highlighted the importance of this collagen in the early-onset form of the disease.

Single amino acid mutations in the COL8A2 gene result in increased collagen VIII accumulation thought to be injurious to the corneal endothelium. Point mutations in the COL8A2 gene give rise to different forms of FECD, these include the $COL8A2^{L450W/L450W}$ (Gottsch et al, 2005) and the $COL8A2^{Q455K/Q455K}$ mutation. A leucine to tryptophan mutation at position 450 (Leu450Trp or L450W) (Gottsch et al, 2005) and a glutamine to lysine at position 455 (Gln455Lys or Q455K) (Biswas et al, 2001) are responsible for altered collagen VIII. The $COL8A2^{L450W/L450W}$ mutation correlates with intra-endothelial cell and extracellular matrix collagen VIII accumulation whilst the mechanism behind the $COL8A2^{Q455K/Q455K}$ form is not yet fully understood (Zhang et al, 2006). Zhang and colleagues found no significant amount of other components, such as fibronectin and collagen IV, within the endothelial cell in early-onset FECD suggesting that they are secreted rapidly whilst collagen type VIII is retained.

FECD advances over decades with a lack of symptoms in the early disease states. As a result, early pathological tissue is unobtainable leaving unanswered questions about the initial pathogenesis of the disease. A number of studies have started looking at the COL8A2 gene

mutations to determine their effects. Recently, a murine, early-onset FECD disease model has been generated with *Col8a2* mutations *(Col8a2*$^{Q455K/Q455K}$ and *Col8a2*$^{L450W/L450W}$) in an attempt to identify if the unfolded protein response (UPR) was activated as previously confirmed in late-onset FECD (Engler et al, 2010). Accumulation of misfolded protein results in endoplasmic reticulum (ER) stress, a feature that is toxic to cells. Activation of the unfolded protein response counteracts this condition by reducing the unfolded protein (Szegezdi et al, 2006). *Col8a2*$^{Q455K/Q455K}$ mutant mice show a 27% endothelial cell decrease at 5 months whereas *Col8a2*$^{L450W/L450W}$ show a 10% reduction in endothelial cell numbers (Jun et al, 2012). These knock-in mutant mice represent the first realistic *in vivo* models for FECD that will allow investigation into the early-onset disease pathogenesis (Jun et al, 2012). The aim of the second part of this chapter was to extend these findings by investigating if the homologous mutations affect the architecture of the corneal extracellular matrix at 5 months of age. Human and mice have similar Descemet's membrane including anterior banded and posterior non-banded zones which makes the mouse model a valuable model when analysing disease.

4.2.1 Methods

4.2.1.1 Col8a2 knock-in mice

The mouse *Col8a2* gene displays 94% amino acid identity to the human COL8A2 gene (protein BLAST, http://blast.ncbi.nlm.nih.gov/Blast.cgi). A targeting vector containing the specific regions of the Col8a2 gene was subcloned into a pBK-CMV vector to generate a gap-repair plasmid. The transformants then had the Q455K substitution (C to A nucleotide) introduced by mutagenesis using specific primers. The vector was verified, embryonic stem cell electroporation and blastocyte injection was performed. Heterozygous were crossed with a Sox2-cre line (Jackson Labs, Bar Harbor, ME) prior to breeding to obtain homozygous WT and MUT genotypes. Generation of the *Col8a2* knock-in mice was carried out in Dr Albert Jun's laboratory (Johns Hopkins University, Baltimore, MD, USA). Corneas from *Col8a2*$^{Q455K/Q455K}$ and *Col8a2*$^{L450W/L450W}$ were examined alongside age/sex-matched homozygous WT littermates to ensure any phenotypes of the mutation occur as a result of mutation and not because of other confounding factors related to genetic background differences. For details please see Jun et al, 2012.

4.2.1.2 TEM

Half corneas from 5-month old wild type and mutant mice, *Col8a2*$^{Q455K/Q455K}$ and *Col8a2*$^{L450W/L450W}$ as published by Jun and colleagues (2012) were prefixed in 4% paraformaldehyde in 1xTris acetate buffer for 10 minutes prior to incubation with glycosaminoglycan (GAG) specific degrading enzymes. Corneas were incubated with i) keratanase ii) chondroitinase ABC or iii) keratanase and chondroitinase ABC for 4 hours to distinguish between keratan sulphate (KS) and chondroitin/dermatan sulphate (CS/DS) proteoglycans. Following enzyme treatment, corneas were rinsed in sodium acetate/0.1M magnesium chloride buffer prior to fixation overnight in 2.5% glutaraldehyde in 25mM sodium acetate buffer (pH 5.7) containing 0.1M $MgCl_2$ and 0.05% Cuprolinic blue. Embedding was then carried out as described in the general methods section. Ultrathin sections of embedded corneal tissue were cut at 100 nm thickness for transmission electron microscopy and collected on uncoated copper grids. Orientation of the tissue was arranged so that peripheral tissue was collected first followed by central cornea. Several sections were collected on multiple girds for each region so micrographs would show accurate representation. A 1% phosphotungstic acid and a saturated uranyl acetate solution were used to stain the grids for 2 and 12 minutes, respectively, prior to examination in an electron microscope (JEOL 1010 transmission electron microscope with Gatan ORIUS SC100 CCD camera). Several grids with sections from peripheral-to-central and anterior-to-posterior cornea were examined for each sample (n=4).

4.2.2 Results

4.2.2.1 Endothelial Examination of Col8a2 Mutant Mice

Specular micrographs taken at 5-months immediately after euthanasia and just prior to excision of the cornea from the eye and its processing for electron microscopy with or without enzyme digestion were used to determine changes in cell shape, size and number. Micrographs revealed darker cells and punctate guttae in both mutants but slightly more so in the *Col8a2*$^{Q455K/Q455K}$ strain (Figure 4.9). Multiple sections of the mutant endothelium were imaged using TEM (Figure 4.10). These showed sparse organelles identified as dilated RER that were not present in wild type mice.

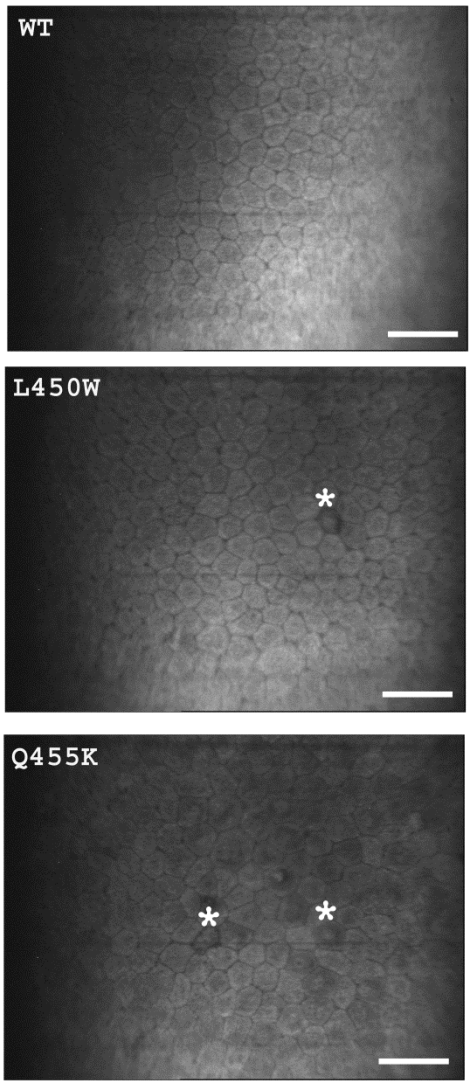

Figure 4.9 Specular micrographs of corneal endothelium. Specular micrographs show punctate guttae and abnormal darkened cells in both mutant strains (*). Scale bar=50 µm. Images taken by Ms Huan Meng.

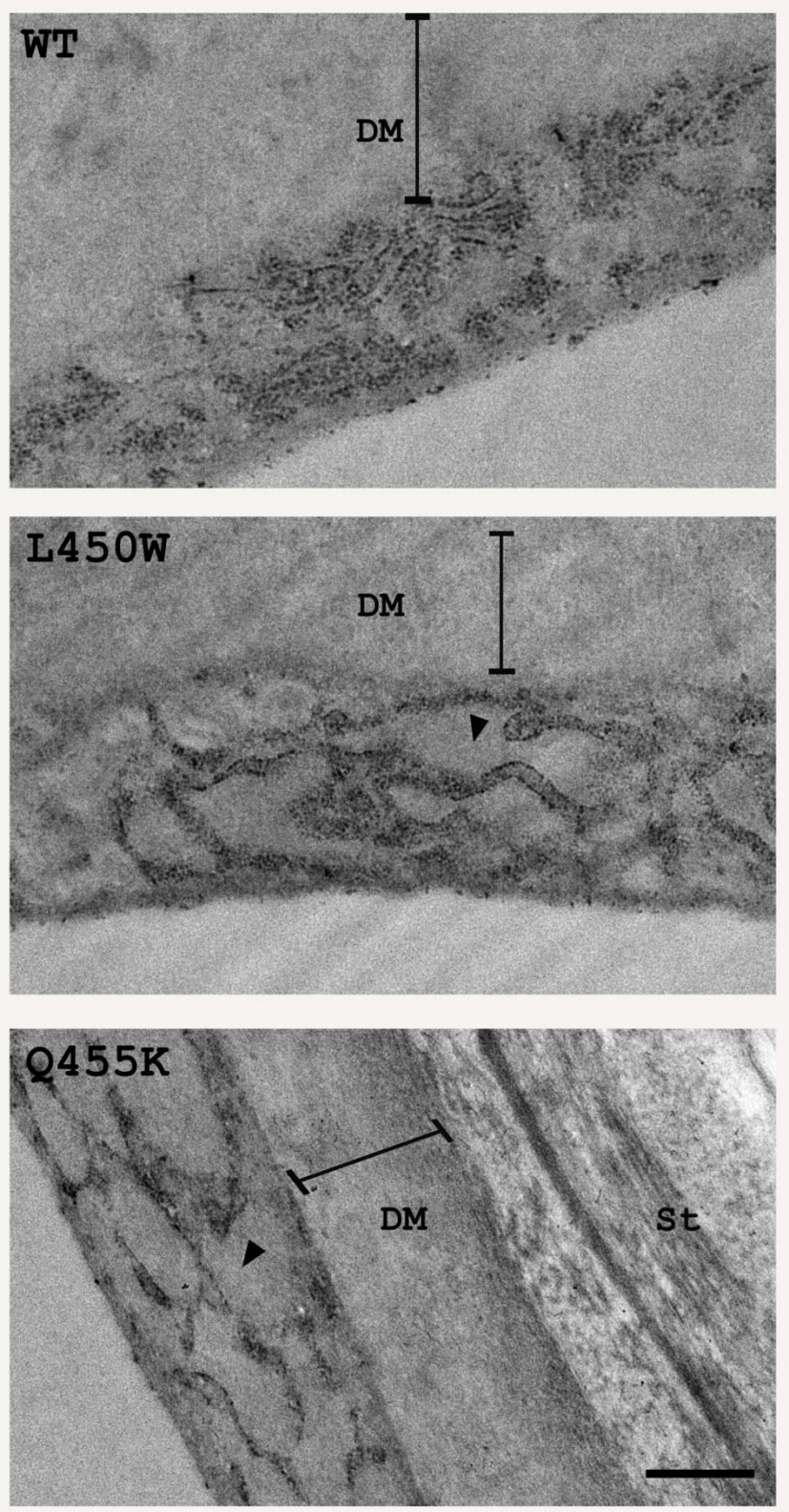

Figure 4.10 TEM of corneal endothelium in wild type and *Col8a2* mutants. Both mutants had dilated RER (arrowhead) present in their endothelial cells when compared to wild type. DM-Descemet's membrane, St-stroma. Scale bar=500 nm.

4.2.2.2 TEM analysis of Col8a2 mutant stroma

Micrographs (Figure 4.11) show the anterior and posterior stroma of the *Col8a2*$^{Q455K/Q455K}$ and *Col8a2*$^{L450W/L450W}$ mutant mouse corneas. No obvious stromal oedema was observed but regions of focal oedema were present in the *Col8a2*$^{Q455K/Q455K}$ mutant. More obvious differences were noted in Descemet's membrane and the endothelial cells.

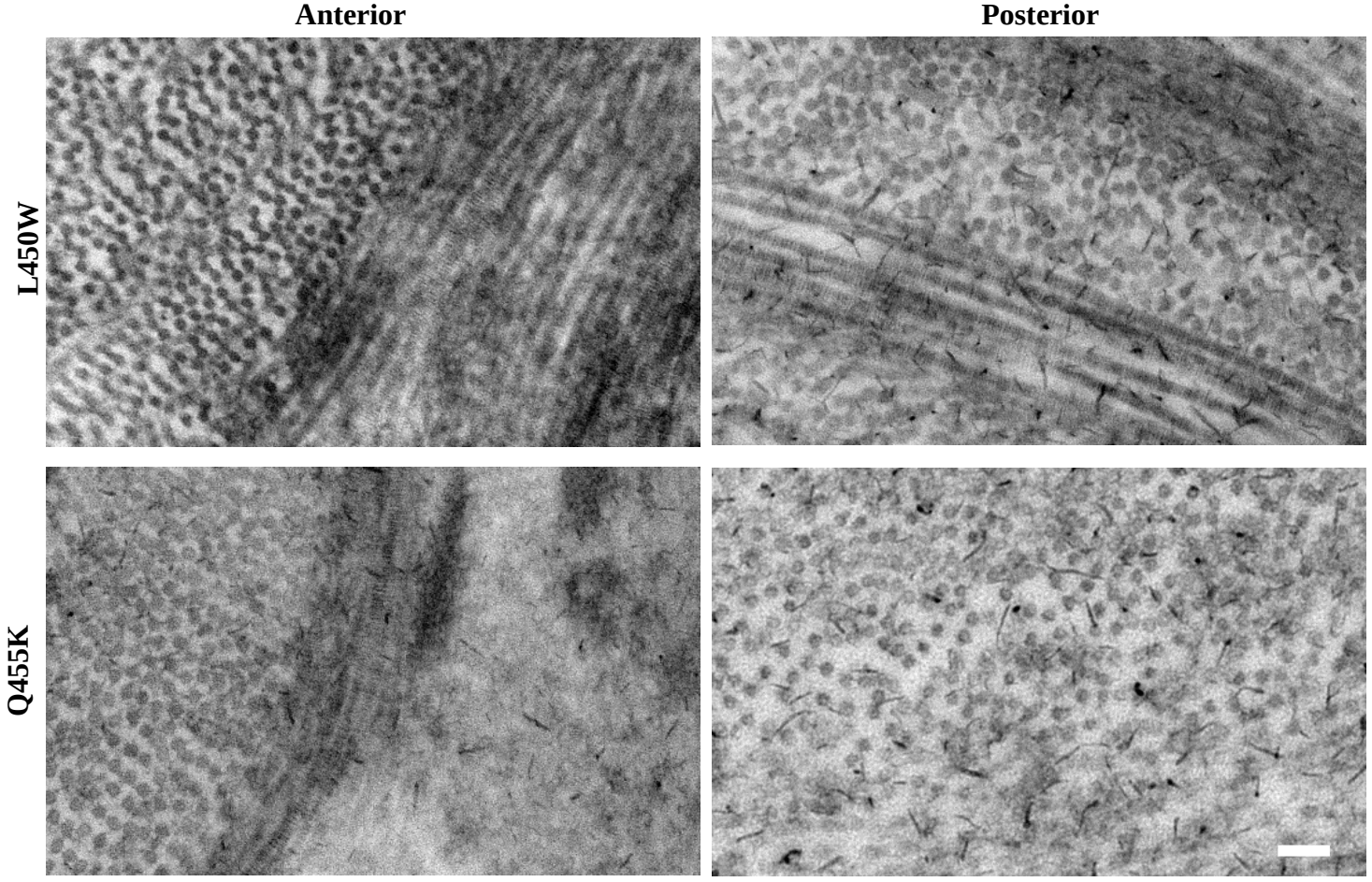

Figure 4.11 TEM micrographs of *Col8a2*$^{L450W/L450W}$ and *Col8a2*$^{Q455K/Q455K}$ homozygous knock-in gene mutant mouse stroma stained with Cuprolinic blue. Focal oedema was observed in the posterior of the *Col8a2*$^{Q455K/Q455K}$ mutant. Micrographs taken from depth of cornea (anterior to posterior). Scale bar=100 nm..

TEM revealed differences in the levels of proteoglycans present in Descemet's membrane and the endothelial monolayer where samples had been stained with Cuprolinic blue. More proteoglycans were noted at the Descemet's endothelial interface in the *Col8a2* mutants compared to wild type samples. The amount of Cuprolinic-blue staining of proteoglycans varied between endothelial cells but was consistently higher in the mutant corneas (Figure 4.12). After observing a higher number of proteoglycans at the Descemet's endothelial interface in the *Col8a2*$^{Q455K/Q455K}$ mutant, the same interface, after enzyme digestion (keratanase and chondroitinase ABC), was examined to determine if the proteoglycans remained (Figure 4.12). This suggested that another proteoglycan, not digested by enzymes employed in these studies, is present at the Descemet's endothelial interface

.

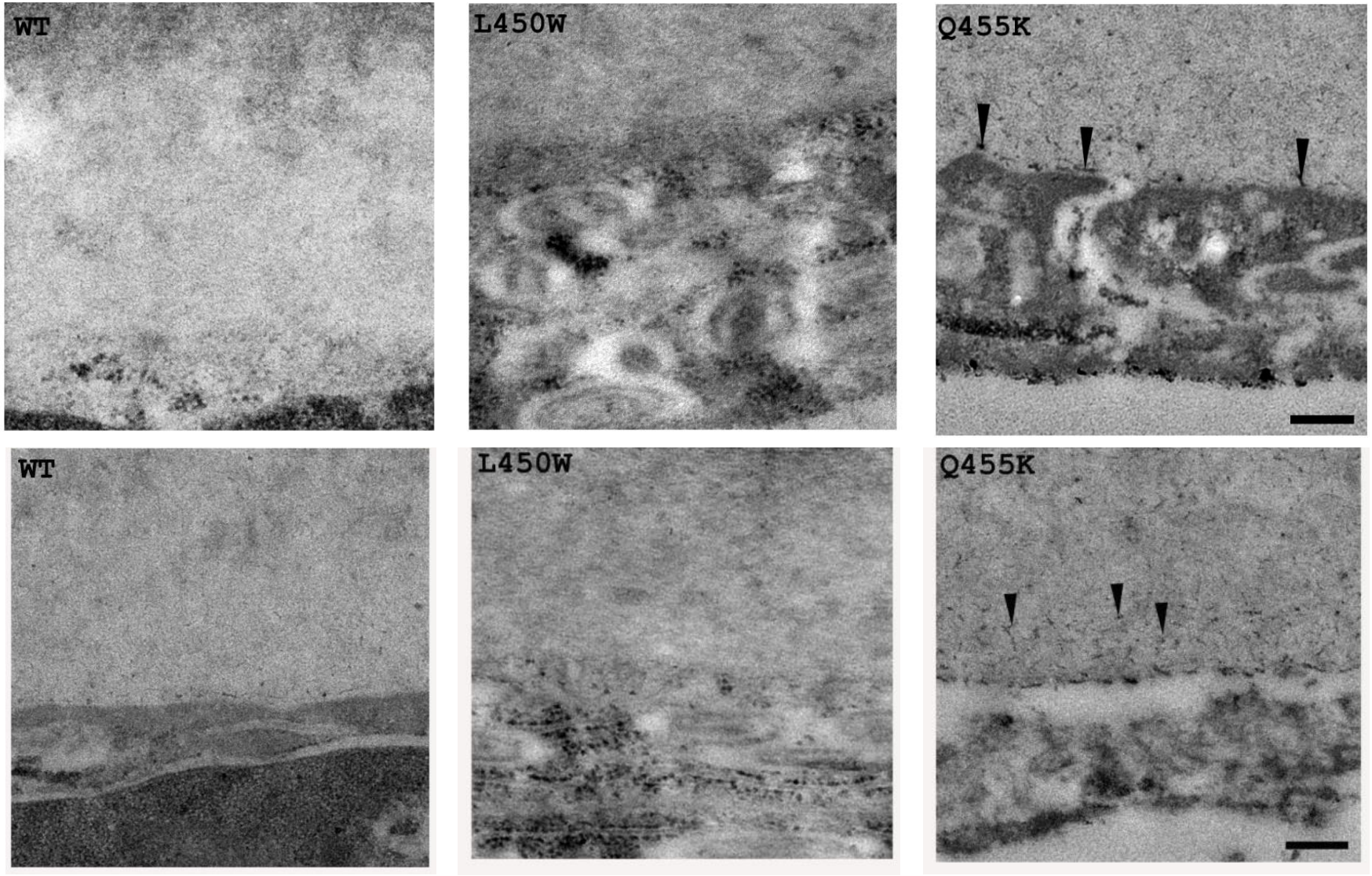

Figure 4.12 Differences in proteoglycan distribution at the Descemet's endothelial interface of wild type and mutant mice. Proteoglycans with (top) and without (bottom) enzyme digestion (keratanase plus chondroitinase ABC) at the Descemet's endothelium interface in wild type (WT), *Col8a2*$^{L450W/L450W}$ (L450W) and *Col8a2*$^{Q455K/Q455K}$ (Q455K). Large amounts of proteoglycans (arrowheads) were observed in the *Col8a2*$^{Q455K/Q455K}$ mutants, compared to wild type. Scale bars =200 nm.

4.2.3 Discussion

Previous mouse models, including a double knock-out *Col8a2* mutant strain, have shown decreased cell density in the endothelial layer, however, this was the only similarity to FECD. No Descemet's membrane thickening or guttae were observed in single or double *Col8a2* knock out mouse models, which are normally seen in the disease (Hopfer et al, 2005). A more recent mouse model showing pathological similarities to those seen in the human form of FECD has now been developed. Results from this model show decreased endothelial cell counts, endothelial cell morphologic changes and Descemet's membrane guttae in their *Col8a2*$^{Q455K/Q455K}$ mutant mouse (Jun et al, 2012). This model may provide a clearer picture into the mechanisms of early-onset FECD. A pathophysiological hypothesis, based on the above mutations, is that the amino acid substitutions decrease the turnover of *Col8a2* leading to an abnormal accumulation of collagen type VIII in Descemet's membrane. Subsequently, this could be a reason for the injurious effects on endothelial cells resulting in apoptosis. This study utilised TEM to determine the effects the *Col8a2* mutations on the corneal stroma, including collagen organisation and proteoglycan distribution, Descemet's membrane and the endothelium.

4.2.3.1 Col8a2 Mutants

Results show TEM of the stroma in both *Col8a2*$^{Q455K/Q455K}$ and *Col8a2*$^{L450W/L450W}$ mutants, whose missense mutations have been associated with the early-onset form of FECD (Biswas et al, 2001). There were no obvious signs of widespread oedema in the stroma, but focal oedematous regions were present in the posterior stroma of the *Col8a2*$^{Q455K/Q455K}$ mutant (Figure 4.13). The relatively young age of the mice is a possible explanation for the lack of widespread oedema, the effects of FECD may not be apparent at this 5-month time point. There are a lack of symptoms in the early stages of FECD despite clinical evidence (guttae, Descemet's membrane thickening) identifying disease onset. This suggests that stromal oedema occurs later on in the disease course when membrane thickening and guttae begin to affect the endothelial cells and consequently stromal hydration. Guttae, thought to cause endothelial degeneration, have been reported at this stage (Jun et al 2012), but these were difficult to locate. Thus, it is likely that the focal posterior oedema is a consequence of the young age of the mice and will possibly increase with time. A study carried out on patients

found that the majority had no or very few guttae, concluding that guttae may be forming but are 're-surfaced' by an increasing secretion of collagen into Descemet's giving the appearance of a uniform surface (Zhang et al, 2006). This may be the case in these mouse samples, a result which could be easily overlooked.

4.2.3.2 The Effect of Col8a2 Mutations on Endothelial Cells.

Jun's studies reported a 27% reduction in endothelial cell count at this 5-month time point (1522±241 versus 2137±155 cells/mm^2, mean ± standard deviation) and a 41% reduction (1240+265 versus 2101+120 cells/mm^2) at 10-month in *Col8a2*$^{Q455K/Q455K}$ versus wild type mice (Jun et al, 2012). It is evident that the mutation affects the endothelial cell count; a 20% reduction is seen between the 5 and 10-month period alone. Nevertheless, it appears that migration and enlargement, a known occurrence in these cells, makes up for the lack of mitosis in response to cell death. This mechanism allows the monolayer to stay confluent with sufficient pump activity down to a cell density of 400-700 cells/mm^2 in man (Bourne and Kaufman, 1976). Therefore, a cell loss of 27%, resulting in a cell density of 1522cells/mm^2, would be adequate for the essential pump mechanism to suffice. More apparent oedema may occur when the cell count is further reduced, perhaps beyond the 10-month stage where the density is still 1240 cells/mm^2 in the *Col8a2*$^{Q455K/Q455K}$ mutant (Jun et al, 2012). Several studies have found an increased pump site density of the Na^+K^+ATPase suggesting that the endothelium is capable of adapting to the decrease in cell number and can upregulate the pumping mechanism (Geroski et al, 1985). Studies determining the effect of guttae on permeability of the endothelium found no change between patients with mild and advanced guttae (Wilson and Bourne, 1988) suggesting that perhaps decreased pump function is responsible for oedematous stroma typically seen in FECD. Further evidence supporting this theory was reported by Zhang (2006) whose study included an individual with no corneal guttae but very few endothelial cells. It may simply be that eventually, even if upregulation of pump sites does occur, there is an insufficient number of cells to maintain stromal deturgescence. In later stages of FECD, when endothelial cells are reduced and Descemet's membrane is thickened, the number of cells will not be sufficient to pump enough fluid through the thicker membrane. Endothelial cell death probably occurs due to the thickened, abnormal Descemet's membrane. A thickened Descemet's membrane would impede the

movement of solutes through the membrane, imposing a damaging amount of stress on the endothelium (Zhang et al, 2006).

Biosynthesis of collagens into their triple helices is undertaken in the RER. The UPR is a system whose role is to reduce misfolded protein accumulation and to restore the correct level of folded protein. If this cannot be completed, UPR-associated apoptosis occurs. The mutant strains, *Col8a2*$^{Q455K/Q455K}$ and *Col8a2*$^{L450W/L450W}$, both had high levels of dilated RER (Figure 4.10). Dilated RER is generally a sign of high protein synthesis and storage, but may also be a sign of UPR. Upregulation of collagen type VIII within the endothelium could result in higher volumes of collagen needing to be assembled within the ER, instigating RER dilation (Jun et al, 2012). Equally, increased abnormal collagen due to the *Col8a2* mutation may give rise to dilated RER, indicative of the UPR. Other studies suggest endothelial cells may be transforming into a fibroblastic type cell, dilated RER and increased ribosome's being one possible indication of this change. Whether or not RER dilation occurs as a result of endothelial cell transformation, abnormal collagen type VIII, its upregulation, or something unforeseen, the mutation is affecting this organelle. One hypothesis is that the amino acid substitutions reduce the turnover of *Col8a2* leading to abnormal accumulation of collagen VIII and subsequently, disruptions in Descemet's membrane. The altered Descemet's membrane will eventually lead to injurious effect on endothelial cells leading to apoptosis.

4.2.3.3 Proteoglycan Labelling

Cuprolinic-blue stained samples were also examined to determine differences in the proteoglycan distribution in the wild type and mutant mice. Noticeable differences in proteoglycan distribution were observed at the Descemet's endothelial interface in the *Col8a2*$^{Q455K/Q455K}$ mutant when compared to wild type. Increased proteoglycans were present at this interface in the mutants compared with wild type, including after enzyme digestion with keratanase and chondroitinase ABC. This result may indicate the remaining proteoglycan is heparan sulphate, a proteoglycan that has been localised to the Descemet's endothelial interface previously (Bairaktaris et al, 1998). Studies have shown that heparan sulphate is increased at the Descemet's endothelial interface in migrating endothelial cells (Davies et al, 1999). This finding may imply individual endothelial cells are migrating, a feature undertaken when cell death occurs to compensate for cell loss in this monolayer

(Svedbergh and Bill, 1972; Laing et al, 1976; Murphy et al, 1984; Landshman et al, 1988). Future work should label heparan sulphate in the cornea to verify this hypothesis. There are limitations with aspects of the analysis as the analysis is primarily observatory which may introduce bias. However, many of the observations made in this study are backed by recent publications with the collaborators. These included activation of the UPR assessed by western blot analysis and real-time PCR, thus, supporting the dilated RER observation in the *Col8a2* mutants as well as other markers including TUNEL signifying apoptosis correlating with specular micrographs (Jun et al 2012, Meng et al, 2013). In conclusion cell death is occurring as a result of the mutation, however, the rate of loss is not high enough at this stage to jeopardise stromal hydration.

Chapter 5: Corneal endothelial cell replacement and regeneration

5.

5.1 Introduction

Human endothelial cells do not proliferate sufficiently *in vivo* and although there are enough to last a lifetime, disease, trauma and infection can result in severely reduced numbers, compromising corneal transparency. Endothelial cells are arrested in the G_1-phase of the cell cycle (Joyce et al, 2002). This is illustrated in various endothelial dystrophies, where the cells do not replicate to replace cell loss, consequently stromal oedema results. FECD, the focus of the previous chapter, is a prominent disease of the corneal endothelium. This chapter addresses the recent advancements in correcting the loss of corneal endothelial cells by replacement and regeneration.

5.1.1 Posterior Corneal Surgery

Until recently almost all endothelial related problems have resulted in corneal transplants involving replacement of the full cornea. Penetrating keratoplasty (PK) has proven very popular and successful in most patients suffering from corneal related vision loss, however, this surgery does carry complications including induced astigmatism and prolonged visual recovery. Numerous other surgeries are now in practice (Table 5.1) including posterior lamellar keratoplasty (PLK), pioneered by Melles (Melles et al, 1998). Benefits include faster recovery, reduced astigmatism and maintenance of globe integrity, overcoming some of the weaknesses existing in PK (Melles et al, 2000; Gorovoy, 2006; Price & Price, 2007). PLK dissects the recipient stroma at 80-90% of its depth also including Descemet's membrane and the endothelial layer before replacing with donor stroma, Descemet's membrane and endothelium via a 9.0mm scleral incision (Melles et al, 1998, 1999; Terry and Ousley, 2001). Recent procedures fold donor tissue so a decreased incision of 5.0mm can be made (Melles et al, 2002). PLK is now referred to as DLEK, the same technique using modified instruments (Terry and Ousley, 2003).

Study	Year	Surgery
Melles et al	1998	PLK/Deep lamellar keratoplasty (DLEK)-manual dissection of recipient stroma (80-90%), Descemet's membrane and endothelium. Replaced with donor stroma, Descemet's and endothelium
Terry and Ousley	2003	DLEK-PLK with modified instruments
Melles et al Terry and Ousley	2002 2005	DLEK with small incision (5.0mm) and self sealing scleral incision
Melles et al	2004	Descemetorhexis-Descemet's stripping, no recipient stroma removed
Price and Price	2005	DSEK-Descemet's stripping before donor insertion
Gorovoy	2006	DSAEK- DSEK procedure using microkeratome
Price and Price Kobayashi et al	2007 2008	nDSAEK- no posterior stripping before donor replacement on host endothelial surface.

Table 5.1 Advancements in posterior corneal surgery over the last decade. Manual dissection and larger incisions originally used in PLK have been replaced by automated dissection and small incisions leading to the development of DSAEK. The nDSAEK procedure evolved from DSAEK, involving the same tissue transplantation but without graft dissection.

5.1.1.1 DSEK/DSAEK

DLEK led to a technique named descemetorhexis involving Descemet's membrane removal from the recipient cornea leaving the stroma fully intact (Melles et al, 2004). This method, later named DSEK (Price and Price, 2005), is quicker and less traumatic than PLK. The use of a microkeratome in this procedure was used to increase precision and smoothness of the graft-host interface (Gorovoy, 2006), a technique now known as DSAEK. DSAEK surgery involves the removal of Descemet's membrane (Melles et al, 2004) and endothelium from the recipient cornea and replacing with donor stroma, Descemet's membrane and endothelium (Price and Price, 2006, Gorovoy, 2006). DSAEK is favoured by many corneal surgeons for correcting endothelial related complications.

5.1.1.2 nDSAEK

nDSAEK uses a similar method to DSAEK (Figure 5.1) but leaves the host cornea fully intact (Kobayashi et al, 2008). It was introduced for the treatment of endothelial dysfunction not associated with guttae. DSAEK surgery will be necessary for diseased endothelial cells,

however, in non-FECD type endothelial dysfunction DSAEK surgery could be replaced by nDSAEK, eliminating the need for Descemet's membrane stripping (Kobayashi et al, 2008). Kobayashi has shown positive results for this surgery with superior visual acuity and little induced astigmatism. It also diminishes the need to remove Descemet's membrane resulting in a simpler procedure. Nevertheless, nDSAEK does carry complications including graft dislocation after surgery (Kobayashi et al, 2008). Questions also remain as to the fate of the sandwiched endothelial cells of the host cornea.

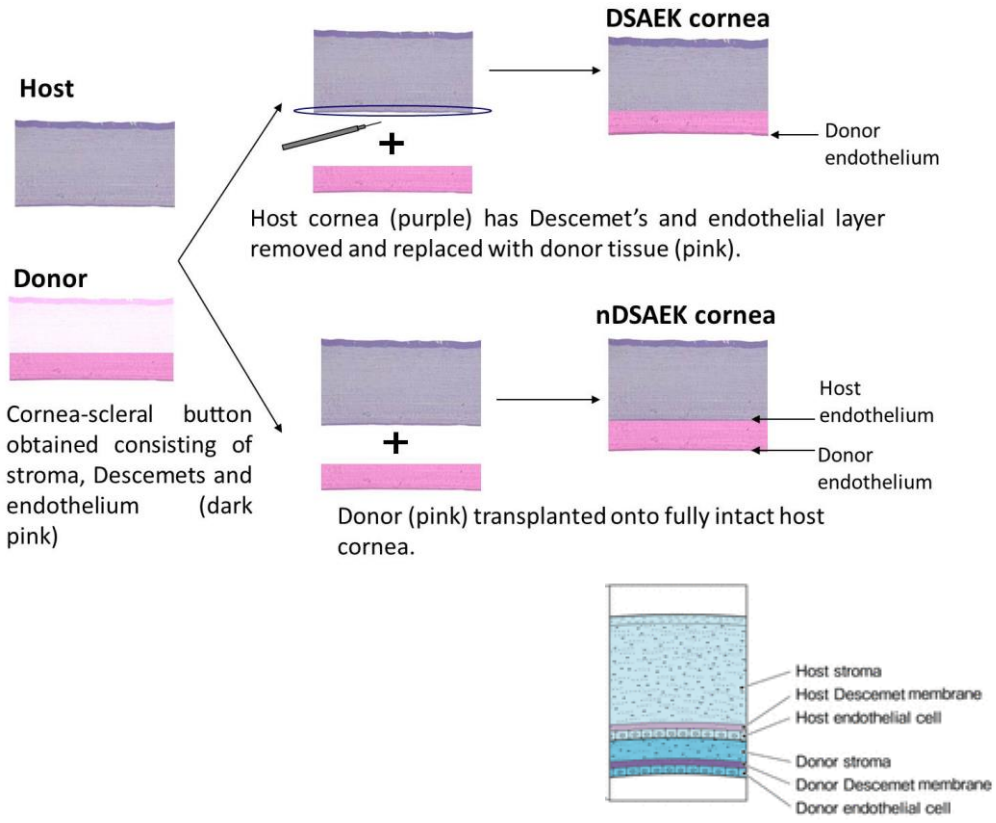

Figure 5.1 Methods used in DSAEK and nDSAEK surgery. DSAEK surgery-Descemet's membrane stripped from host. Posterior donor cornea trimmed (posterior stroma, Descemet's membrane and endothelium). Posterior donor cornea transplanted onto posterior host cornea resulting in DSAEK cornea. **nDSAEK surgery**-Posterior donor cornea transplanted onto posterior surface of full host cornea to achieve nDSAEK cornea. nDSAEK cornea represented in inset schematic (adapted from Masaki et al, 2012).

5.1.2 Rho-Associated Kinase Inhibitors

As well as corneal surgery there are now studies investigating implantation of cultured endothelial sheets, overcoming the problem of donor tissue shortage (Ishino et al, 2004; Koizumi et al, 2007). These studies have reported promising results for this technique,

including typical endothelial morphology and function. The addition of pharmacological agents has also meant that the proliferative ability of the cells can be increased (Koizumi et al, 2007).

A new, non-surgical treatment is now under investigation whose application is based on the Rho-Rho kinase pathway. The Rho family of guanosine triphosphatases (GTPases), including Rho, Rac, and Cdc42, control many intracellular processes and cytoskeleton functions. Rho was first described in the early 1990s as a new member of the Ras family responsible for the assembly of contractile actin-myosin filaments in Swiss 3T3 fibroblasts (Ridley and Hall, 1992). GDP-Rho (inactive) is converted to GTP-Rho (active) by extracellular signals, effectively acting as a molecular switch to control signal transduction pathways. Recently, many Rho effector molecules have been identified including Rho-associated kinase (ROCK). ROCK belongs to the serine/threonine family of kinases consisting of an amino terminal domain, a central coiled region, and a carboxyl terminus. It is involved in the cytoskeleton function, actin-myosin mediated contraction, cell cycle progression and apoptosis. For example, ROCK can phosphorylate the myosin light chain (MLC) and inactivate myosin phosphatase; this enables it to regulate MLC phosphorylation, responsible for smooth muscle contraction (Amano et al, 1996). The amino terminus hosts the kinase, whilst the carboxyl terminus consists of the Rho-binding domain and a pleckstrin homology (PH) domain (Figure 5.2). ROCK is retained in its inactive state by an autoinhibitory loop whereby the PH and Rho binding domain bind to the amino terminal. Activated Rho can bind to the Rho-binding domain of ROCK which allows an open conformation of the kinase, thus, activating the kinase activity of ROCK. From here, ROCK can increase contraction, migration and proliferation.

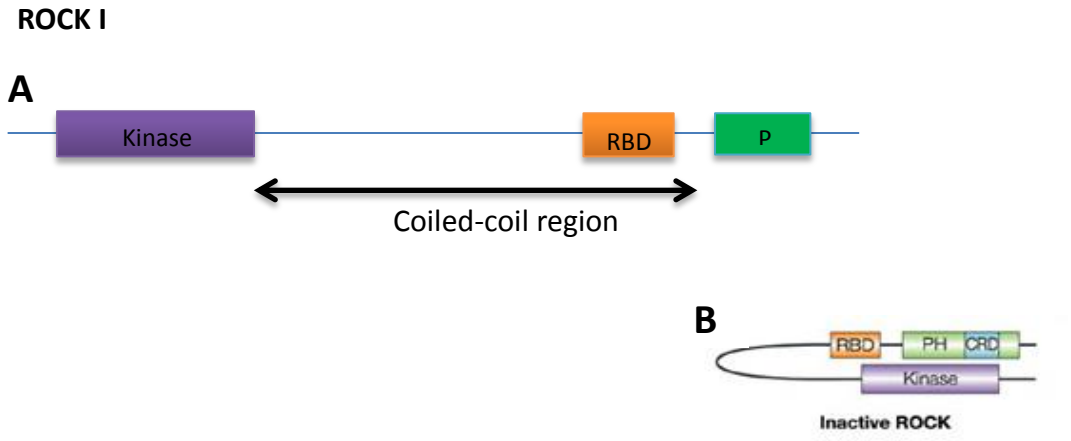

Figure 5.2 ROCK I. A) ROCK is composed of an amino terminus, coiled-coil region and a carboxyl terminus. B) Autoinhibitory loop formed to inactivate ROCK. RBD-Rho-binding domain, PH-Pleckstrin homology.

Rho GTPases are known to play an important role in cell cycle progression. There have been numerous studies reporting that Rho inactivation results in blockade of the G_1-S phase progression. This blockade of progression has been reported in Swiss 3T3 fibroblasts (Olson et al, 1995) together with blockade of cell cycle proteins in the hearts of cardiomyocytes (Zhao and Rivkees, 2003). ROCK inhibition is thought to decrease certain cyclins and cyclin dependent kinases which are important in the cell cycle, hence, their ability to cause disruption in cell cycle progression. However, a recent study has found the opposite, reporting that inhibition of ROCK promotes proliferation and cell migration whilst decreasing apoptosis in monkey corneal endothelial cells (MCECs) (Okumura et al, 2009). Anti-apoptotic effects have been reported not only in MCECs but also in studies in spinal cord injury (Dubreuil et al, 2003) and dissociated human embryonic stem cells (Wantanabe et al, 2007). Y-27632 is widely used as a specific ROCK inhibitor (Uehata et al, 1997) able to compete with ATP for binding to the kinases. Reported findings could have a huge impact on the regeneration of corneal endothelial cells which have been depleted in surgery, trauma, and endotheliopathies. It would also be beneficial in corneal transplatation, preserving endothelial cells during transport of tissue for surgery.

The main aims of this study were to better understand the effects of

i) posterior corneal surgery and the changes that occur to the endothelial cells within the cornea
ii) ROCK inhibitor, Y-27632, on endothelial cells.

5.2 Material and Methods

5.2.1 Posterior Corneal Surgery

Tissue used in this study was obtained from Dr Hiroki Hatanaka (Kyoto Prefectural University of Medicine, Kyoto, Japan) who performed the experimental nDSAEK surgery. Eyes were allowed to heal for two weeks post-surgery before being studied (n=3).

5.2.1.1 Graft Tissue Preparation

Donor lenticules from Japanese white rabbits (female, 2-3kg body weight, Shimizu Laboratory Supplies Co., Ltd, Kyoto, Japan) were obtained after death by injection with pentobarbital sodium. Corneo-scleral buttons, 100-200µm thick, 8.0mm in diameter, were dissected manually before unilateral transplantation into the graft tissue. Recipient rabbits were anesthetised (ketamine hydrochloride, xylazine and tropical oxybuprocaine) prior to the surgery using the procedure carried out by Price (Price and Price, 2005).

5.2.1.2 DSAEK/nDSAEK

DSAEK surgery involved the creation of a 3.0mm limbal-corneal incision prior to Descemet's membrane stripping of an area measuring 9.0mm in diameter. The graft tissue was inserted into a Busin glide (endothelium facing anterior chamber) before being pulled into place with forceps. An air bubble was used to aid graft to recipient attachment before stitching the incision. Descemet's membrane was not scraped in nDSAEK surgery (see Hatanaka et al 2012 for full details). Several ultra-thin sections from limbus, central and peripheral regions of the cornea were collected on each grid and examined to determine key alterations in the tissue n=3.

5.2.2 Rho-Associated Kinase Inhibitor

A pair of corneas from the same human donor were obtained, one stored in Optisol, the other stored in Optisol with ROCK inhibitor, Y-27632. TEM was used to examine the effect of Y-27632 on the morphology of the treated and untreated endothelial cells. The second part of the study involved TEM examination of rabbit corneas injected with differing endothelial cell densities prior to treatment with Y-27632 to determine the appropriate density required for complete monolayer regeneration.

5.2.2.1 Corneal Storage with ROCK Inhibitor

Human corneas stored in Optisol with ROCK inhibitor, Y-27632 (10µm), had specific inclusion and exclusion criteria to ensure any differences observed were related to the ROCK inhibitor. These included:

- A pair of corneas from the same individual
- No endothelial disease or severe epithelial damage
- No less than 2000cells/mm^2 of endothelial cells
- No more than 12 hours between death and preservation in Optisol
- No more than 300cells/mm^2 difference between left and right cornea.

One cornea was placed into Optisol (n=4), the other into Optisol with Y-27632 (n=4) before being processed for TEM. Microscopy was carried out to determine differences between control and ROCK inhibited endothelial cells. Several sections were cut for each sample in different regions of the block to ensure all areas were analysed.

5.2.2.2 Endothelial Cell Injection with Y-27632 in vivo

The second part of the study injected different concentrations of rabbit endothelial cells ($2x10^5$, $5x10^5$ and $1x10^6$ cells) into rabbit cornea *in vivo* to find the number of cells required for monolayer assembly with Y-27632 (10µm).

5.2.3 TEM

Tissue was fixed for 3 hours in 2.5% glutaraldehyde and 2% paraformaldehyde in appropriate buffers for 2-3 hours. TEM processing was carried out as described in the general methods. Semi (500 nm) and ultra-thin (100 nm) sections were cut and collected on glass slides or uncoated copper grids, respectively, prior to staining with uranyl acetate and Reynolds lead citrate for 12 and 5 min, respectively. Toluidine blue (1%) was used to stain semi-thin sections used for light microscopy.

5.3 Results

5.3.1 Posterior Corneal Surgery

5.3.1.1 Low Magnification Graft-Host Interface

Figure 5.3 shows light micrographs of DSAEK and nDSAEK corneas two weeks after surgery. The boundary between the donor and host tissue can be seen in both micrographs, these are shown by black arrowheads. The interface is less predominant in DSAEK surgery as there is a stroma-stroma interface as opposed to a stroma-endothelium interface in nDSAEK. The interface stands out as a result of the host endothelial cells and Descemet's membrane positioned in the posterior third of the nDSAEK cornea. One thing that is common in both micrographs is the good adherence in both surgeries. There does not appear to be any dissociation between the two tissues.

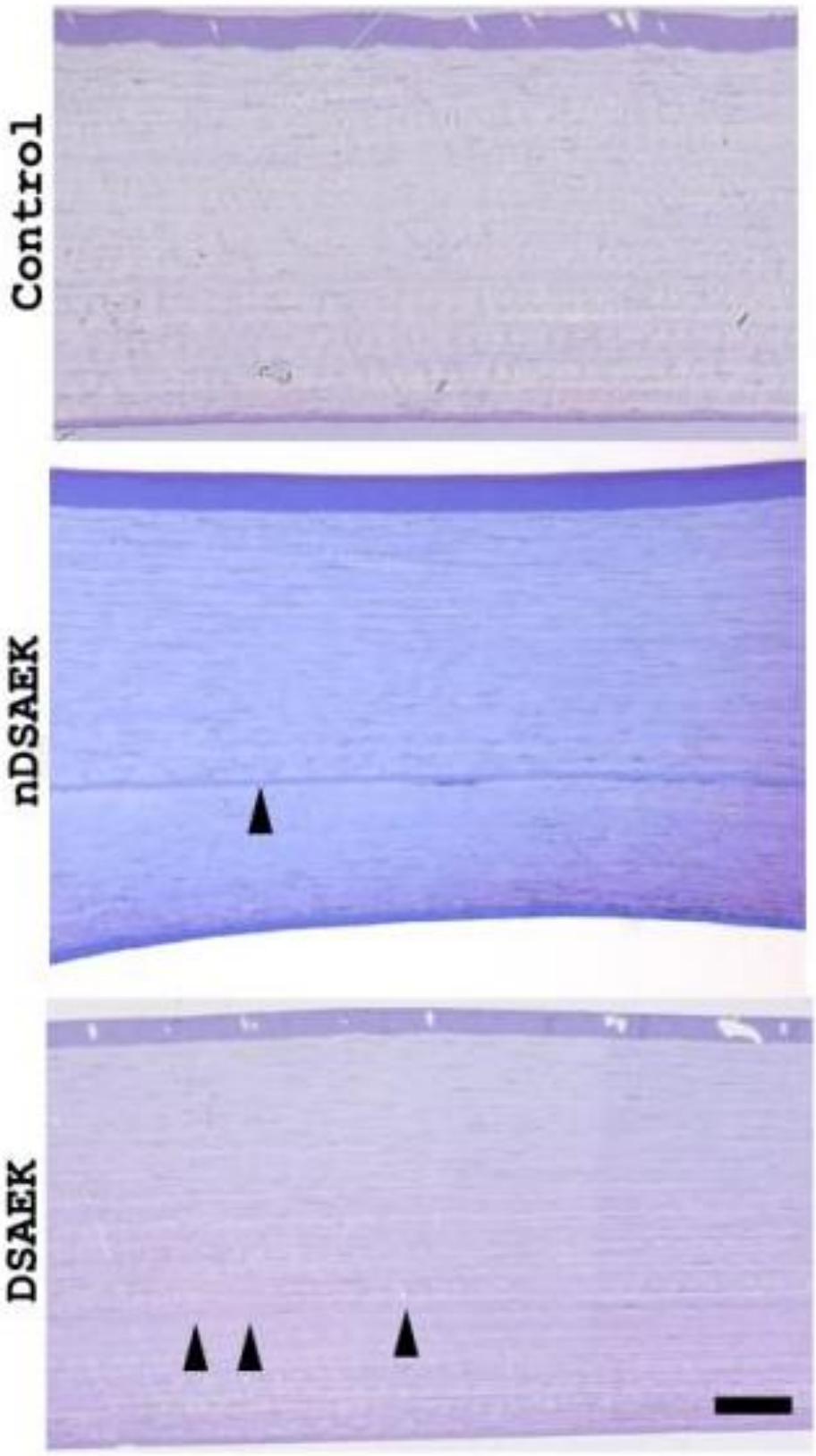

Figure 5.3 Toluidine blue (1%) stained light micrographs taken from resin embedded semi-thin sections of control, nDSAEK and DSAEK corneas 14 days post-surgery. Graft-host interface is indicated by arrowheads in nDSAEK and DSAEK. Clear retention of Descemet's membrane is observed in nDSAEK cornea, sandwiched between host and graft stroma. Scale bar= 50 μm.

5.3.1.2 TEM

Figure 5.4 shows TEM images of the endothelial cells on the posterior of the cornea in control, nDSAEK and DSAEK rabbit tissue. Cell morphology of nDSAEK and DSAEK tissue was comparable to control.

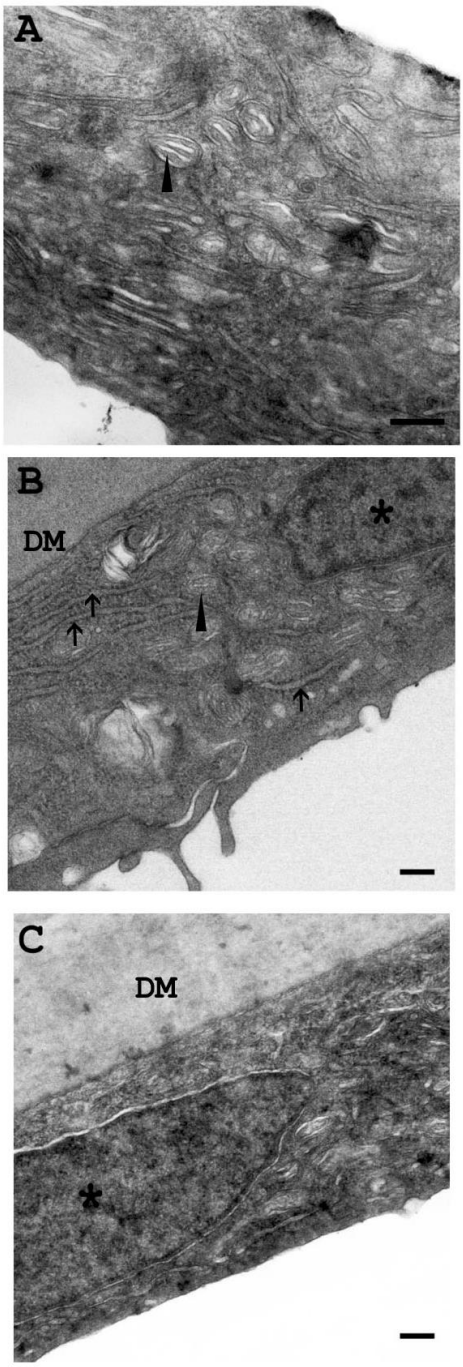

Figure 5.4 Transmission electron micrographs of posterior endothelial cell layer. (A) Control (B) nDSAEK (C) DSAEK. Organelles are highlighted, mitochondria (arrowheads), nucleus (*), rough endoplasmic reticulum (arrows), DM-Descemet's membrane. Scale bars=200 nm.

TEM examination of nDSAEK and DSAEK corneas revealed very different interfaces. This was primarily due to the sandwiched host endothelial cells present in the nDSAEK cornea compared to a stroma-stroma interface in DSAEK tissue.

Micrographs from the nDSAEK cornea indicate the host endothelial layer becomes incomplete two weeks post-surgery (Figure 5.5). The cells appear to degenerate at various points in the monolayer leaving gaps which are only visible by TEM. A fibrous material appears between these cells, although it is uncertain what this material is, a possible source may be the host endothelial cells. We speculate that the fibrotic-like tissue represents the early stages of cellular transformation. Duplication of a basement membrane on the host endothelial posterior surface was the final feature of this tissue. This resulted in cells having a membrane on both its apical and basal surface.

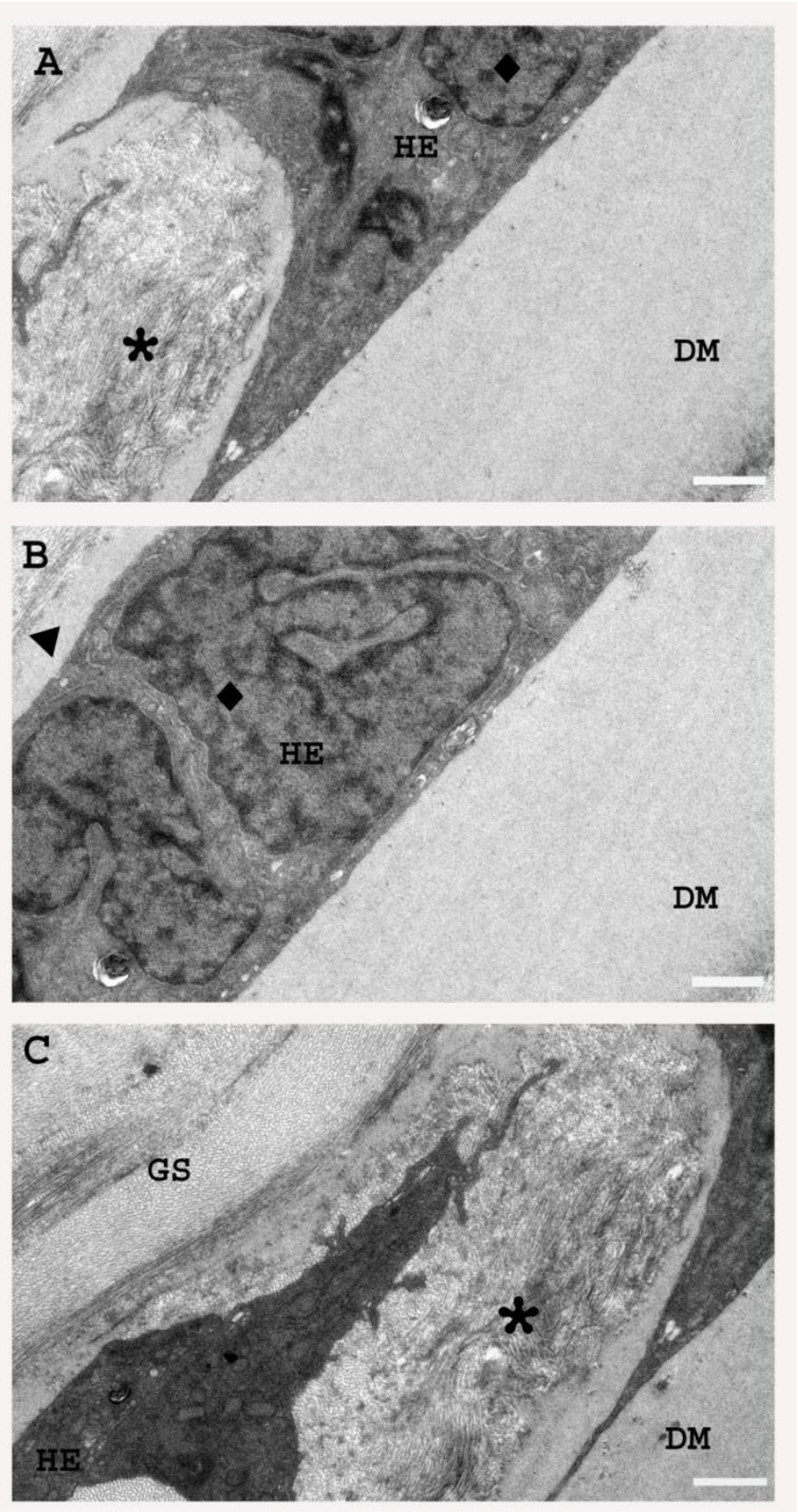

Figure 5.5 TEM micrographs from nDSAEK tissue two weeks post-surgery. (A) Fibrotic material between host endothelial cells (*). (B) Duplication of Descemet's membrane (arrowhead). (C) Incomplete host endothelium and fibrous tissue (*) between endothelial cells and Descemet's membrane. HE-host endothelium, DM-Descemet's membrane, GS-graft stroma, ◊-nucleus. Scale bars=1 µm.

Although the interface in DSAEK tissue was less distinct in the light micrographs it was still present. The interface was located due to the presence of a thin layer of fibrous-like material in the posterior third of the cornea (Figure 5.6).

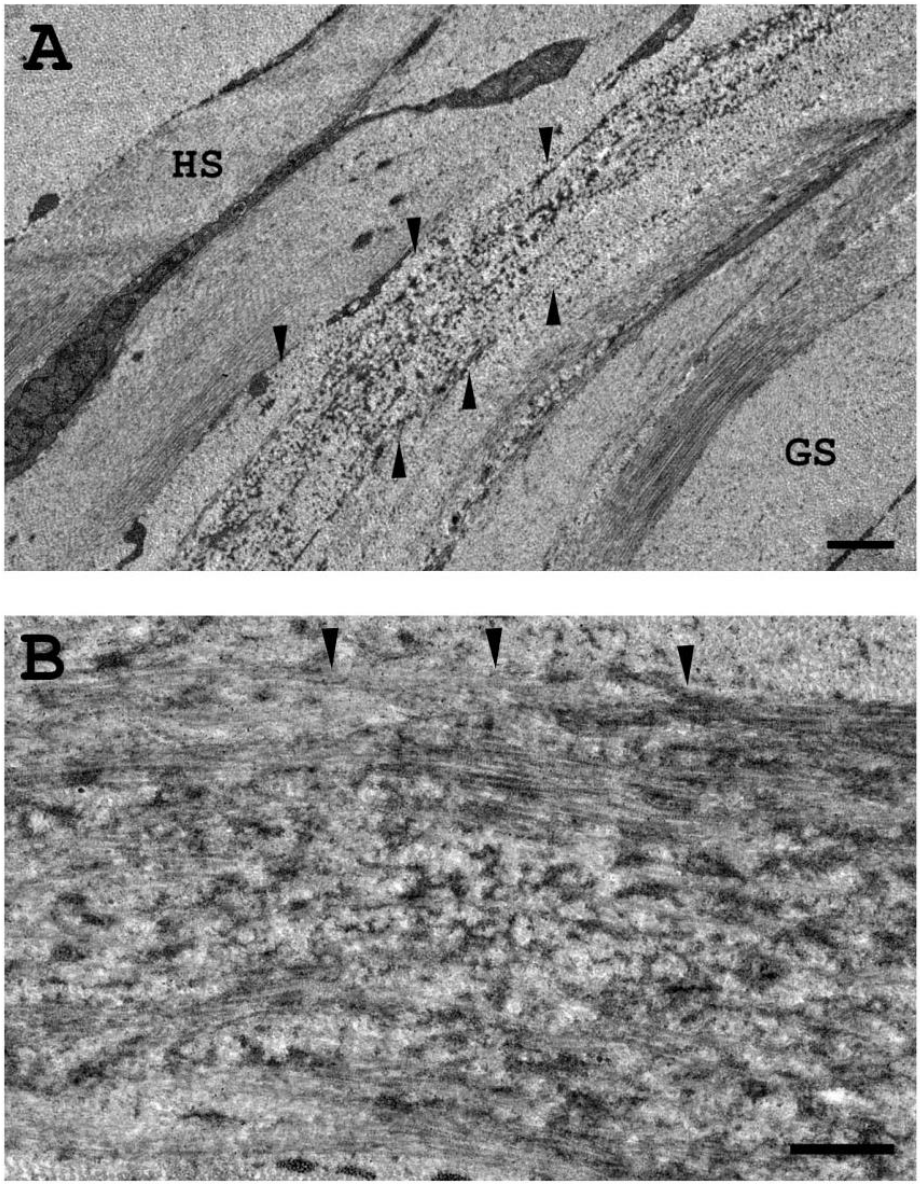

Figure 5.6 Micrographs of the DSAEK interface. Scar/fibrotic tissue (arrowheads) is clearly visible between host (HS) and graft (GS) stroma (A). This region was imaged at higher magnifications (B) showing disorganised tissue noticeably different from typical stroma. Scale bars=1 µm.

5.3.2 ROCK Inhibitor (Y-27632)

5.3.2.1 Human Corneal Storage with Y-27632

Both peripheral and central regions of endothelium in human corneas were examined in control and Y-27632 treated tissue to determine the effects of the ROCK inhibitor (n=4). No obvious differences were observed between the groups, both layers looked healthy and organelles appeared unchanged (Figure 5.7).

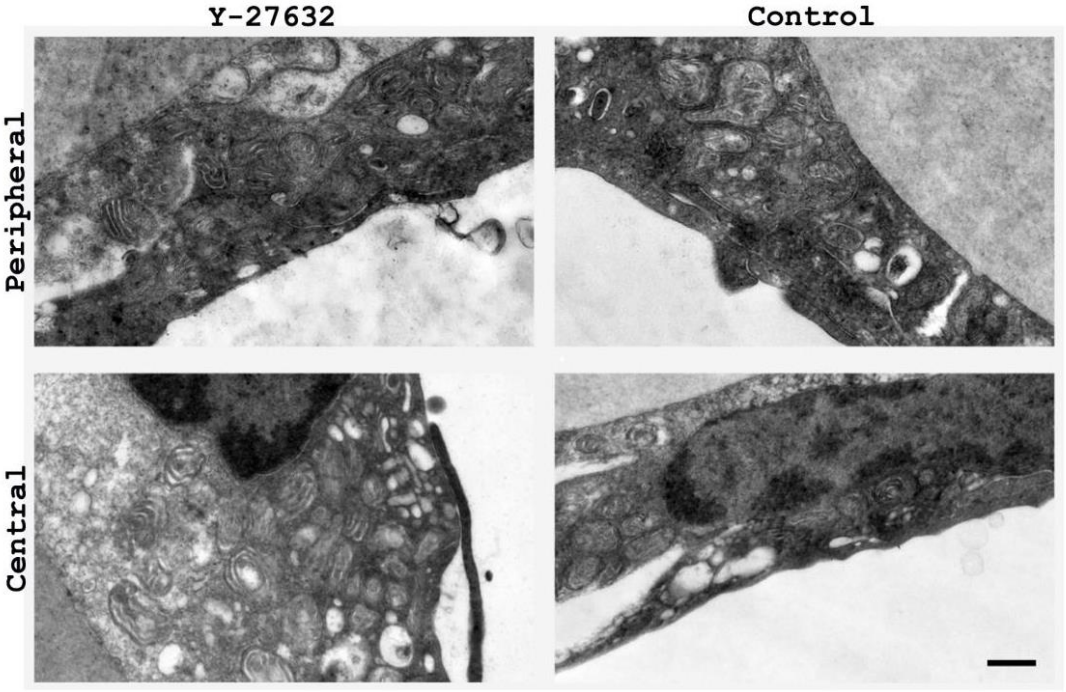

Figure 5.7 Y-27632 treated and un-treated peripheral and central endothelial cells. Morphology of the endothelial cells were comparable to control cornea. Scale bar=0.5 µm

5.3.2.2 Endothelial Cell Injection with Y-27632

Three different densities of endothelial cells were injected into rabbits with removed endothelium to determine the number of cells required to reproduce the monolayer with Y-27632. Cell numbers were calculated to determine a density of $5.0x10^5$ cells was required for monolayer regeneration (Research Center for Regenerative Medicine, Doshisha University, Kyoto, Japan). TEM was carried out to examine individual endothelial cells at each of the cell injection densities ($2.0x10^5$, $5.0x10^5$ and $1.0x10^6$ cells). Figure 5.8 shows micrographs of the stroma and endothelium of injected rabbit corneas. The lowest density of injected endothelial cells had an oedematous stroma anterior to a thinned endothelial cell monolayer. The stroma of corneas injected with $5.0x10^5$ and $1.0x10^6$ cells appeared normal with

regularly arranged fibrils within the stroma and a healthy endothelial monolayer. TEM analysis confirms that an injection of $5.0x10^5$ cells appears to be adequate for endothelial monolayer renewal whereas the introduction of $2.0x10^5$ cells results in areas of oedema within the stroma possibly due to insufficient endothelial cells.

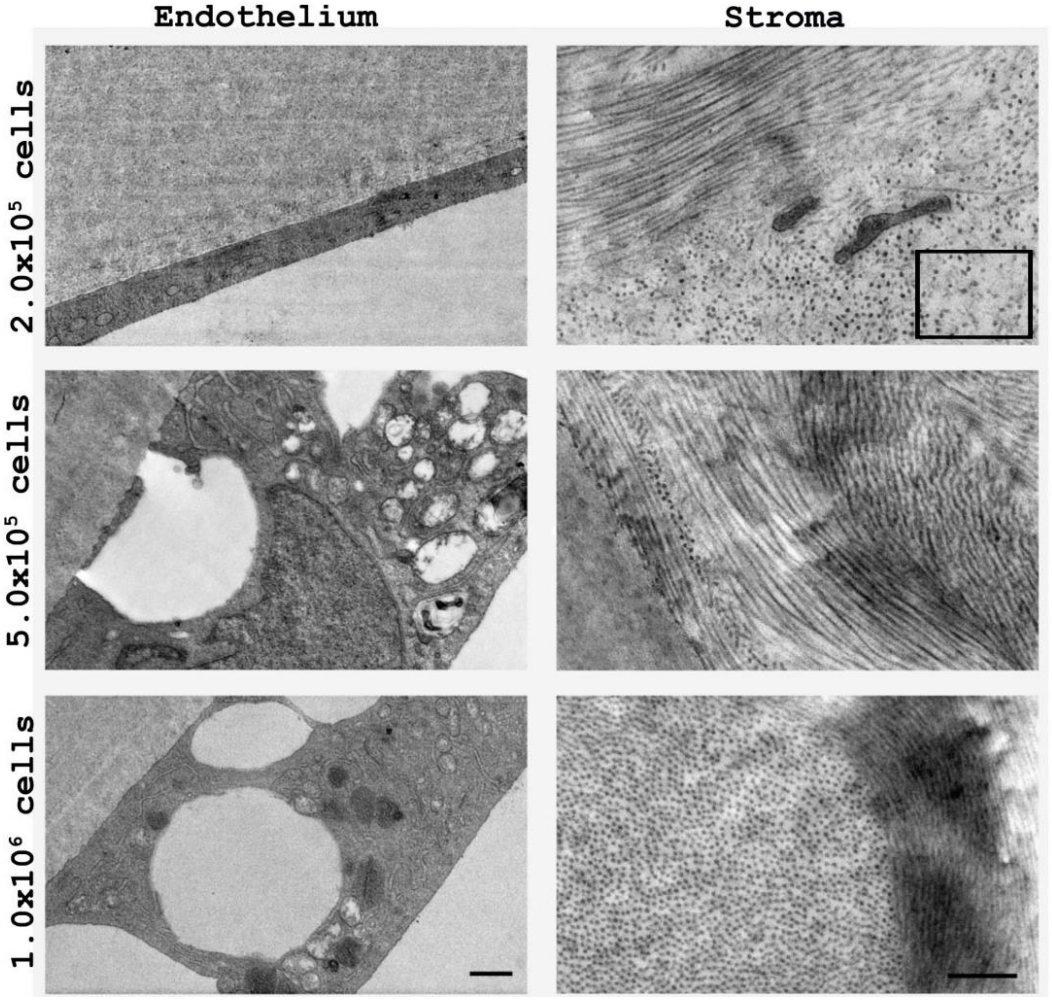

Figure 5.8 Micrographs of rabbit stroma and endothelium with different injected cell numbers. A cell density of $2.0x10^5$ cells resulted in an oedematous stroma (squared) with thinned endothelial cells. Higher cell densities ($5x10^5$ and $1x10^6$ cells) resulted in regularly arranged collagen fibrils and endothelial cells resembling typical morphological structure. Scale bars-endothelium=1 µm, stroma=500 nm.

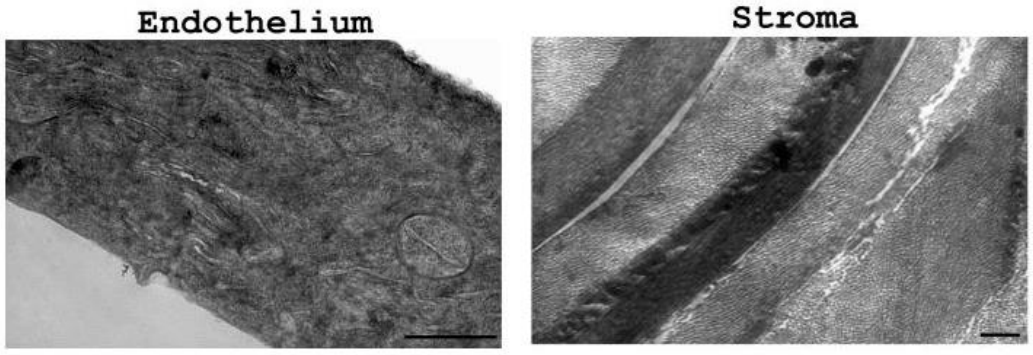

Figure 5.9 Micrographs representing control corneas devoid of cell injection with Y-27632. Scale bars=500 µm, stroma=500 µm.

5.4 Discussion

5.4.1 Posterior Corneal Surgery

nDSAEK surgery is now being used in patients with encouraging results. Nevertheless, there is still little known about the host endothelial cells and Descemet's membrane sandwiched between the host and graft stroma. Kobayashi and colleagues have reported that some patients suffer from donor dislocation post nDSAEK surgery (Kobayashi et al, 2008) and perhaps the reason stems from the presence of remaining host Descemet's membrane and endothelial cells. This study was carried out to determine the structural integrity of the host endothelial cells, Descemet's membrane, and how well the graft adheres to the host tissue in rabbit. The stroma was also investigated to see if the surgery had altered its architecture. Both TEM and light microscopy were used to determine the effects on the tissue which had undergone nDSAEK surgery two weeks prior.

Together with TEM, light micrographs show that host endothelial cells and Descemet's membrane are still present two weeks after nDSAEK surgery. Light micrographs showed a well adhered graft with a thin, distinct interface where the host endothelium meets graft stroma. Electron micrographs support this result as clear endothelium and Descemet's membrane are visible in the posterior third of the cornea. These cells stained positively for Na^+K^+ ATPase (Figure 5.10), a protein involved in the endothelial pumping system suggesting that they have retained some of their functionality (Hatanaka et al, 2012). This activity, however, does not seem to affect the visual acuity of patients (Kobayashi et al, 2008). If the Na^+K^+ATPase is still functional in the host endothelial cells then there is a possibility that a dual bicarbonate pump is functioning within the same cornea. There does not appear to be any reason why these trapped cells would not function and move fluid out of the host stroma into the graft resulting in a more hydrated graft stroma. However, Hodson carried out a series of experiments that challenges this theory. His results showed that when the fluid (i.e. aqueous humor) is removed from the endothelium's apical surface, the pump ceased (personal communication). This related to the build-up of lactic acid around the endothelium, an occurrence which would likely transpire in nDSAEK surgery if the pump persisted. Thus, based on this finding it is unlikely that these sandwiched cells retain any pump functionality.

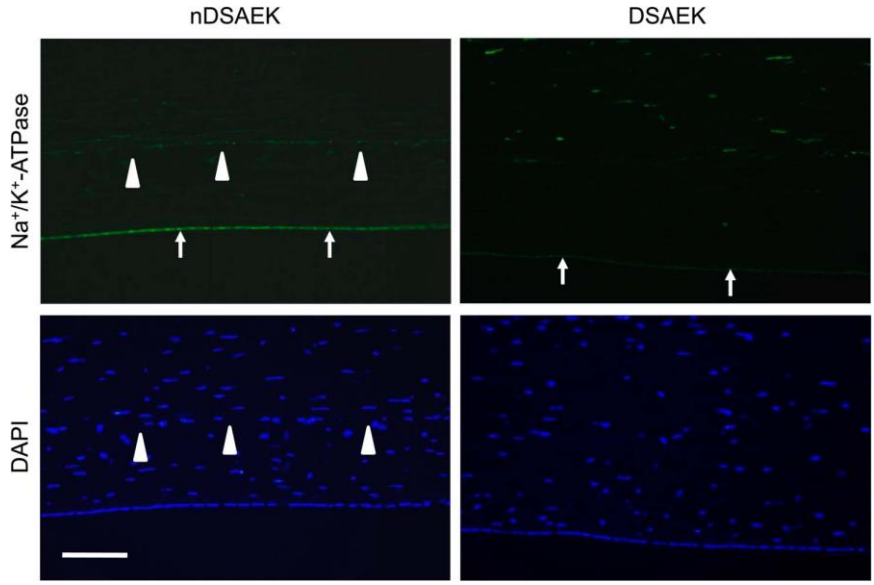

Figure 5.10 Na^+K^+ATPase expression in DSAEK and nDSAEK tissue 14 days post-surgery. Host (arrowheads) and graft (arrows) corneal endothelial cells expressed Na^+K^+ATPase in nDSAEK surgery, DAPI (blue) nuclear stain highlights a discontinuous line at the graft-host interface (arrows). Na^+K^+ATPase expression (green) also present in graft endothelial cells in DSAEK tissue. Scale bar=100 µm. Taken from Hatanaka et al, 2012.

As previously discussed, host endothelial cells are present at the interface two weeks post-surgery in nDSAEK, however, at this time-point the host endothelial layer is incomplete and what appears to be a fibrotic tissue is being deposited. The composition of this material is not known but it may be produced by the host endothelial layer in response to the graft tissue on its posterior surface. TEM also shows endothelial cell extensions into the graft stroma. Endothelial cell extensions, together with the fibrotic material observed at the interface implies that the endothelial cells are transforming. The cells may be under stress resulting in phagocytic activity and possibly migration into the stroma. Duplication of Descemet's membrane on the apical surface of endothelial cells is also observed (Figure5.5B). Type IV collagen is deposited by the corneal endothelium on its distal surface, it may be that it is also deposited on its proximal surface but under normal conditions is removed by the aqueous humour that bathes the cells. The absence of aqueous humour posterior to the sandwiched endothelial cells may result in the duplication of Descemet's membrane. The presence of endothelial cells, the unidentified fibrous tissue and what appears to be duplication of Descemet's membrane may have an effect on graft adherence, however, dislocation of the graft was not seen in these studies. Nevertheless, this surgery is still in its early stages and

although graft detachment was not seen in our experiments it may differ in human tissue. The majority of patients that have undergone nDSAEK did not experience graft dislocation (16.7% dislocated graft, Kobayashi et al, 2008), some studies reporting no graft dissociation (Masaki et al, 2012). There are still many unknowns surrounding this technique, mainly the long-term outcomes of the surgery including the morphology and location of the host endothelial cells.

Studies using confocal and slit lamp images have reported normal epithelial cells and keratocytes but also observed particles present at the graft-donor interface (Kobayashi et al, 2009). Kobayashi found that nDSAEK graft-recipient interface particles were larger than those observed in DSAEK. He concluded that either Descemet's membrane or the compressed necrotic endothelial cells are responsible for this (Kobayashi et al, 2009). Based on our TEM analysis, I would agree with this conclusion as we were still able to image the host endothelial layer. Kobayashi's study was carried out 3 months after surgery suggesting that the cells are still present at the time point or that the unidentified tissue we observed (scar, or new Descemet's produced by endothelium) is responsible. Perhaps then, up to at least 3-months post-nDSAEK surgery, remnants of the endothelial layer or Descemet's membrane are still visible at the interface but are dispersing as shown by the reduced interface haze in Kobayashi's study (Kobayashi et al, 2009).

nDSAEK surgery could be useful in non-FECD type endothelial dysfunction where the endothelial layer is not pathogenic. It may also be beneficial in eyes without lens or iris which become challenging in DSEK surgeries. Fragments of Descemet's membrane from the donor cornea can drop down during DSEK surgery which interferes with retinal function if there is no barrier between the anterior and posterior eye, i.e. lens. When Descemet's membrane is not stripped this problem is avoided (Price et al, 2007). This surgery can also be carried out for failed PKs, the original purpose for this surgery was to correct endothelial dysfunction after failed PK. Descemet's membrane and Bowman's membrane are thought to adhere most strongly after PK surgery. In failed PKs, where the endothelial cell count is low, nDSAEK may be beneficial.

DSAEK surgery has become increasingly popular over recent years after the initial success of posterior lamellar keratoplasty by Melles and colleagues (Melles et al, 1998). These

procedures have progressed rapidly as more advanced instruments, including the microkeratome and Busin glide, have been developed allowing more precise donor button cutting and smaller initial recipient incision. Results from this study support the positive results surrounding DSAEK surgery. Slit lamp imaging demonstrates that corneas become clear one week post-surgery (Hatanaka et al, 2012) with well adhered graft demonstrated by light microscopy (Figure 5.3). The difficulty in finding the interface by both TEM and light microscopy is likely to signify good graft adherence. It is already known that the stroma-stroma interface provides good adhesion, with lower graft detachment rates than those seen in nDSAEK (Price and Price, 2005; Price et al, 2010). It is thought that DSAEK surgery is much like laser-assisted in situ keratomileusis (LASIK) in that both result in a stroma-stroma interface. LASIK is an effective surgical procedure for correcting refractive errors and has rare cases of flap displacement (Lin and Maloney, 1999). Tissue stained positively for Na^+K^+ATPase (Figure 5.9), a sign that the graft endothelial cells are functional. As previously mentioned, the interface was difficult to find especially by TEM examination. When located, it appeared as a zone of granular tissue at the junction between the host and graft stroma. *In-vivo* confocal studies have reported interface haze and high levels of interface particle density post DSEAK surgery. These levels decrease during the 6-month study period, nevertheless, levels are higher than those observed in nDSAEK at every time-point. The material we observe with TEM may be responsible for this haze, just at a later stage. This material will probably have an effect on visual acuity, which in Kobayashi's DSAEK study could be why the majority of patients did not reach 20/20 or better (Kobayashi et al, 2008). The presence of granular material suggests that even a stroma-stroma interface can cause interface haze.

DSAEK techniques have evolved further and now include ultra-thin DSAEK, a procedure where the donor button comprises of endothelium, Descemet's membrane and an ultra-thin layer of stroma (approx. 100 µm). Ultra-thin DSAEK achieves similar visual results to those reported in DMEK without the difficult donor preparation (Busin et al, 2012). DMEK surgery is also available, however, preparation of the thin donor tissue is challenging, resulting in high numbers of lost grafts, increased graft detachment, increased donor preparation time and unfolding challenges (McCauley et al, 2009). These are just a few examples of how DSAEK surgery has, and is still advancing to overcome some of the complications that have emerged.

The stroma-stroma interface formed in DSAEK has better adherence compared with stroma-endothelium interface present in nDSAEK. This is demonstrated well by the increased graft dissociation in nDSAEK surgery (Kobayashi et al, 2008). Although nDSAEK surgery will not replace DSAEK it is a good alternative that avoids Descemet's membrane stripping in cases with no endothelial guttae, opacities or other endothelial abnormalities. This two week post-operative study has provided evidence that graft tissue adheres well in nDSAEK. An incomplete endothelial layer resides at the interface with fibrous stroma-like tissue and what appears to be duplication of Descemet's membrane on the host endothelial apical membrane. The fate of the host endothelial cells is yet to be determined, however, it seems that they will eventually become absent. These results identify the ultrastructural changes occurring after DSAEK and nDSAEK surgery that may provide a clue as to why certain grafts take longer to achieve good visual acuity than others. It also demonstrates the changes that occur in the host endothelial cells in the period following nDSAEK surgery, a factor that is not yet fully understood.

5.4.2 The Effect of ROCK Inhibitor on Corneal Endothelial Cells

Endothelial cell death is a common problem encountered in all corneal surgery, corneal transportation, disease and trauma. Disruption of this cell layer results in stromal swelling as endothelial cells are unable to pump adequate fluid out of the stroma. Due to the delicate nature of this cell layer, damage can occur very easily, one study found a cell loss of 33.6% one year after PK (Culbertson et al, 1982). Migration and enlargement of endothelial cells occurs after cell loss due to the limited proliferative capabilities of corneal endothelial cells. Corneal endothelial cells are known to be arrested in the G_1-phase of the cell cycle (Joyce et al, 2002), a quality that, in certain circumstances, can jeopardise corneal transparency. If there are insufficient cell numbers to remove excess stromal fluid, the cornea becomes oedematous. Good storage conditions have become an important part of corneal transplantation and over the past two decades have been developed in an attempt to optimise corneal storage environment. Optisol, the main storage media used today, has proved to be effective in maintaining the cornea in a sufficient state for transplantation, however, there is still significant endothelial cell death (Means et al, 1995). Recent studies examining endothelial cell death, proliferation and adhesion after the addition of a ROCK inhibitor have shown interesting results that may be beneficial in future endothelial treatment. Early results

from corneal treatment with ROCK inhibitor Y-27632 have been encouraging, decreasing apoptosis (12.4%±4.6% in control versus 2.0%±1.6% in Y-27632 treated, annexin-V positive cells) whilst promoting proliferation (Ki67 expression and Brd-U labelling) and cell migration (Okumura et al, 2009). Overall the number of viable cultivated monkey corneal endothelial cells was enhanced with larger cell colonies in the Y-27632 treated group when compared to control. This treatment could be very beneficial in corneal transport before transplantation and as a pharmaceutical agent post-surgery to reduce cell death and to possibly increase proliferation.

Whilst immunohistochemistry has been undertaken to determine the number of proliferating and apoptotic cells, the general morphology of the cells and state of the stroma is still unknown. This study provides additional data supporting Y-27632 as an effective agent in endothelial cell health with TEM analysis. The morphology of the Y-27632 treated cells was comparable to the controls with typical organelles. Okumura's study (Okumura et al, 2009) reported a decrease in the number of cells undergoing apoptosis. TEM analysis did not reveal any necrotic or abnormal cell morphology in the treated group. Cell structure and organelles appeared normal in all sections and regions through corneal depth imaged with no signs of cell degradation or duplication of the endothelial cell monolayer. This data is reassuring and based on the morphological analysis the drug treatment does not appear to have any negative effects. Okumura's study on Y-27632 primate treated cells shows increased adhesion of cells in culture (Okumura et al, 2009); it is possible that suppression of migration leads to increased adhesion.

The second study used rabbit cornea to determine the number of endothelial cells required for complete monolayer regeneration and to give an insight into how these cells behave post injection *in vivo*. Three different cell volumes were injected. The lowest density ($2x10^5$ cells) resulted in an oedematous posterior stroma, an outcome probably due to a lack of cells to counteract the fluid leaking into the stroma via the pump mechanism. The endothelial cells in these micrographs also appeared thinner and stretched, possibly due to excessive cell spreading to compensate for the inadequate number of cells overall. Organelles were sparse with not nearly the same volumes as we would normally expect to see in these cells, a possible sign that these cells are stressed and cannot sustain typical cell functions and the maintenance of organelles. This was not the case in the corneas injected with the higher cell

densities. There was no evidence of stromal oedema in these rabbits, endothelial cells looked normal with characteristic organelles. These findings helped to establish that a density of $5x10^5$ cells was adequate to form a sufficient cell monolayer, capable of maintaining stromal deturgescence. These data also show a clear suggesting that the cell volume injected does not cause duplication of the cells; an outcome that could jeopardise the pumping mechanism and therefore stromal hydration and transparency.

Previous studies working on adult human corneal endothelial cells found that they retain the essential functions required to maintain stromal dehydration *in vivo* (Mimura et al, 2004), a quality meaning these cells would also be viable for transplantation. New techniques for posterior corneal surgery are frequently being developed with the general consensus that the thinner the graft the better the outcome (Dapena et al, 2009). However, due to the fragile nature of transplanting endothelial cells alone, many surgeries include stroma and Descemet's membrane; a practice that could be avoided if the surgery was combined with Y-27632 treatment. Studies on DMEK, a surgical procedure only replacing Descemet's membrane and the diseased endothelium, have shown quicker and near complete visual recovery within 1-3 months (Ham et al, 2009). Hence, DMEK is one procedure that could benefit from this treatment. Transport and storage of tissue before transplantation is another area where ROCK inhibitors could be used. Although the current methods of corneal storage, namely Optisol, are adequate, there is still significant cell loss as mentioned above (Means et al, 1995). The time between tissue removal and surgery is a period of endothelial degeneration which together with surgery, results in a substantial loss of cells. An agent capable of reducing apoptosis and increasing proliferation would help increase the viability of the cornea for transplantation and reduce the chance of oedema post-surgery. In the future, Y-27632 may serve as a topical agent for the cornea, and as a result, a less invasive therapy for endothelial dysfunction.

There are still challenges ahead for this treatment. Establishing the number of functional endothelial cells is an important factor in this study. There may be an increase in the cell density but their functionality may not be characteristic of normal endothelial cells. Studies on Schlemm's canal endothelial cells found Y-27632 decreased transendothelial electrical resistance, increasing the paracellular permeability thought alterations in the tight junctions (Kameda et al, 2012). If the same result was to occur in the endothelial cells of the cornea,

this could give rise to an oedematous stroma. Even if the inhibitor did have adverse side effects on the endothelial cells, it does not appear to change their morphology. Questions may also be raised about the cell injection studies, including the fate of the remaining endothelial cells once the monolayer has formed. The cells are thought to be removed from the aqueous humor, with no effect on intraocular pressure. There are no reported effects of Y-27632 on keratocytes, however, this factor still needs to be considered and observed in the long-term. They are still cell components of the cornea and may be affected by ROCK inhibition. Future work examining the long-term effects of this agent on the endothelial cells and the cornea as a whole are going to be important to determine the drug parameters. Studies will help define the treatment time required for sufficient endothelial regeneration and potential adverse effects of Y-27632. Some of this data can be analysed *in vitro*, whilst other areas will need *in vivo* studies and clinical trials. Clinical trials would be beneficial in establishing the outcomes in patients and to support integration into the clinic.

This study has helped establish the number of cells required for monolayer regeneration without monolayer duplication post Descemet's stripping and the morphological effects of the ROCK inhibitor, Y-27632. Images provide evidence that in environments with too few cells, stretched and thinned cells result which may reduce efficacy of the vital pump function discussed in chapter 3. It is important to determine how these cells behave in their new environment with drug intervention; this analysis has helped elucidate this and provides evidence that no atypical morphology was observed.

Corneal endothelial replacement and regeneration offer alternatives to traditional PK which have reduced adverse effects and faster recovery. DSAEK and nDSAEK surgeries provide effective surgical procedures for the replacement of corneal endothelial cells until techniques involving the transplantation of endothelia cells only are perfected. ROCK inhibition, on the other hand, offers endothelium regeneration without the need for invasive surgery. The combination of the two treatments could reduce the number of failed surgeries as a result of low endothelial cell count. ROCK inhibition used solely will also be beneficial corneal transport. Both posterior corneal surgery and ROCK inhibition offer additional and possible alternatives for corneal endothelium correction. Although long-term outcomes are required for both interventions, the benefits are clear and establish both as definite contenders in endothelial cell correction after depletion.

Chapter 6: Overall Discussion

6.

The importance of the cornea's endothelial layer is recognised in development, disease, and surgery, demonstrated in this thesis. The limited replicative capability of these cells in adult tissue (Joyce et al, 1996) reinforces the need for intervention, whether surgical or pharmaceutical, to increase the endothelial cell number to maintain stromal deturgescence. The main aim of this thesis was to better understand corneal endothelial cells in development, disease and intervention. It was important to determine the changes the cells undergo in each of these environments and to better understand how they react and their adaptability in circumstances where they are under stress. The findings give an insight into the morphology and protein expression of the developmental endothelial cells and how they might influence the developing stroma. The research also highlights the effects of a knock-in mutation on the endothelial cells and subsequently the corneal stroma, as well as recent advancements in endothelial replacement and regeneration via surgery and a Rho-associated kinase inhibitor, respectively. These interventions will be beneficial to patients who are susceptible to endothelial cell loss such as those diagnosed with FECD.

6.1 Endothelial Development

One key role of endothelial cells is to maintain correct stromal hydration in order for corneal transparency to prevail. This is achieved by a pumping mechanism whose role is to counteract the leak of fluid into the stroma through the paracellular tight junction route. Chapter 3 investigated the development of the endothelial cells in embryonic chick cornea. Observation of the cell layer at low magnification depicted a general view of the posterior tissue including stroma and Descemet's membrane. Stromal density and organisation was seen to increase as development progressed alongside a growing Descemet's membrane. Endothelial cells consisted of numerous organelles including mitochondria whose responsibility is to provide the energy required for pump function correlating with early studies on developmental tissue (Wulle, 1972). Immunolocalisation employing a rabbit anti-$Na^{+}HCO_3^{-}$ antibody revealed the presence of the NBC in all stages labelled (E10-E14). The importance of this cotransporter has previously been highlighted in adult tissue (Sun and Bonanno, 2003), and is one of the major transporters of HCO_3^{-} residing on the basolateral

membrane. Its presence at these early stages in development suggests it may also have a role in embryonic stromal hydration. Studies have reported compaction and dehydration in the latter stages of development, this helps increase the transparency of the cornea to 96% by E19 (Coulombre and Coulombre, 1958). NBC, labelled at this time point, may influence this compaction and onset of transparency. A study carried out by Conrad et al (2006) measured NBC gene expression in the embryonic chick, finding that its expression increased through development and into the post-hatching period. These studies correlate with Conrad's data and helps reinforce the concept that the cotransporter plays a role in development as well adulthood. The final experiment undertaken in chapter 3 used A-scan ultrasonography to determine the changes in thickness during the E9-E18 developmental period. This technique avoided the need for tissue fixation and dehydration, measuring the corneal thickness in fresh tissue. Alterations in the methodology led to a final experiment measuring fresh corneal tissue on one day in one eye. These data revealed three key trends. The first was a thickness increase from E9-E12 followed by a plateau in the E12-E15 developmental period and finally, a decrease in thickness till E18 where the final measurement was taken. Early studies (Hay and Revel, 1969) on cornea suggest the initial increase occurs due to primary stromal swelling in preparation for mesenchymal cell invasion, along with the corneal keratocytes populating the matrix, forming the secondary stroma. The plateau observed between E12-E15 may be a period of stromal reorganisation before final dehydration and compaction of the collagen fibrils. This relates to a study measuring interfibrillar Bragg spacing reporting that two dehydration phases occur during avian corneal development. The first between E13-E14 suggested to be as a result of water loss from non-collagenous regions, the second between E16-E17, thought to be due to a decrease in interfibrillar Bragg spacing (Siegler and Quantock, 2002). Our thickness decrease, post E15, correlates with their result reporting interfibrillar Bragg spacing decrease. We postulate that the endothelium is involved in water regulation and deturgescence at this period of development and that there may be two phases of endothelial pump activity.

The majority of data collected in chapter 3 correlates with previous literature including NBC gene expression supporting our immunolocalisation data and the compaction studies carried out in embryonic chick correlating with our corneal thickness data. However, Hay and Revel reported thickness results which contradicted ours; I believe this was as a result of the tissue dehydration they used in their study. Now that the expression and importance of the NBC is

recognised, it will be important to determine when the cotransporter is not only expressed but is functional to define more specifically its role in corneal development.

6.2 Part I-The Ultrastructure of Descemet's membrane

Descemet's membrane is the basement membrane of the corneal endothelium providing it with a structural support that allows the movement of fluid through. When this membrane was examined long spacing structures with a periodicity of 100 nm are observed in the transverse section plane. These structures were still present in en face sections alongside the more typical polygonal lattice formations we would expect in this membrane (Sawada et al, 1990, Shuttleworth, 1997). The collagen responsible for the polygonal structures is now recognised as type VIII collagen (Sawada et al, 1990) and it is likely that the elongated structures observed in both planes are also composed of the same type. Early studies on Descemet's membrane show how a polygonal lattice represents a structural solution, solving the problem of resisting compression whilst maintaining a porous structure (Ninomiya et al, 1990). Three-dimensional analysis revealed how the globular domains appear to be stacked directly on top of one another supporting this idea of lattice structures in Descemet's membrane which stack on top of one another capable of allowing fluid through the membrane. The model created combines the elongated structures observed in both planes with the typical polygonal formations. The model demonstrates how both types of structure would allow Descemet's membrane to be permeable. Occasionally interbands were visible within the elongated structures. After visualising en face sections it was concluded that these interbands are likely to be formed by the central globular domain we observe in the polygonal formations. Based on the polygonal structures it was proposed that the dominant bands are formed by stacked globular domains. This is also conceivably true for the intermediate bands observed in transverse sections of Descemet's membrane, however, the less distinct banding is probably due to globular domains not being in the same plane as the distinct bands, thus, a weaker structure is imaged.

Cuprolinic blue staining and three-dimensional analysis revealed the presence of proteoglycans associating with the internodal regions of the elongated structures we believe to be type VIII collagen. The binding of proteoglycans to the helical part of this collagen may assist in maintaining the arrangement of type VIII in either the polygonal lattice or the

elongated structures observed via the collagenous regions of the molecule. These results support previously published literature on the structure of Descemet's membrane with additional evidence on the assembly of collagen type VIII. Proteoglycan labelling in Descemet's membrane has been previously reported (Bairaktaris et al, 1998; Davies et al, 1999), however, this is the first data that shows proteoglycans associating with intermodal regions of type VIII collagen in Descemet's membrane. This may imply they have a role in maintaining the unique structure of type VIII collagen in Descemet's membrane.

6.2 Part II-*Col8a2* FECD Model

Endothelial cells become compromised by trauma, surgery, infection and disease. Whilst they can adapt to cell loss by migration and enlargement of remaining cells, if the cell count becomes too low, stromal swelling will transpire. As in most diseases, early diagnosis is essential so that preventative treatment can be used to decrease the symptoms and inhibit disease onset. Due to the lack of symptoms in the early stages of FECD, the only tissue available for examination is from PKs where the features of the disease are most severe and represent the latter stages of FECD. This has meant that little is known about the early disease pathogenesis due to the lack of tissue available for examination. This has highlighted the need for disease models to identify the factors contributing to the pathogenesis and the time-points within the disease course where symptoms are revealed. Chapter 4 identified the ultrastructural changes within the stroma of *Col8a2* knock-in murine mutants, a recently developed mouse model for early-onset FECD (Jun et al, 2012). It has been well established that corneal swelling and thickened Descemet's membrane are features present in patients with the disease (Waring et al, 1978). Disorganised collagen VIII in Descemet's membrane has led to studies based on mutations in this collagen (Biswas et al, 2001; Gottsch et al, 2005). The symptoms presented in *Col8a2* mutants in these studies mirror those seen in FECD, establishing them as disease targets. The more evident differences in our results were observed in the endothelial layer, including dilated RER and increased proteoglycans at the Descemet's endothelial interface, suggesting the initial effects of the disease occur in this region. Dilated RER is a sign of high protein synthesis that is likely due to accumulation of collagen VIII in these mutants and activation of the UPR. The lack of evident oedema in the corneas, which would have been expected if endothelial pump function was compromised, was assumed to be due to the relatively young age of the mice. Recent studies on these

models have reported significant endothelial cell loss (Jun et al, 2012), however, this may not be adequate to compromise the pump leak system operating in the endothelial cells. The increased proteoglycans present at the Descemet's endothelial interface in the *Col8a2*$^{Q455K/Q455K}$ mutant are thought to be a product of the endothelial cells, visualised even after enzyme digestion with keratanase and chondroitinase ABC. This correlated with studies identifying changes in proteoglycans in wounded and normal cornea. Davies found increases in both CS and heparan sulphate in migrating endothelial cells (Davies et al, 1999). This may indicate that proteoglycans are playing a key role in the cellular processes in this disease model. These results demonstrate the resilience of the endothelial cell layer; even with a significant cell loss the remaining cells are clearly capable of maintaining stromal deturgescence.

The results obtained in chapter 4 reinforce the *Col8a2* knock-in murine mouse model as an important tool in determining the disease pathogenesis in FECD. Defining the features that occur in the disease will help better understand the sequence of events and ways to resolve them. The ultrastructural changes in the *Col8a2* knock-in mouse models signify that similar studies at later time-points are required so that a more extensive representation of the effects of the disease can be obtained. This would help reveal the changes that occur between the initial and latter stages of the disease, and may help outline the detrimental effects on the cornea that need to be targeted. TEM at the Descemet's endothelial interface highlighted the presence of proteoglycans in the *Col8a2*$^{Q455K/Q455K}$ mutant. It is assumed heparan sulphate is the proteoglycan responsible as its presence remains after digestion with keratanase and chondroitinase ABC. However, due to time and tissue constraints, this proteoglycan was not labelled. Future work should include immunohistochemistry to identify this proteoglycan. It will also be beneficial to label collagen VIII in Descemet's membrane to determine if its structure is altered and whether the proteoglycans observed at the interface are linked to this collagen.

6.3 Corneal Endothelial Cell Replacement and Regeneration

The prevalence of diseases such as FECD, has resulted in the development of procedures to replace the pathological tissue present in the cornea. The most common procedure carried out in corneal tissue, which is irreversibly damaged, is PK. Chapter 5 observed the ultrastructural

changes that occurred in partial corneal transplants which have become more favoured by corneal surgeons in recent years. Newer procedures aim to replace only the damaged/diseased areas of the cornea, reducing some of the problems that develop post PK. Developments in posterior corneal surgery have included smaller incisions, the use of automated equipment (Gorovoy, 2006) and decreasing the thickness of the donor grafts. Light microscopy of DSAEK and nDSAEK surgeries demonstrated that the adherence of both grafts was good. Investigation with TEM allowed a more detailed view of this interface in both surgeries. Host Descemet's membrane and endothelial cells were still present 2 weeks post-surgery in nDSAEK and extended into the graft stroma along with scar tissue on the posterior surface of the host endothelial cells. The presence of Descemet's membrane, endothelium and the scar tissue does not appear to interfere with visual acuity or the adherence of the graft tissue. However, the fibrotic scar tissue we report here, along with the host Descemet's membrane and endothelium are likely to be responsible for graft dissociation in those reports studying nDSAEK (Kobayashi et al, 2008).

DSAEK has become increasingly popular over the last few years after the initial success of PLK by Melles (Melles et el, 1998). The adherence of the graft is good; this was supported by the difficulty in finding the interface by TEM. This backs the low graft detachment rates previously reported for DSAEK surgery (Price and Price, 2005; 2010). The interface examined by TEM appeared as a layer of granular tissue between the graft and host stroma. Some studies have reported interface haze in DSAEK (Kobayashi et al, 2008) that may be due to this granular material and may be a key reason why some patients do not reach 20/20 or better.

Both DSAEK and nDSAEK are now being carried out in patients and have proved to be effective. Although nDSAEK cannot be used for FECD or in any problem where the endothelium is diseased, it will be beneficial in patients with low endothelial cell counts and those with failed PKs not associated with guttae. DSAEK can be used in those with diseased endothelium, as these cells are removed. This will be advantageous over PK as the current host tissue has good adherence, particularly at the basement membranes (Bowmans and Descemet's). Removal of these structures will reduce the integrity of the cornea and disrupt the globe; hence, partial corneal replacement is a good advancement in this field.

The long term effects on the cornea post DSAEK and nDSAEK surgery is the main unknown. The first DSAEK study carried out in patients was in 2006, this is fairly recent and there is little data available on the changes within the tissue at higher magnification. Once patient DSAEK corneas do become available it will be important to observe the interface and remaining endothelial cells to determine the effects of time on the tissue. I think the most important feature in this surgery will be the interface, especially in nDSAEK surgery where the original endothelial cells reside and a scar-like tissue is present. What happens to the host endothelial cells and the overall state of the interface after longer durations? Partial surgeries have developed further and have helped pave the way to ultra-thin DSAEK and even replacement with only Descemet's membrane and endothelium, although the latter has proven difficult due to the delicate nature of the tissue. This is the future in posterior corneal surgery and investigation into the ultrastructure of this tissue should also be considered.

Corneal transplantation is not the only method for correcting corneal endothelial cell loss. Recently, studies investigating a ROCK inhibitor have shown increased proliferation, adhesion and decreased apoptosis in the corneal endothelium (Okumura et al, 2009). The second part of Chapter 5 examined the effects of the ROCK inhibitor, Y-27632, on the morphology of the corneal endothelium in human and rabbit samples. Results from TEM analysis illustrate that the endothelial cells present in the Y-27632 treated group were comparable to control samples in human corneas. This data correlates with previous findings reported by Okumura and colleagues that apoptosis is decreased in these cells after treatment with ROCK inhibitor (Okumura et al, 2009). The second part of the ROCK inhibitor investigation into corneal endothelial cells was concerned with cell injection studies. Initially, increasing cell volumes were injected into endothelial stripped rabbit corneas to determine the cell density required to form a new, complete monolayer. After discovering that a cell density of $2x10^5$ cells resulted in an oedematous stroma and thinned endothelial cells, a cell density of $5x10^5$ cells was established as an appropriate volume to be used. Together with previous studies, this data supports the notion that endothelial cells can be injected, and with the support of the ROCK inhibitor, Y-27632, are capable of regenerating the endothelial cell layer.

The use of Y-27632 in cell injection therapies is beneficial but it is important to note that this ROCK inhibitor has the potential to be used in such surgeries as DSAEK/nDSAEK as well as

a component of storage media's used to transport and store corneal tissue. Thus, Y-27632 is a promising novel therapy for the treatment of corneal endothelium dysfunction.

A number of challenges lie ahead for the ROCK inhibitor studies. So far, the main research for Y-27632 has been based on animal models. The next logical step for this treatment is clinical trials to conclude whether or not the same results can be replicated in man. Treatment time required in patients and any long term effects on the ocular tissue are other parameters that need to be determined. Increased intraocular pressure and the abnormal deposition of endothelial cells on the posterior cornea have not been reported in any of the studies so far but should be considered in future trials (Okumura et al, 2012).

6.4 Summary

The techniques used to study the morphology of the corneal endothelium and the expression of the pump show how the cells change through development. It also demonstrates how the thickness of the cornea can change in a short period of time, an important process in development and a feature that needs to be controlled into adulthood. In addition these studies have also shown that disease can severely affect the cells of this monolayer by both attenuation and decreased cell density that consequently, affects stromal hydration. FECD is a primary corneal endotheliopathy responsible for many PKs. The initial pathogenesis of FECD is still not fully understood due to the lack of tissue available in the early disease stages. The production of a murine model based on knock-in mutations previously established by Biswas and Gottsch (Biswas et al, 2001; Gottsch et al, 2005) has allowed us to determine the early changes that exist in FECD corneas. The final chapter focusing on corrective procedures/interventions will aid endothelial cell loss. Corneal surgery has been developed as a direct result of these diseases, as well as infection and trauma. Recent developments in posterior corneal surgery have produced promising results. DSAEK and nDSAEK are increasingly chosen over traditional PK because of faster visual recovery and reduced astigmatism. Although there are changes to the corneal ultrastructure after these surgeries, they do not appear to affect the outcomes in patients nor do they compromise the graft. They are an important development in this field and have led to further developments in the form of ultra-thin DSAEK and DMEK. Recently, ROCK inhibition has also generated interest as a result of its proliferative effects on endothelial cells. The results reported here supply

additional evidence that this inhibitor has beneficial effects on the endothelial cells whilst not interfering with general cell morphology. The importance of the endothelial layer is highlighted in this thesis, where enough disruption will lead to stromal oedema. This has resulted in extensive research into replacement and regeneration of the cell layer that has a crucial role in maintaining stromal deturgescence, a feature vital to corneal transparency.

References

References

Abuladze N, Lee I, Newman D, Hwang J, Boorer K, Pushkin A and Kurtz I (1998) Molecular cloning, chromosomal localization, tissue distribution, and functional expression of the human pancreatic sodium bicarbonate cotransporter. *Journal of Biological Chemistry*. 273*:*17689–17695.

Adamis AP, Filatov V, Tripathi BJ and Tripathi RC (1993) Fuchs'' endothelial dystrophy of the cornea. *Survey of Ophthalmology.* 38:149-168

Airiani S, Trokel SL and Lee SM (2006) Evaluating central corneal thickness measurements with noncontact optical low-coherence reflectometry and contact ultrasound pachymetry. *American Journal of Ophthalmology*. 142: 164–165.

Akimoto Y, Sawada H, Ohara-Imaizumi M, Nagamatsu S and Kawakami H (2008) Change in long-spacing collagen in Descemet's membrane of diabetic goto-kakizaki rats and its suppression by antidiabetic agents. *Experimental Diabetes Research.* 2008: 818341.

Allan BD, Terry MA, Price FW Jr, Price MO, Griffin NB and Claesson M (2007) Corneal transplant rejection rate and severity after endothelial keratoplasty. *Cornea.* 26: 1039-1042

Amano M, Iot M, Kimura K, Fukata Y, Chihara K, Nakano T, Matsuura Y, et al (1996) Phosphorylation and activation of myosin by Rho-associated kinase (Rho-kinase). *Journal of Biological Chemistry*. 271: 20246–20249.

Anseth A (1961) Glycosaminoglycan's in the Developing Corneal Stroma. *Experimental Eye Research.* 1: 116-121.

Aronson P (1985) Kinetic properties of the plasma membrane Na-H exchanger *Annual Review of Physiology.* 47: 545.

Bairaktaris G, Davis L, Fullwood N, Nieduszynski I, Marcyniuk B, Quantock A and Ridgway A (1998) An ultrastructural investigation into proteoglycan distribution in human corneas. *Cornea*. 17: 396–402.

Bard J and Kratochwil K (1987) Corneal morphogenesis in the Mov13 mutant mouse is characterized by normal cellular organization but disordered and thin collagen. *Development.* 101: 547–55.

Bard J, Hay ED and Meller S (1975) Formation of the endothelium of the avian cornea: a study of cell movement in vivo. *Developmental Biology.* 42: 334-361.

Benya P (1980) EC collagen: Biosynthesis by corneal endothelial cells and separation from type IV without pepsin treatment or denaturation. *Renal Physiology*. 3:30-35.

Bettelheim F and Plessy B (1975) The hydration of Proteoglycans of bovine cornea. *Biochimica et Biophysica Acta.* 381: 203-214.

Birk D E, Fitch J, and Linsenmayer T F (1986) Organization of Collagen Types I and V in the Embryonic Chicken Cornea. *Investigative Ophthalmology & Visual Science.* 27: 1470-1477.

Birk DE, Fitch JM, Babiarz JP and Linsenmayer TF (1988) Collagen type I and type V are present in the same fibril in the avian corneal stroma. *Journal of Cell Biology*. 106: 999–1008

Birk D E, Fitch J, Babiarz J, Doane M, and Linsenmayer T (1990) Collagen Fibrillogenesis Invitro- Interaction of Type -I and Type-V Collagen Regulates Collagen Fibril Diameter. *Journal of Cell Science.* 94: 649-657.

Biswas S, Munier FL, Yardley J, Hart-Holden N, Perveen R, Cousin P, Sutphin JE, et al (2001) Missense mutations in COL8A2, the gene encoding the alpha2 chain of type VIII collagen, cause two forms of corneal endothelial dystrophy. *Human Molecular Genetics*. 10: 2415–2423.

Blair S, Seabrooks D, Shields W, Pillai S and Cavanagh H (1992) Bilateral progressive iris atrophy and keratoconus with coincident features of posterior polymorphous dystrophy- A case report and proposed pathogenesis. *Cornea.* 11: 255–261.

Blochberger T, Cornuet P, and Hassel J (1992) Isolation and partial characterization of lumican and decorin from adult chicken corneas- A keratan sulphate-containing isoform of decorin is developmentally regulated. *Journal of Biological Chemistry.* 267: 20613-20619

Bonanno J and Giasson C (1992) Intracellular pH regulation in fresh and cultured bovine corneal endothelium, II. NaH:CO3 cotransport and Cl/HCO3 exchange. *Investigative Ophthalmology and Visual Science*. 33: 3068-3079.

Bonanno JA, Yi G, Kang XJ and Srinivas SP (1998) Reevaluation of Cl-/HCO3- exchange in cultured bovine endothelial cells. *Investigative Ophthalmology and Visual Science*. 39:2713-2722.

Bonanno J, Guan Y, Jelamskii S, and Kang X (1999) Apical and basolateral CO_2-HCO_3 permeability in cultured bovine corneal endothelial cells. *The American Journal of Physiology.* 277: C545-C553.

Bonanno J (2003) Identity and regulation of ion transport mechanisms in the corneal endothelium. *Progress in Retinal and Eye Research*. 22: 69–94.

Boruchoff SA and Kuwabara T (1971) Electron microscopy of posterior polymorphous degeneration. *American Journal of Ophthalmology.* 72: 879-887.

Bourne W and Kaufman H (1976) Specular microscopy of the human corneal endothelium in vivo. *American Journal of Ophthalmology.* 81: 319-323.

Bozzola J and Russell L (1999) *Electron Microscopy* .2nd Edition. Jones and Bartlett Publishers International, Toronto.

Bredrup C, Knappskog PM, Majewski J, Rødahl E and Boman H (2005) Congenital stromal dystrophy of the cornea caused by a mutation in the decorin gene. *Investigative Ophthalmology & Visual Science.* 46: 420–6.

Bron R, Tripathi RC, and Tripathi BI (1997). Wolff's anatomy of the eye and orbit. 8th Edition. Chapman & Hall (London).

Busin M, Patel AK, Scorcia V and Ponzin D. (2012). Microkeratome-assisted preparation of ultrathin grafts for Descemet's stripping automated endothelial keratoplasty. *Investigative Ophthalmology & Visual Science*. 53: 521–4.

Cai CX, Fitch JM, Svoboda KKH, Birk DE and Linsenmayer TF (1994) Cellular invasion and collagen type-IX in the primary corneal stroma in-vitro. *Developmental Dynamics.* 201:206-215

Callaghan M, Hand C, Kennedy S, Fitzsimon J, Collum L, and Parfrey N (1998) Homozygosity mapping and linkage analysis demonstrate that autosomal recessive congenital hereditary endothelial dystrophy (CHED) and autosomal dominant CHED are genetically distinct. *British Journal of Ophthalmology.* 83: 115-119.

Calmettes L, Deodati F, Planel H and Bec P (1956) Etude histologique et histochimique de l'epithelium anterieur de la cornee et de ses basales. *Archives of Ophthalmology.* 16: 481-506.

Chakravarti S, Magnuson T, Lass J, Jepsen K, LaMantia C, and Carroll H (1998) Lumican regulates collagen fibril assembly: Skin fragility and corneal opacity in the absence of lumican. *Journal of Cell Biology.* 141: 1277- 1286.

Chan CC, Green WR, Barraquer J, Barraquer-Somers E and de la Cruz ZC (1982) Similarities between posterior polymorphous and congenital hereditary endothelial dystrophies: a study of 14 buttons of 11 cases. *Cornea.* 1: 155–172.

Chandler PA (1955) Atrophy of the stroma of the iris: Endothelial dystrophy, corneal edema, and glaucoma. *American Journal of Ophthalmology.* 41:607-615

Chapman JA, Tzaphlidou, M, Meek KM and Kadler KE (1990) The collagen fibril--a model system for studying the staining and fixation of a protein. *Electron Microscopy Reviews.* 3: 143-182.

Chen J, Guerriero E, Lathrop K and SundarRaj N. (2008) Rho/ROCK signalling in regulation of corneal epithelial cell cycle progression. *Investigative Ophthalmology & Visual Science*. 49: 175–183.

Chen Q, Fitch JM, Gibney E and Linsenmayer TF (1993) Type II collagen during cartilage and corneal development: immunohistochemical analysis with an anti-telopeptide antibody. *Developmental Dynamics.* 196: 47–53.

Cintron C, Covington H, and Kublin C (1983) Morphogenesis of rabbit corneal stroma. *Investigative Ophthalmology & Visual Science.* 24: 543-556.

Cintron C, Hassinger L, Kublin C, and Cannon D (1978) Biochemical and ultrastructural changes in collagen during corneal wound healing. *Journal of Ultrastructure Research.* 65: 13-22.

Conrad A, and Conrad G (2003) The keratocan gene is expressed in both ocular and non-ocular tissues during early chick development. *Matrix Biology*. 22: 323-337.

Conrad A, Zhang Y, Walker A, Olberding L, Hanzlick A, Zimmer A, Morffi R, et al. (2006). Thyroxine affects expression of KSPG-related genes, the carbonic anhydrase II gene, and KS sulfation in the embryonic chicken cornea. *Investigative Ophthalmology and Visual Science*. 47: 120–132.

Cornuet P, Blochberger T, and Hassel J (1994) Molecular polymorphism of lumican during corneal development. *Investigative Ophthalmology & Visual Science.* 35: 870-877.

Corpuz L, Funderburgh J, Funderburgh M, Bottomley G, Prakash S, and Conrad G (1996) Molecular cloning and tissue distribution of keratocan - Bovine corneal keratan sulfate PG 37A. *Journal of Biological Chemistry.* 271: 9759-9763

Coulombre AJ and Coulombre JL (1958). Corneal development. I. Corneal transparency. *Journal of Cellular and Comparative Physiology*. 51: 1–11.

Coulombre A and Coulombre J (1961) *The development of the structural and optical properties of the cornea*. New York, Academic press.

Cox J, Farrell R, Hart R, and Langham M (1970) The transparency of the mammalian cornea. *Journal of Physiology.* 210: 601-616.

Cribs C, Krachmer J, Phelps C and Weingeist T (1977) The clinical spectrum of posterior polymorphous dystrophy. *Archives in Ophthalmology.* 95: 1529-1537.

Crow J, Lima P, Agapitos P, and Nelson J (1994) Effects of insulin and EGF on DNA synthesis in bovine endothelial cultures: flow cytometric analysis. *Investigative Ophthalmology & Visual Science.* 35: 128-133.

Culbertson W, Abbott R and Forster R (1982). Endothelial-cell loss in penetrating keratoplasty. *Ophthalmology*. 89: 600–604.

Dapena I, Ham L and Melles G (2009) Endothelial keratoplasty: DSEK/DSAEK or DMEK-the thinner the better? *Current Opinion in Ophthalmology*. 20: 299–307.

Davanger M, and Evensen A (1971) Role of Pericorneal Papillary Structure in Renewal of Corneal Epithelium. *Nature.* 229: 560-561.

Davies Y, Lewis D, Fullwood N, Nieduszynski I, Marcyniuk B, Albon J and Tullo A. (1999). Proteoglycans on normal and migrating human corneal endothelium. *Experimental Eye Research*. 68: 303–311.

DelMonte DW and Kim T (2011) Anatomy and physiology of the cornea. *Journal of Cataract and Refractive Surgery.* 37: 588-598

Doane M and Dohlman C (1970) Physiological Response of the Cornea to an Artificial Epithelium. *Experimental Eye Research.* 9: 158–164.

Dua H, and Azuara-Blanco A (2000) Limbal stem cells of the corneal epithelium. *Survey of Ophthalmology.* 44: 415-425.

Dublin I (1970) Comparative Embryologic Investigations of Early Development of Cornea and Pupillary membrane in reptiles, birds, and mammals. *Acta Anatomica* .76: 381.

Dubreuil C, Winton M and McKerracher L (2003) Rho activation patterns after spinal cord injury and the role of activated Rho in apoptosis in the central nervous system. *Journal of Cell Biology*. 162: 233–243.

Dunlevy J, Beales M, Berryhill B, Cornuet P, and Hassell J (2000) Expression of the keratan sulfate Proteoglycans lumican, keratocan and osteoglycin/mimecan during chick corneal development. *Experimental Eye Research.* 70: 349-362.

Edelhauser H (2006) The balance between corneal transparency and edema. *Investigative Ophthalmology & Visual Science* 47:1755-1767.

Ehlers N, Modis L and Møller-Pedersen (1998) A morphological and functional study of Congenital Hereditary Endothelial Dystrophy. *Acta Ophthalmologica Scandinavica.* 76: 314-318

Elliott G, and Hodson S (1998) Cornea, and the swelling of polyelectrolyte gels of biological interest. *Reports on Progress in Physics.* 61: 1325-1365

Engelmann K, Bohnke M, and Friedl P (1988) Isolation and Long-Term Cultivation of Human Corneal Endothelial Cells. *Investigative Ophthalmology & Visual Science.* 29: 1656-1662.

Engler C, Kelliher C, Spitze AR, Speck CL, Eberhart CG and Jun AS (2010). Unfolded protein response in Fuchs' endothelial corneal dystrophy: a unifying pathogenic pathway? *American Journal of Ophthalmology*. 149: 194–202.

Esko JD, Kimata K and Lindahl U (2009) Proteoglycans and Sulfated Glycosaminoglycan's. In: *Essentials of Glycobiology*. 2nd edition. Cold Spring Harbor (NY): Cold Spring Harbor Laboratory Press

Ewer M (1970) Early development of Stroma Corneae and Pupillary Membrane in Humans. *Acta Anatomica.* 75: 37.

Fabricant R, Salisbury J, Berkowitz R, and Kaufman H (1982) Regenerative effects of epidermal growth factor after penetrating keratoplasty in primates. *Archives of Ophthalmology.* 100: 994-995.

Farrell R, and Hart R (1969) On the theory of spatial organization of macromolecules in connective tissues. *Bulletin of Mathematical Biophysics.* 31: 727-760.

Feldman S, Gately D, Schonthal A, and Feramisco J (1992) Fos expression and growth regulation in bovine corneal endothelial cells. *Investigative Ophthalmology & Visual Science*. 33: 3307-3314.

Fischbarg J, and Lim J (1974) Role of cations, anions, and carbonic anhydrase in fluid transport across rabbit corneal endothelium. *Journal of Physiology.* 241: 647-675.

Fitch JM (1990). The spatial organization of Descemet's membrane-associated type IV collagen in the avian cornea. *The Journal of Cell Biology.* 110: 1457–1468.

Fitch JM, Gross J, Mayne R, Johnson-Wint B and Linsenmayer TF (1984) Organization of collagen types I and V in the embryonic chicken cornea: monoclonal antibody studies. *Proceedings of the National Academy of Sciences of the United States of America.* 81: 2791–2795.

Fitch JM, Mentzer A, Mayne R and Linsenmayer TF (1988) Acquisition of type-IX collagen by the developing avian primary corneal stroma and vitreous. *Developmental Biology.* 128: 396–405.

Fitch JM, Kidder JM and Linsenmayer TF (2005) Cellular invasion of the chicken corneal stroma during development: Regulation by multiple matrix metalloproteases and the lens. *Developmental Dynamics*. 232:106-118

Frank J (ed) (2006) Electron Tomography :Methods for Three-Dimensional Visualization of Structures in the Cell. 2nd Edition. Springer.

Fuchs' E (1910) Dystrophia epithelialis corneae. Albrecht von Graefes Archiv für *Ophthalmologie*. 76:478

Funderburgh J, Caterson B, and Conrad G (1986) Keratan sulfate PG during embryonic development of the chicken cornea. *Developmental Biology.* 116: 267-277.

Funderburgh J, Funderburgh M, Brown S, Vergnes J, Hassell J, Mann M and Conrad G (1993) Sequence and structural implications of a bovine corneal keratan sulphate PG core protein. Protein 37B represents bovine lumican and proteins 37A and 25 are unique. *Journal of Biological Chemistry.* 268: 11874-11880.

Gandhi NS and Mancera RL (2008) The Structure of Glycosaminoglycan's and their Interactions with Proteins. *Chemical Biology and Drug Design.* 72: 455-482

Geroski DH, Matsuda M, Yee RW, Edelhauser HF and Sugar J (1985). Pump function of the human corneal endothelium-effects of age and cornea guttata. *Ophthalmology.* 92:759-763

Gordon M K, Foley J, Birk D E, and Linsenmayer C (1994) Type-V Collagen and Bowmans Membrane- Quantitation of Messenger-RNA in Corneal Epithelium and Stroma. *Journal of Biological Chemistry.* 269: 24959-24966

Gordon S (1988) Changes in distribution of extracellular matrix proteins during wound repair in corneal endothelium. *Journal of Histochemistry and Cytochemistry.* 36: 409-416.

Gordon MK, Gerecke DR, Dublet B, Van der Rest M and Olsen BR (1989) Type XII collagen. A larger multidomain molecule with partial homology to type IX collagen. *Journal of Biological Chemistry*. 264: 19772-19778

Gorovoy MS (2006) Descemet's-stripping automated endothelial keratoplasty. *Cornea.* 25: 886–9.

Gospodarowicz D, Mescher A, and Birdwell C (1977) Stimulation of Cornea1 Endothelial Cell Proliferation in vitro by Fibroblast and Epidermal Growth Factors. *Experimental Eye Research.* 25: 75-89.

Gospodarowicz D, Greenburg G, Vlodavsky I, Alvardo J, and Johnson L (1979) The identification and localization of fibronectin in cultured corneal endothelial cells: Cell surface polarity and physiological implications. *Experimental Eye Research.* 29: 485-509.

Gottsch JD, Sundin OH, Liu SH, Jun AS, Broman KW, Stark WJ, Vito ECL et al (2005). Inheritance of a novel COL8A2 mutation defines a distinct early-onset subtype of Fuchs' corneal dystrophy. *Investigative Ophthalmology & Visual Science.* 46:1934–1939.

Grimes PA, Stone RA, Laties AM, and Li W (1982) Carboxyfluorescein. A probe of the blood-ocular barriers with lower membrane permeability than fluorescein. *Archives of Ophthalmology* 100: 635-639

Green K (1991) Corneal endothelial structure and function under normal and toxic conditions. *Cell Biology Reviews* 25: 169-207

Gross E, Hawkins K, Abuladze N, Pushkin A, Cotton C, Hopfer U, and Kurtz I (2001a) The stoichiometry of the electrogenic sodium bicarbonate cotransporter NBC1 is cell-type dependent. *Journal of Physiology*: 597-603.

Ham L, Balachandran C, Verschoor C, Van Der Wees, J and Melles G (2009) Visual rehabilitation rate after isolated Descemet's membrane transplantation Descemet membrane endothelial keratoplasty. *Archives of Ophthalmology*. 127: 252–255.

Hanna C, Bicknell D, and O'Brian J (1961) Cell turnover in the adult human eye *Archives in Ophthalmology.* 65:695-698

Hart G (1976) Biosynthesis of glycosaminoglycan's during corneal development. *Journal of Biological Chemistry.* 251: 6573-6521.

Hart R and Farrell R (1969) Light Scattering in the Cornea. *Journal of the Optical Society of America* 59: 776-773.

Hassell J, Cintron C, Kublin C and Newsome D (1983) Proteoglycan changes during restoration of transparency in corneal scars. *Archives of Biochemistry and Biophysics* 222: 362-369.

Hassell JR, Kimura JH and Hascall V (1986) Proteoglycan core protein families. *Annual Review of Biochemistry*. 55: 539-567

Hatanaka H, Koizumi N, Okumura N, Takahashi H, Tanioka H, Young RD, Jones FE, et al. (2012). A study of host corneal endothelial cells after non-Descemet stripping automated endothelial keratoplasty. *Cornea*. 32:76-80

Hay ED and Dodson JW (1973). Secretion of collagen by corneal epithelium. I. Morphology of the collagenous products produced by isolated epithelia grown on frozen-killed lens. *The Journal of Cell Biology* 57: 190–213.

Hay ED and Revel J (1969) *Fine structure of the developing avian cornea*. Basel, New York, Karger, 1969.

Hecquet C, Morisset S, Lorans G, Plouet J and Adolphe M (1990) Effects of acidic and basic fibroblast growth factors on the proliferation of rabbit corneal cells. *Current Eye Research.* 9: 429-433

Hendrix M, Hay E, Mark K, and Linsenmayer T (1982) Immunohistochemical localization of collagen types I and II in the developing chick cornea and tibia by electron microscopy. *Investigative Ophthalmology & Visual Science* 22: 359-375.

Hirsch M, Renard G, Faure J, and Pouliquen Y (1976) Formation of Intercellular Spaces and Junctions in Regenerating Rabbit Corneal Endothelium. *Experimental Eye Research* 23: 385-397.

Hirsch M, Renard G Faure, JP and Pouliquen Y (1977) Study of ultrastructure of rabbit corneal endothelium by freeze-fracture technique - apical and lateral junctions. *Experimental Eye Research* 25: 277-288.

Hodson S (1971) Evidence for a bicarbonate-dependent sodium pump in corneal endothelium. *Experimental Eye Research* 11: 20-29.

Hodson S (1974) The regulation of corneal hydration by a salt pump requiring the presence of sodium and bicarbonate ions. *Journal of Physiology* 236: 271-302.

Hodson S and Mayes KR. (1978). Inter-cellular spaces and coupled water transport in rabbit cornea. *Journal of Physiology*. 284:146–146.

Hodson SA and Hodson GA (1988) The absence of bicarbonate-stimulated ATPase activity in the plasma membranes of the bicarbonate secreting ox corneal endothelial cells. *Biochimica et Biophysica Acta (BBA) – Biomembranes* 937: 241-246

Hodson S, and Miller F (1976) The Bicarbonate Ion Pump in the Endothelium which Regulates the Hydration of Rabbit Cornea. *Journal of Physiology* 263: 563-577.

Hongo M, Itoi M, Yamaguchi N, and Imanishi J (1992) Distribution of epidermal growth factor (EGF) receptors in rabbit corneal epithelial cells, keratocvtes and endothelial cells, and the changes induced by transforming growth factor-131. *Experimental Eye Research* 54: 9-16.

Hopfer U, Fukai N, Hopfer H, Wolf G, Joyce N, Li E and Olsen BR (2005) Targeted disruption of Col8a2 and Col8a2 genes in mice leads to anterior segment abnormalities in the eye. *FASEB Journal* 10:1232-1244

Hoppenreijs V, Pels E, Vrensen G, Felton PC and Treffers WF (1993) Platelet-Derived Growth Factor: Receptor Expression in Corneas and Effects on Corneal Cells. *Ophthalmology & Visual Science* 34:637-649

Hoppenreijs V, Pels E, Vrensen G, and Treffers W (1994) Effects of platelet-derived growth factor on endothelial wound healing of human corneas. *Investigative Ophthalmology & Visual Science* 35: 150-161.

Huff J and Green K. (1981). Demonstration of active sodium-transport across the isolated rabbit corneal endothelium. *Current Eye Research*. 2: 113–114.

Huff J and Green K. (1983). Characteristic of bicarbonate, sodium, and chloride fluxes in the rabbit corneal endothelium. *Experimental Eye Research*. 36: 607–615.

Iozzo RV, Moscatello AD, McQuillan DJ and Eichstetter (1999) Decorin is a biological ligand for the epidermal growth factor receptor. *Journal of Cell Biology.* 274:4489-4492

Ishino Y, Sano Y, Nakamura T, Connon CJ, Rigby H, Fullwood N and Kinoshita S (2004.) Amniotic membrane as a carrier for cultivated human corneal endothelial cell transplantation. *Investigative Ophthalmology & Visual Science*. 45:800–806.

Iwamoto T and DeVoe AG (1971) Electron microscopic studies on Fuchs'' combined dystrophy. I. Posterior portion of the cornea. *Investigative Ophthalmology and Visual Sciences* 10:9–28

Jakus MA (1956) Studies on the cornea. II. The fine structure of Descemet's membrane. *The Journal of Biophysical and Biochemical Cytology.* 25:243-252.

Jenstch T, Keller S, Kock M, and Wiederholt M (1984) Evidence for Coupled Transport of Bicarbonate and Sodium in Cultured Bovine Corneal Endothelial Cells. *The Journal of Membrane Biology.* 81: 189-204.

Jentsch T, Stahlknecht T, Hollwede H, Fischer D, Keller S and Wiederholt M (1985) A bicarbonate-dependent process inhabitable by disulfonic stilbenes and a Na+/H+ exchange mediate Na-22(+) uptake into cultured bovine corneal endothelium. *Journal of Biological Chemistry.* 260:795–801.

Jentsch T, Keller S, and Wiederholt M (1985) Ion Transport Mechanisms in Cultured Bovine Corneal Endothelial Cells. *Current Eye Research.* 4: 361-369.

Johnston M C, Noden D M, Hazelton R D, Coulombre J L, and Coulombre AJ (1979) Origins of avian ocular and periocular tissues. *Experimental Eye Research.* 29: 27-43.

Joyce NC, Meklir B, Joyce SJ and Zieske JD (1996) Cell cycle protein expression and proliferative status in human corneal cells. *Investigative Ophthalmology Visual Science* 37:645–655

Joyce N C, Harris D, and Mello D (2002) Mechanisms of mitotic inhibition in corneal endothelium: contact inhibition and TGF-β2. *Investigative Ophthalmology & Visual Science* 43: 2152-2159.

Joyce N C, Meklir B and Neufeld A H (1990) In Vitro Pharmacologic Separation of Corneal Endothelial Migration and Spreading Responses. *Investigative Ophthalmology & Visual Science.* 34: 1816- 1826.

Jumblatt M (1981). Intracellular potentials of cultured rabbit corneal endothelial cells: Response to temperature and ouabain. *Vision Research.* 21; 45–47

Jun AS, Meng H, Ramanan N, Matthaei M, Chakravarti S, Bonshek R, Black GCM et al (2012) An alpha 2 collagen VIII transgenic knock-in mouse model of Fuchs' endothelial corneal dystrophy shows early endothelial cell unfolded protein response and apoptosis. *Human Molecular Genetics* 21:384–93.

Kadler K, Hojima Y and Prockop D (1987) Assembly of collagen fibrils de novo by cleavage of the type I PC-collagen with procollagen C-proteinase assay of critical concentration demonstrates that collagen self-assembly is a classical example of an entropy driven process. *Journal of Biological Chemistry*. 262: 15696–15701.

Kameda T, Inoue T, Inatani M, Fujimoto T, Honjo M, Kasaoka N, Inoue-Mochita, M., et al (2012) The Effect of Rho-Associated Protein Kinase Inhibitor on Monkey Schlemm's Canal Endothelial Cells. *Investigative Ophthalmology & Visual Science*. 53: 3092–103.

Kao W and Liu C (2003) Roles of lumican and keratocan on corneal transparency. *Glycoconjugate Journal.* 19: 275-285.

Kapoor R., Sakai LY, Funk S, Roux E, Bornstein P and Sage EH (1988) Type VIII collagen has a restricted distribution in specialized extracellular matrices. *The Journal of Cell Biology*. 107: 721–30.

Kaufman H, and Katz J (1977) Pathology of the corneal endothelium. *Investigative Ophthalmology & Visual Science* 16: 265-268.

Kaye G, Sibley R, and Hoefle F (1973) Recent studies on the nature and function of the corneal endothelial barrier. *Experimental Eye Research* 15: 585-613.

Kay E, Gu X, Ninomiya Y, and Smith R (1993) Corneal endothelial modulation: a factor released by leukocytes induces basic fibroblast growth factor that modulates cell shape and collagen. *Investigative Ophthalmology & Visual Science* 34: 663-672.

Keenan TDL, Carley F, Yeates D, Jones MNA, Rushton S and Goldacre MJ (2010) Trends in corneal graft surgery in the UK. *British Journal of Ophthalmology*. 95:468-472

Kefalides N, Cameron J, Tomichek E, and Yanoff A (1976) Biosynthesis of basement membrane collagen by rabbit corneal endothelium in vitro. *Journal of Biological Chemistry* 251: 730-733.

Kenyon K (1969) The synthesis of the basement membrane of the corneal epithelium in bulbous keratopathy *Investigative Ophthalmology* 8: 156-168.

Kenyon K, and Maumenee A (1973) Further studies of congenital hereditary endothelial dystrophy of the cornea. *American Journal of Ophthalmology* 76: 419-439.

Kielty CM and Grant ME (2003) The Collagen Family: Structure, Assembly, and Organization in the Extracellular Matrix, in Connective Tissue and Its Heritable Disorders. In *Molecular, Genetic, and Medical Aspects.* 2nd ed. John Wiley & Sons, Inc., Hoboken, NJ, USA.

Kinsey V and Cogan D (1942) The cornea IV. Hydration properties of the whole cornea. *Archives of Ophthalmology*. 28: 449–463

Klintworth GK (2009). Corneal dystrophies. *Orphanet Journal of Rare Diseases*. *4*: 1–38.

Kobayashi A, Yokogawa H and Sugiyama K (2008) Non-Descemet Stripping Automated Endothelial Keratoplasty for Endothelial Dysfunction Secondary to Argon Laser Iridotomy. *American Journal of Ophthalmology* 146: 543-549

Kobayashi A, Mawatari Y, Yokogawa H and Sugiyama K (2008) In vivo laser confocal microscopy after descemet stripping with automated endothelial keratoplasty. *American Journal of Ophthalmology*. 145: 977-985.

Kobayashi A, Yokogawa H and Sugiyama K (2009) In vivo laser confocal microscopy after non-Descemet's stripping automated endothelial keratoplasty. *Ophthalmology*. 116: 1306–1313.

Koizumi N, Sakamoto Y, Okumura N, Okahara N, Tsuchiya, H, Torii R, Cooper L, et al (2007) Cultivated corneal endothelial cell sheet transplantation in a primate model. *Investigative Ophthalmology & Visual Science*. 48: 4519–4526.

Krachmer J (1985) Posterior polymorphous corneal dystrophy: a disease characterized by epithelial-like endothelial cells which influence management and prognosis. *Transactions of the American Ophthalmology Society*. 83:413-475

Kuang K, Xu M, Koniarek J P, and Fischbarg J (1990) Effects of ambient bicarbonate, phosphate and carbonic anhydrase inhibitors on fluid transport across rabbit corneal endothelium. *Experimental Eye Research* 50: 487-493.

Kwan APL, Cummings CE, Chapman JA and Grant ME (1991). Mascromolecular organization of chicken type X collagen in vitro. *Journal of Cellular Biology* 114:597-604.

Laing R A, Sandstrom M M, Berrospi A R, and Leibowitz H M (1976) Changes in Corneal Endothelium as a Function of Age. *Experimental Eye Research* 22: 587-594.

Landshman N, Ben-Hanan I, Assia E, Ben-Chaim O, and Belkin M (1988) Relationship between morphology and functional ability of regenerated corneal endothelium. *Investigative Ophthalmology & Visual Science* 29: 1100-1109.

Levy S, McCartney A, Baghai M, Barrett M, and Moss J (1995) Pathology of the iridocorneal-endothelial syndrome: The ICE-cell. *Investigative Ophthalmology & Visual Science* 363: 2592-2601.

Lewis P, Pinali C, Young R, Meek K, Quantock A, and Knupp C (2010) Structural interactions between collagen and Proteoglycans are elucidated by three-dimensional electron tomography of bovine cornea. *Cell Press* 18: 239-245.

Li W, Vergnes JP, Cornuet PK and Hassell JR(1992) cDNA clone to chick corneal chondroitin/dermatan sulfate proteoglycan reveals identity to decorin. *Archives of Biochemistry and Biophysics*. 296:190-197

Liebovitch L, and Fischbarg J (1982) Effects of inhibitors of passive Na+ and HCO3- fluxes on electrical potential and fluid transport across rabbit corneal endothelium. *Current Eye Research*. 2*:* 183–186.

Liles M, Palka BP, Harris A, Hughes C, Young RD, Meek KM, Caterson B and Quantock AJ (2010) Differential relative sulfation of keratan sulphate glycosaminoglycan in the chick cornea during embryonic development. *Investigative Ophthalmology and Visual Sciences.* 51:1365-1372

Lim J and Fischbarg J (1981) Electrical-properties of rabbit corneal endothelium as determined from impedance. *Biophysical Journal*. 36*:* 677–695.

Lin R and Maloney R (1999) Flap complications associated with lamellar refractive surgery. *American Journal of Ophthalmology.* 127: 129–136.

Linsenmayer TF, Smith G and Hay E (1977) Synthesis of 2 collagen types by embryonic chick corneal epithelium in vitro. *Proceedings of the National Academy of Sciences of the United States of America*. 74: 39–43.

Linsenmayer TF, Fitch JM and Mayne R (1984) Extracellular matrices in the developing avian eye-type-V collagen in corneal and noncorneal tissues. *Investigative Ophthalmology Visual Science*. 47:41-47.

Linsenmayer TF, Gibney E, Gordon MK, Marchant JK, Hayashi M and Fitch JM (1990) Extracellular matrices of the developing chick retina and cornea-localization of messenger-RNAs for collagen type-II and type-IX by insitu hybridization. *Investigative Ophthalmology and Visual Sciences*. 31:1271-1276.

Mann K, Jander R, Korsching E, Kuhn K and Rauterberg J (1990) The primary structure of a triple-helical domain of collagen type-VIII from bovine Descemet's-membrane. *FENS letters*. 273:168-172.

Masaki T, Kobayashi A, Yokogawa H, Saito Y and Sugiyama K (2012) Clinical evaluation of non-Descemet's stripping automated endothelial keratoplasty (nDSAEK). *Japanese Journal of Ophthalmology*. *56*: 203–207.

Materson E, Edelhauser H and Horn DLV (1977) The role of thyroid hormone in the development of the chick corneal endothelium and epithelium. *Investigative Ophthalmology & Visual Science*. *16*: 105–115.

Maurice D (1957) The Structure and Transparency of the Cornea. *Journal of Physiology* 136: 263-286.

McCauley M, Price F and Price MO (2009) Descemet's membrane automated endothelial keratoplasty. *Journal of Cataract and Refractive Surgery*. 35:1659–1664.

Means T, Geroski D, Hadley A, Lynn M and Edelhauser H (1995) Viability of human corneal endothelium following Optisol-GS storage. *Archives of Ophthalmology*. 113: 805–809.

Mehta D and Malik A (2006) Signalling mechanisms regulating endothelial permeability. *Physiological Reviews*. *86*: 279–367.

Melles G, Eggink F, Lander F, Pels E, Rietveld F, Beekhuis W and Binder P (1998) A surgical technique for posterior lamellar keratoplasty. *Cornea*. *17*: 618–625.

Melles G, Lander F, Rietveld F, Remeijer L, Beekhuis W and Binder P (1999) A new surgical technique for deep stromal, anterior lamellar keratoplasty. *British Journal of Ophthalmology*. *83*: 327–333.

Melles G, Lander F, Dooren BTHV, Pels E and Beekhuis W (2000) Preliminary clinical results of posterior lamellar keratoplasty through a sclerocorneal pocket incision. *Ophthalmology*. *107*: 1850–1856.

Melles GRJ, Lander F and Rietveld FJR (2002) Transplantation of Descemet ' s Membrane Carrying Viable Endothelium Through a Small Scleral Incision. *Cornea*. *21:* 415–418

Melles GRJ, Wijdh R and Nieuwendaal C (2004) A technique to exercise the Descemet's membrane from a recipient cornea (descemetorhexis). *Cornea*. *23*: 286–288.

Miller A (1976) Molecular packing in collagen fibrils. In *Biochemistry of Collagen* (Ramachandran GN, Reddi AH, eds), pp 85–136, Plenum, New York.

Mimura T, Amano S, Usui T, Araie M, Ono K, Akihiro H, Yokoo S, et al (2004) Transplantation of corneas reconstructed with cultured adult human corneal endothelial cells in nude rats. *Experimental Eye Research*. 79: 231–237.

Montiani-Ferreira F, Cardoso F and Petersen-Jones S (2004) Postnatal development of central corneal thickness in chicks of Gallus gallus domesticus. *Veterinary Ophthalmology*. 7: 37–9.

Morton K, Hutchinson C, Jeanny J, Karpouzas I, Pouliquen Y, and Courtois Y (1989) Colocalization of fibroblast growth factor binding sites with extracellular matrix components in normal and keratoconus corneas. *Current Eye Research* 8: 975-987.

Muller L, Pels E, Schurmans L, and Vrensen G (2004) A new three-dimensional model of the organization of Proteoglycans and collagen fibrils in the human corneal stroma. *Experimental Eye Research* 78: 493-501.

Murphy C, Alvarado J, and Juster R (1984) Prenatal and Postnatal Growth of Human Descemet's Membrane. *Investigative Ophthalmology & Visual Science* 25: 1402-1415.

Nakayasu K, Tanaka M, Konomi H and Hayshi T (1986) Distribution of type-I, type II, type IV and type V collagen in normal and keratoconus corneas. *Ophthalmic Research*. 18:1-10

Nayak S, and Binder P (1984) The growth of endothelium from human corneal rims in tissue culture. *Investigative Ophthalmology & Visual Science* 25: 1213-1216.

Ninomiya Y, Castagnola P, Gerecke D, Gordon MK, Jacenko O, LuValle P, McCarthy M, Muragaki Y, Nishimura I, Oh S, Rosenblum N, Sato N, Sugrue S, Taylor R, Vasios G, Yamaguchi N, Olsen BR (1990) The molecular biology of collagens with short triple-helical domains. *In Extracellular Matrix Genes*. New York: Academic Press, Inc.;:pp 79–114

Okumura N, Ueno M, Koizumi N, Sakamoto Y, Hirata K, Hamuro J and Kinoshita S (2009). Enhancement on primate corneal endothelial cell survival in vitro by a ROCK inhibitor. *Investigative Ophthalmology & Visual Science*. 50: 3680–3687.

Okumura N, Koizumi N, Ueno M, Sakamoto Y, Takahashi H, Tsuchiya H, Hamuro, J, et al (2012) ROCK inhibitor converts corneal endothelial cells into a phenotype capable of regenerating in vivo endothelial tissue. *The American Journal of Pathology*. 181: 268–277.

Olson M, Ashworth A and Hall A (1995) An essential role for Rho, Rac and Cdc42 GTPases in cell cycle progression through G2. *Science*. 269: 1270–1272.

Ozanics V, Rayborn N, and Sagun D (1977) Observations on morphology of developing primate cornea-epithelium, its innervation and anterior stroma. *Journal of Morphology* 153: 263-297.

Perlman M, and Baum J (1974) Synthesis of a collagenous basal membrane by rabbit corneal endothelial cell. *Archives in Ophthalmology* 92: 238-239.

Piez KA, Eigner EA and Lewis MS (1963) The chromatographic separation and amino acid composition of the subunits of several collagens. *Biochemistry* 2:58–66.

Price FW and Price MO (2005) Descemet's Stripping With Endothelial Keratoplasty in 50 Eyes: A Refractive Neutral Corneal Transplant. *Journal of Refractive Surgery*. 21: 339–345.

Price FW and Price MO (2006). Endothelial keratoplasty to restore clarity to a failed penetrating graft. *Cornea*. 25*:*895–9.

Price MO, and Price FW (2007) Descemet's stripping endothelial keratoplasty. *Current Opinion in Ophthalmology* 18: 290-294

Price MO and Price FW (2010) Endothelial keratoplasty - a review. *Clinical & Experimental Ophthalmology*. 38: 128–40.

Quantock AJ, Kinoshita S, Capel MS and Schanzlin DJ (1998). A Synchotron X-ray diffraction study of developing chick corneas. *Biophysics Journal.* 74: 995-998.

Rainer G, Petternel V, Findl O, Schmetterer L, Skorpik C, Luksch A and Drexler W (2002). Comparison of ultrasound pachymetry and partial coherence interferometry in the measurement of central corneal thickness. *Journal of Cataract and Refractive Surgery*. 28: 2142–5.

Raymond G, Jumblatt M, Bartels S, and Neufeld A (1986) Rabbit corneal endothelial cells in vitro: Effects of EGF. *Investigative Ophthalmology & Visual Science* 27: 474-479.

Ress DB, Harlow ML, Marshall RM and McMahan UJ (2004). Methods for generating high-resolution structural models from electron microscope tomography data. *Structure*. 12: 1763-1774

Richardson W, and Hettinger M (1985) Endothelial and epithelial-like cell formations in a case of posterior polymorphous dystrophy. *Archives in Ophthalmology* 103: 1520-1524.

Ridley AJ and Hall A (1992) The small GTP-binding protein rho regulates the assembly of focal adhesions and actin stress fibers in response to growth factors. *Cell*. 70: 389–99.

Riley MV (1971) The role of the epithelium in control of corneal hydration. *Experimental Eye Research*. 12: 128–37.

Riley M, Winkler B, Czajkowski C, and Peters M (1995) The roles of bicarbonate and CO_2 in transendothelial fluid movement and control of corneal thickness. *Investigative Ophthalmology and Visual Science* 36: 103-112.

Romero M and Boron W (1999) Electrogenic Na^+/HCO_3-cotransporter: cloning and physiology. *Annual review of Physiology*. 61: 699–723.

Romero M, Fong P, Berger U, Hediger M and Boron W (1998) Cloning and functional expression of rNBC, an electrogenic Na(+)-HCO3(-) cotransporter from rat kidney. *American Journal of Physiology-Renal Physiology*. 274: 425–432.

Rosenblum ND, Briscoe DM, Karnovsky MJ and Olsen BR (1993) Alpha 1-VIII collagen is expressed in the rat glomerulus and in resident glomerular cells. *American Journal of Physiology*. 264:1003-1010.

Sage H, Trüeb B and Bornstein P (1983) Biosynthetic and structural properties of endothelial cell type VIII collagen. *The Journal of Biological Chemistry*. *258:* 13391–401.

Samples J, Binder P, and Nayak S (1991) Propagation of human corneal endothelium in vitro effect of growth factors. *Experimental Eye Research* 52: 121-128.

Sawada H,Konomi H and Nagai Y(1984).The basement membrane of bovine endothelial corneal cells in culture with β-aminopropionitrile: Biosynthesis of hexagonal lattices composed of a 160 nm dumbbell- shaped structure. *European Journal of Cell Biology* 35:226–234.

Sawada H, Konomi H and Hirosawa, K (1990) Characterization of the Collagen in the Hexagonal Lattice of Descemet's Membrane: Its Relation to Type VIII Collagen

Immunoelectron Microscopy of Matrices lmmunoelectron Microscopy of DMs In Situ. *Journal of Cell Biology*. *110:* 219–227.

Schimmelpfennig B (1984) Direct and indirect determination of nonuniform cell density distribution in human corneal endothelium. *Investigative Ophthalmology & Visual Science* 25: 223-229.

Scott JE (1975) Physiological Function and Chemical Composition of Pericellular Proteoglycan (an Evolutionary View). *Philosophical Transactions of the Royal Society*. 271 235-242

Scott J (1992) Morphometry of cupromeronic blue-stained PG molecules in animal corneas, versus that of purified PG molecules in animal corneas, versus that of purified Proteoglycans stained in vitro, implies that tertiary structures contribute to corneal ultrastructure. *Journal of Anatomy.* 180: 155-164.

Scott JE (1996) Proteodermatan and proteokeratan sulfate (decorin, lumican/fibromodulin) proteins are horseshoe shaped. Implications for their interactions with collagen. *Biochemistry.* 35:8795–8799

Scott J, and Haigh M (1985) Small PG- collagen interactions-keratin sulphate proteoglycans associates with rabbit corneal collagen fibrils at the A-bands and c-bands. *Bioscience Reports* 5: 765-774.

Senoo T, Obara Y, and Joyce N C (2000) EDTA: a promoter of proliferation in human corneal endothelium. *Investigative Ophthalmology and Visual Science* 41: 2930-2935.

Senoo T, and Joyce N C (2000) Cell cycle kinetics in corneal endothelium from old and young donors. *Investigative Ophthalmology & Visual Science* 41: 660-667.

Shuttleworth CA (1997) Type VIII collagen. *The International Journal of Biochemistry & Cell Biology*. 29:1145–8.

Siegler V, and Quantock A (2002). Two-stage compaction of the secondary avian cornea during development. *Experimental Eye Research*. 74:427–431.

Smelser GK and Ozanics V (1965) New concepts in anatomy and histology of the cornea. In: King JH, McTigue JW, eds. *The Cornea.* Washington, DC: Butterworth, London. 1-20.

Speakman J (1959) Endothelial cell vacuolation in the cornea. *The British Journal of Ophthalmology*. 43:139–46.

Sramek S, Wallow I, Bindley C, and Sterken G (1987) Fibronectin Distribution in the Rat Eye. *Investigative Ophthalmology & Vision Science.* 28: 500-505.

Srinivas SP, Satpathy M Gallagher P Lariviere E and Van Driessche W (2004) Adenosine induces dephosphorylation of myosin II regulatory light chain in cultured bovine corneal endothelial cells. *Experimental Eye Research* 79: 543-541

Srinivas SP and Sangly P (2010) Dynamic regulation of barrier integrity of the corneal endothelium. *Optometry and Vision Science*. 87: 239-254

Stiemke M, McCartney M, Cantu- Crouch D and Edelhauser H (1991) Maturation of the corneal endothelial tight junction. *Investigative Ophthalmology & Visual Science.* 32:2757-2765.

Sun X, Bonanno J, Jelamskii S, and Xie Q (2000) Expression and localization of Na1-HCO32 cotransporter in bovine corneal endothelium. *American Journal of Physiology.* 279: 1648-1655.

Sun X, and Bonanno J (2003) Identification and Cloning of the Na/HCO3- Cotransporter (NBC) in Human Corneal Endothelium. *Experimental Eye Research* 77: 287-295.

Svedbergh B, and Bill A (1972) Scanning electron microscopic studies of the corneal endothelium in man and monkeys. *Acta Ophthalmologica.* 50: 321-326.

Svoboda KK, Nishimura I, Sugrue S, Ninomiya Y and Olsen B (1988) Embryonic chicken cornea and cartilage sythesize type-IX collagen molecules with different amino-terminal domains. *Proceedings of the National Academy of Sciences of the United States of America*. 85: 7496–7500.

Szegezdi E, Logue SE, Gorman AM and Samali A (2006) Mediators of endoplasmic reticulum stress-induced apoptosis. *EMBO Reports.* 7:880-885.

Tamura Y, Konomi H, Sawada H, Takashima S, and Nakajima A (1991) Tissue Distribution of Type VIII Collagen in Human Adult and Fetal Eyes. *Investigative Ophthalmology & Visual Science* 32: 2636-2644.

Terry M and Ousley PJ (2001). Replacing the endothelium without corneal surface incisions or sutures- The first United States clinical series using the deep lamellar endothelial keratoplasty procedure. *Ophthalmology*. 110:755–764.

Terry MA and Ousley PJ (2003) In pursuit of emmetropia: Spherical equivalent refraction results with deep lamellar endothelial keratoplasty (DLEK). *Cornea.* 22: 619–626.

Terry MA and Ousley PJ (2005) Small-incision deep lamellar endothelial keratoplasty (DLEK). *Cornea*. 24: 59–65.

Tervo T, Sulonen J, Valtonen S, Vannas A, and Virtanen I (1986) Distribution of Fibronectin in Human and Rabbit Corneas. *Experimental Eye Research* 42: 399-406.

Toole B, and Gross J (1971) Extracellular matrix of regenerating newt limb-synthesis and removal of hyaluronate prior to differentiation. *Developmental Biology* 25: 57-77.

Toole B, and Trelstad R (1971) Hyaluronate production and removal during corneal development in the chick. *Developmental Biology* 26: 28-35.

Trelstad R, Hayashi K, and Toole B (1974) Epithelial collagens and Glycosaminoglycan's in the Embryonic cornea. *The Journal of Cell Biology* 62: 815-830.

Uehata M, Ishizaki T, Satoh H, Ono T, Kawahara T, Morishita T, Tamakawa H, et al (1997) Calcium sensitization of smooth muscle mediated by a Rho-associated protein kinase in hypertension. *Nature*. 389: 990–994.

Usui T, Seki G, Amano S, Oshika T, Miyata K, Kunimi M, Taniguchi S, et al (1999) Functional and molecular evidence for Na(+)-HCO3- cotransporter in human corneal endothelial cells. *Pflügers Archiv - European Journal of Physiology*. 438: 458–462.

Von Der Mark K, Von der Mark H, Timpl R, and Trelstad R (1977) Immunofluorescent localization of collagen types I, II, and III in the embryonic chick eye. *Developmental Biology* 59:75-85

Wantanabe S, Nishikawa S, Muguruma K and Sasai Y (2007) A ROCK inhibitor permits survival of dissociated human embryonic stem cells. *Nature Biotechnology*. 25: 681–686.

Waring G (1982) Posterior collagenous layer of the cornea-ultrastructural classification of abnormal collagenous tissue posterior to Descemet's membrane in 30 cases. *Archives of Ophthalmology*. 100: 122–134.

Waring G, Rodrigues M, and Laibson P (1978) Corneal dystrophies. II. Endothelial dystrophies. *Survey of Ophthalmology* 23: 147-168.

Watsky M, McCartney M, Mclaughlin B, and Edelhauser H (1990) Corneal Endothelial Junctions and the Effect of Ouabain. *Investigative Ophthalmology & Visual Science* 31: 933-941.

Weber IT, Harrison RW and Iozzo RV (1996) Model structure of decorin and implications for collagen fibrillogenesis. *The Journal of Biological Chemistry*. 271: 31767–31770.

Whikehart D, Vaughn A, Holley G, and Edelhauser H (2002) Telomerase activity in the human corneal endothelial limbus. *ARVO* 2002 Annual Meeting Abstract and Program Planner accessed at www.arvo.org.: Abstract#1627.

Wiederholt M and Koch M (1978) Intracellular-potentials of isolated rabbit and human corneal endothelium. *Experimental Eye Research*. 27: 511–518.

Wigham C, Guggenheim J, and Hodson S (1994) Sodium movement into and out of corneal endothelium. *European Journal of Physiology* 428: 577-582.

Wigham C and Hodson S (1985) The movement of sodium across short-circuited rabbit corneal endothelium. *Current Eye Research*. 4:1241–1245.

Wilson S, Bourne W M, and Brubaker R F (1988) Effect of dexamethasone on corneal endothelial dysfunction in Fuchs'' dystrophy. *Investigative Ophthalmology & Visual Science* 29: 357-361.

Wilson SE and Bourne WM (1988) Fuchs'' dystrophy. *Cornea* 7:2–18

Woost P, Jumblatt M, Eiferman R, and Schultz G (1992) Growth factors and corneal endothelial cells: I. Stimulation of bovine corneal endothelial cell DNA synthesis by defined growth factors. *Cornea* 11: 1-10.

Wulle K and Lerche W (1969) Electron microscopic observations of the early development of the human corneal endothelium and Descemet's membrane. *Ophthalmologica.* 157:451-461.

Wulle K (1972) Electron microscopy of the fetal development of the corneal endothelium and Descemet's membrane of the human eye. *Investigative Ophthalmology*. 11:897-904.

Yamaguchi N, Benya P, van der Rest M and Ninomiya Y (1989) The cloning and sequencing of alpha 1(VIII) collagen cDNAs demonstrate that type VIII collagen is a short chain collagen and contains triple-helical and carboxyl-terminal non-triple-helical domains similar to those of type X collagen. *The Journal of Biological Chemistry*. 264: 16022–16029.

Zhao Z and Rivkees S (2003) Rho-associated kinases play an essential role in cardiac morphogenesis and cardiomyocyte proliferation. *Developmental Dynamics*. 226: 24–32.

Zhang C, Bell WR, Sundin OH, De La Cruz Z, Stark WJ, Green WR and Gottsch JD (2006) Immunohistochemistry and electron microscopy of early-onset Fuchs' corneal dystrophy in three cases with the same L450W COL8A2 mutation. *Transactions of the American Ophthalmological Society*. 104: 85–97.

Online References

Royles Opticians. Available at
http://www.royles-opticians.co.uk/glossary.shtml
accessed 17.01.2013

Webvision. Available at
http://webvision.med.utah.edu/book/part-i-foundations/simple-anatomy-of-the-retina/
accessed on 17.01.2013

Appendix I

1. Embryonic chick corneal thickness data

The following tables contain the average raw data values measured in embryonic chick cornea for the separate experiments carried out.

Embryonic day	Average corneal thickness (µm)	Standard deviation
9	158.9	30.2
10	179.4	10.1
11	202.9	16.3
12	244.1	46.1
13	270.3	16.9
14	292	16.1
15	266.6	12
16	243.4	3.6
17	210.2	15.5
18	190.2	7.57

Corneal thickness in both eyes of embryonic chick. Table shows the average corneal thickness and standard deviation measured from both eyes on one day between the E9-E18 developmental period in embryonic chick corneas.

Embryonic day	Average corneal thickness (µm)		Standard deviation	
	Left cornea	Right cornea	Left cornea	Right cornea
9	178.6	138.1	22.22	22.8
10	186.5	169.2	3.0	7.1
11	216.2	194.8	13.5	14.7
12	267.3	222.9	38.1	43.8
13	284.3	256	12.1	5.2
14	301.8	282.2	7.3	16.6
15	266.7	266.6	15.2	8.3
16	244.3	242.4	4.5	2.4
17	202.6	215	12.7	13.3
18	184.9	195.4	3.8	6.7

Left and right corneal thickness measurements in embryonic chick cornea. Values are average thickness measurements and standard deviation for each embryonic day (E9-E18).

Embryonic day	Average corneal thickness (µm)	Standard deviation
9	164.8	16.6
10	203	13.5
11	220.4	11.7
12	260.3	18.7
13	264.8	14.3
14	266.6	18.2
15	271.2	12.2
16	232.4	12.8
17	216.4	10.7
18	205.5	12.3

Corneal thickness in left eye only from final experiment. Table shows average corneal thickness and standard deviation of thickness data measured in the left eye only between the E9-E18 developmental period.

Embryonic day	Average corneal thickness (µm)	Standard deviation
9	169.9	19.6
10	206.2	25.9
11	217.8	13.2
12	257.5	44.7
13	280	23.4
14	285.8	25.6
15	287.3	33.4
16	246.1	22.6
17	220.2	19.1
18	209.1	25.8

Combined left corneal thickness data. Standard deviation and averaged corneal thickness data collected from all left corneal data.

Comparison	Difference	q	P value
E9 vs E10	-0.02047	5.172 *	P<0.05
E9 vs E11	-0.04395	11.487 ***	P<0.001
E9 vs E12	-0.08519	21.249 ***	P<0.001
E9 vs E13	-0.1113	28.131 ***	P<0.001
E9 vs E14	-0.1330	36.416 ***	P<0.001
E9 vs E15	-0.1077	27.204 ***	P<0.001
E9 vs E16	-0.08443	21.331 ***	P<0.001
E9 vs E17	-0.05122	13.096 ***	P<0.001
E9 vs E18	-0.03122	7.888 ***	P<0.001
E10 vs E11	-0.02347	5.602 **	P<0.01
E10 vs E12	-0.06471	14.849 ***	P<0.001
E10 vs E13	-0.09088	21.077 ***	P<0.001
E10 vs E14	-0.1126	27.907 ***	P<0.001
E10 vs E15	-0.08721	20.227 ***	P<0.001
E10 vs E16	-0.06396	14.834 ***	P<0.001
E10 vs E17	-0.03074	7.203 ***	P<0.001
E10 vs E18	-0.01075	2.493 ns	P>0.05
E11 vs E12	-0.04124	9.731 ***	P<0.001
E11 vs E13	-0.06740	16.086 ***	P<0.001
E11 vs E14	-0.08908	22.824 ***	P<0.001
E11 vs E15	-0.06374	15.211 ***	P<0.001
E11 vs E16	-0.04049	9.662 ***	P<0.001
E11 vs E17	-0.007271	1.754 ns	P>0.05
E11 vs E18	0.01272	3.036 ns	P>0.05
E12 vs E13	-0.02616	6.003 **	P<0.01
E12 vs E14	-0.04784	11.717 ***	P<0.001
E12 vs E15	-0.02249	5.162 *	P<0.05
E12 vs E16	0.0007554	0.1733 ns	P>0.05
E12 vs E17	0.03397	7.872 ***	P<0.001
E12 vs E18	0.05396	12.382 ***	P<0.001
E13 vs E14	-0.02168	5.375 **	P<0.01
E13 vs E15	0.003667	0.8504 ns	P>0.05
E13 vs E16	0.02692	6.243 ***	P<0.001
E13 vs E17	0.06013	14.088 ***	P<0.001
E13 vs E18	0.08013	18.584 ***	P<0.001
E14 vs E15	0.02534	6.284 ***	P<0.001
E14 vs E16	0.04859	12.049 ***	P<0.001
E14 vs E17	0.08181	20.520 ***	P<0.001
E14 vs E18	0.1018	25.242 ***	P<0.001
E15 vs E16	0.02325	5.393 **	P<0.01
E15 vs E17	0.05647	13.229 ***	P<0.001
E15 vs E18	0.07646	17.734 ***	P<0.001
E16 vs E17	0.03321	7.782 ***	P<0.001
E16 vs E18	0.05321	12.341 ***	P<0.001
E17 vs E18	0.01999	4.684 *	P<0.05

Tukey-Kramer multiple comparisons test multiple comparisons test for experiment 2.

Comparison	Difference	q		P value
E9 vs E10	-0.03824	16.465	***	P<0.001
E9 vs E11	-0.05556	22.643	***	P<0.001
E9 vs E12	-0.09554	34.892	***	P<0.001
E9 vs E13	-0.09999	40.748	***	P<0.001
E9 vs E14	-0.1018	39.610	***	P<0.001
E9 vs E15	-0.1064	43.902	***	P<0.001
E9 vs E16	-0.06764	28.090	***	P<0.001
E9 vs E17	-0.05159	20.729	***	P<0.001
E9 vs E18	-0.04171	16.760	***	P<0.001
E10 vs E11	-0.01733	7.727	***	P<0.001
E10 vs E12	-0.05730	22.469	***	P<0.001
E10 vs E13	-0.06176	27.540	***	P<0.001
E10 vs E14	-0.06358	26.833	***	P<0.001
E10 vs E15	-0.06812	30.850	***	P<0.001
E10 vs E16	-0.02940	13.413	***	P<0.001
E10 vs E17	-0.01335	5.854	**	P<0.01
E10 vs E18	-0.003471	1.522	ns	P>0.05
E11 vs E12	-0.03998	14.969	***	P<0.001
E11 vs E13	-0.04443	18.680	***	P<0.001
E11 vs E14	-0.04625	18.511	***	P<0.001
E11 vs E15	-0.05079	21.649	***	P<0.001
E11 vs E16	-0.01208	5.181	*	P<0.05
E11 vs E17	0.003977	1.648	ns	P>0.05
E11 vs E18	0.01386	5.740	**	P<0.01
E12 vs E13	**-0.004452**	**1.667**	**ns**	**P>0.05**
E12 vs E14	-0.006273	2.258	ns	P>0.05
E12 vs E15	-0.01081	4.093	ns	P>0.05
E12 vs E16	0.02790	10.614	***	P<0.001
E12 vs E17	0.04395	16.264	***	P<0.001
E12 vs E18	0.05383	19.919	***	P<0.001
E13 vs E14	**-0.001821**	**0.7287**	**ns**	**P>0.05**
E13 vs E15	-0.006362	2.712	ns	P>0.05
E13 vs E16	0.03235	13.879	***	P<0.001
E13 vs E17	0.04841	20.051	***	P<0.001
E13 vs E18	0.05828	24.143	***	P<0.001
E14 vs E15	**-0.004541**	**1.840**	**ns**	**P>0.05**
E14 vs E16	0.03417	13.929	***	P<0.001
E14 vs E17	0.05023	19.833	***	P<0.001
E14 vs E18	0.06011	23.734	***	P<0.001
E15 vs E16	0.03871	16.847	***	P<0.001
E15 vs E17	0.05477	22.989	***	P<0.001
E15 vs E18	0.06465	27.136	***	P<0.001
E16 vs E17	0.01605	6.781	***	P<0.001
E16 vs E18	0.02593	10.953	***	P<0.001
E17 vs E18	0.009879	4.033	ns	P>0.05

Tukey-Kramer multiple comparisons test for experiment 3. Period of thickness plateau is in bold.

Source of Variation	% of total variation	P value	Significant?
Interaction	4.933	0.0834	No
Developmental day	80.16	< 0.0001	Yes
Left/right	3.248	0.0018	Yes

Two-way ANOVA for left eye right eye interaction over E9-E18. The analysis suggests that left/right cornea has the same effect at all values measured at each developmental day ($p \geq 0.01$). It also shows that developmental day and cornea (left/right) account for 80.16% ($p \leq 0.01$) and 3.25% ($p \leq 0.01$) of total variance, respecitvely suggesting that both factors play a role in the measurement of corneal thickness.

2. Grey value data

Grey value plots used to determine association of globular domains of type VIII collagen. Different peaks are produced depending on the arrangement of the globular domains. A parallel arrangement would produce asymmetric/double peaks as a result of stacked NC1 domains adjacent to stacked NC2 domains. An anti-parallel association would produce large symmetrical peaks caused by alternate stacked NC1 and NC2 domains. The elongated structures measured in Descemet's membrane in this study generated symmetrical peaks; hence, our model was based on an anti-parallel association.

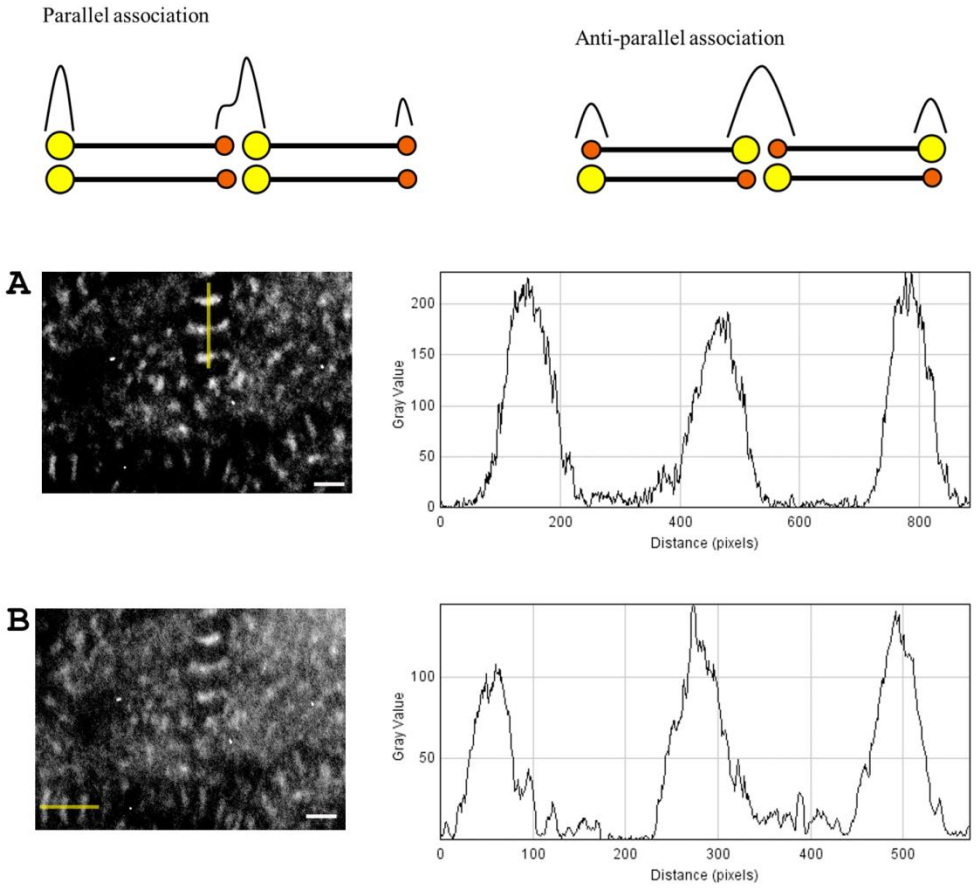

Type VIII collagen associations based on grey value. Schematic (top) displays the possible arrangements of type VIII collagen within the Descemet's membrane lattice. Parallel association results would result in double or asymmetric peaks formed by the large (NC1 [yellow]) and small (NC2 [orange]) globular domains, whereas anti-parallel associations would result in tall, wide peaks as a result of the alternating large and small globular domains stacking on top of one another. Selected micrographs showing the clearest elongated structures were selected from the tilt series and grey values were calculated using Fiji/ImageJ software. A and B show the different peaks obtained from the highlighted area (yellow) for each elongated structure. Scale bar=100 nm.

3. Buffers

0.1M sodium acetate buffer

13.6g $CH_3CO_2Na*3H_20$/1000ml dH_2O
6g CH_3COOH/1000ml dH_2O

181ml $CH_3CO_2Na*3H_20$ added to 19ml CH_3COOH to achieve a pH of 5.7

Dilute as required and add 2.03g MgCl2 to 100ml to make 0.1M MgCl2 in sodium acetate

0.2M sodium cacodylate buffer

42.8g $Na(CH_3)_2As0_2*3H_20$/1000ml dH_2O
Add HCl to achieve pH 7.2-7.4

0.2M sørensen buffer

27.6g $NaH_2PO_4*H_20$/1000ml dH_2O
35.61g $Na_2HPO_4*2H_20$/1000ml dH_2O

28ml of 0.2M NaH_2PO_4 added to 72ml of 0.2M Na_2HPO_4 to achieve 0.1M sørensen buffer pH 7.2.

10X Tris acetate buffer

Tris base 19.4g
Glacial acetic acid 4.6ml
EDTA 0.5M (pH8) 16ml

Make up to 400ml using dH_20

4. Araldite Resin

Araldite resin mixture

14ml Araldite monomer CY212
16ml DDSA Hardener
0.6ml BDMA Accelerator

Modify for volume required

5. Staining

Lead citrate

1.33g $Pb(NO_3)$+ 1.76g $Na_3C_6H_5O_7$ into 30ml dH_2O +8ml NaOH. Make up to 50ml with dH_2O

Appendix II

BASIC INVESTIGATION

A Study of Host Corneal Endothelial Cells After Non-Descemet Stripping Automated Endothelial Keratoplasty

Hiroki Hatanaka, MD, Noriko Koizumi, MD, PhD,† Naoki Okumura, MD, PhD,*† Hiroaki Takahashi, MS,† Hidetoshi Tanioka, PhD,* Robert D. Young, PhD,‡ Frances E. Jones, BSc,‡ Andrew J. Quantock, PhD,‡ and Shigeru Kinoshita, MD, PhD**

Purpose: To determine the short-term fate of the host endothelium and Descemet membrane after non-Descemet stripping automated endothelial keratoplasty (nDSAEK).

Methods: Eight unilateral DSAEK (n = 4) or nDSAEK (n = 4) surgeries were performed in the right eyes of 8 rabbits. Corneal transparency and thickness were followed-up by slit-lamp microscopy, and 2 weeks postoperatively, corneas were evaluated by immunohistochemistry and transmission electron microscopy.

Results: Corneas remained clear after both DSAEK and nDSAEK. One week after DSAEK, the stroma-to-stroma surgical interface was identifiable as a zone of fibrotic tissue a few microns thick, whereas in the nDSAEK group, the recipient corneal endothelium and Descemet membrane were clearly visible at the graft–host interface. The retained endothelial cells were positive for Na^+/K^+-ATPase but assumed a markedly different morphology from healthy endothelial cells, with cell processes extending into the graft stroma or engulfing strands of irregularly dissected grafted stromal tissue where they occasionally appeared to compartmentalize the transplanted matrix and became detached from the underlying Descemet membrane.

Conclusions: Host endothelial cells 2 weeks after nDSAEK express markers of pump function, but appear to be morphologically altered, occasionally detaching from the adjacent Descemet membrane, extending into the graft stroma or engulfing strands of the grafted stroma at the interface. The short-term persistence and subsequent phenotypical alteration of residual endothelial cells, aligned to structural changes to Descemet membrane, might influence graft adherence after nDSAEK.

Received for publication October 21, 2011; revision received April 12, 2012; accepted May 2, 2012.

From the *Department of Ophthalmology, Kyoto Prefectural University of Medicine, Kyoto, Japan; †Department of Biomedical Engineering, Faculty of Life and Medical Sciences, Doshisha University, Kyotanabe, Japan; and ‡Structural Biophysics Group, School of Optometry and Vision Sciences, Cardiff University, Cardiff, United Kingdom.

Supported by the Funding Program for Next Generation World-Leading Researchers from the Cabinet Office in Japan (to N.K.; LS117). Ms Jones is a graduate student funded by the Engineering and Physical Sciences Research Council (United Kingdom).

The authors state that they have no conflicts of interest to declare.

Reprints: Noriko Koizumi, Department of Biomedical Engineering, Faculty of Life and Medical Sciences, Doshisha University, Kyotanabe 610-0321, Japan (e-mail: nkoizumi@mail.doshisha.ac.jp).

Key Words: nDSAEK, DSAEK, host endothelium, adhesion, pump function

(*Cornea* 2013;32:76–80)

Corneal endothelial disorders such as Fuchs endothelial dystrophy or pseudophakic bullous keratopathy lead to irreversible corneal endothelial dysfunction. Penetrating keratoplasty has been widely performed for the restoration of endothelial function. However, this has several potential adverse effects such as the occurrence of irregular astigmatism, suture-induced problems, and fragility against trauma. Alternative methods for replacing the endothelium have been developed lately and include posterior lamellar keratoplasty, deep lamellar endothelial keratoplasty, Descemet stripping endothelial keratoplasty, Descemet stripping automated endothelial keratoplasty (DSAEK), and Descemet membrane endothelial keratoplasty.[1–4]

Recently, a new modified form of DSAEK has been reported, which has been termed non-Descemet stripping automated endothelial keratoplasty (nDSAEK).[5] This procedure differs from DSAEK in that the host Descemet membrane and endothelium are not surgically removed before the introduction of the posterior lamellar graft. nDSAEK has been shown to be efficient for the treatment of endothelial dysfunction not associated with guttata, with rapid visual recovery and minimal induced astigmatism.[5] In contrast, donor dislocation has been reported after nDSAEK,[5] and subclinical corneal abnormalities have been observed by laser confocal microscopy.[6] We hypothesize that the continued presence of the host endothelium and Descemet membrane may adversely affect the adherence of the posterior graft tissue. The aim of this study was to understand more fully the change of function and anatomy of the residual endothelial cells in the immediate post-nDSAEK period in a rabbit model.

MATERIALS AND METHODS

Surgical Procedure

Japanese white rabbits (female, 9–10 weeks old, 2–3 kg body weight; Shimizu Laboratory Supplies Co, Ltd, Kyoto, Japan) were used as an animal model for corneal endothelial

transplantation and treated in accordance with the Association for Research in Vision and Ophthalmology Statement for the Use of Animals in Ophthalmic and Vision Research. The experimental procedures were approved by the Animal Care and Use Committee of Kyoto Prefectural University of Medicine (Approval No. 12-12).

Eight corneas of 4 rabbits, euthanized by injection with pentobarbital sodium (130 mg/kg; Kyoritsu, Tokyo, Japan), were used as donor material, with preparation of donor lenticules immediately preceding the DSAEK or nDSAEK procedures. First, a donor corneoscleral button was placed on a Barron artificial anterior chamber (Katena Products, Denville, NJ), after which saline was infused into the chamber. For each button, a corneal endothelial graft, 100 to 200 μm thick and 8 mm in diameter, was dissected manually using a DALK spatula set (Dutch Ophthalmic Research Center, Zuidland, the Netherlands) and separated by dermal punch using the technique described by Melles et al.[7] These 8 graft tissues were then implanted unilaterally into the right eyes of 8 rabbits as described in the following, 4 using the DSAEK technique and 4 using nDSAEK.

One week before the DSAEK and nDSAEK surgeries, lensectomies and peripheral iridectomies were performed in the right eyes of the 8 rabbits. At surgery, recipient rabbits were anesthetized by intramuscular injection of a mixture of ketamine hydrochloride (70.4 mg/kg; Sankyo, Tokyo, Japan), xylazine (11.8 mg/kg; Bayer, Munich, Germany), and topical oxybuprocaine. Pupils were expanded with topical tropicamide. Surgery was performed on the right eye of each rabbit using the modified technique described by Price et al.[3] First, for DSAEK, a 3-mm limbal-corneal incision was made and the endothelium/Descemet membrane was mechanically scraped using a modified Price-Sinskey hook (ASICO, Westmont, IL) while infusing air into the anterior chamber through a 25-gauge cannula. The scraped area measured at least 9 mm in diameter, and the denuded area was confirmed by 0.04% trypan blue staining during surgery. Descemet membrane scraping was not done in the nDSAEK group. Next, a Busin glide (Moria, Doylestown, PA) was loaded with the donor tissue, oriented so that its endothelial side faced the anterior chamber. This was coated with Viscoat (Alcon, Fort Worth, TX) to protect the cells from physical damage. The graft was pulled into the Busin glide opening, and a 25-gauge anterior capsular forceps (Inami, Tokyo, Japan) that entered the opposite side of the anterior chamber through a small incision was used to grasp the graft. The inserted graft was then attached to the recipient cornea by air injection, and the incision was closed with 10-0 nylon sutures. After surgery, all animals received 0.3% ofloxacin ointment and were maintained with the right side of the face facing downward for 30 to 60 minutes. At days 1, 3, 5, 7, and 14 after surgery, corneal transparency was assessed by the use of a slit-lamp microscope.

Immunohistochemistry

Two weeks after surgery, animals were killed by injection with pentobarbital sodium (130 mg/kg; Kyoritsu), and 4% paraformaldehyde was perfused into the anterior chamber and applied dropwise to the ocular surface for 5 to 10 minutes. Corneoscleral buttons were then excised and immersed in 20% sucrose overnight at 4°C and embedded in optimal cutting temperature compound at −80°C. Sections (10 μm thick) were cut, fixed in 4% formaldehyde for 5 minutes at room temperature, permeabilized for 5 minutes in phosphate-buffered saline (PBS) containing 0.5% Triton X-100, washed, and incubated for 60 minutes with 1% bovine serum albumin. This was followed by overnight incubation at 4°C with 1:100 diluted mouse anti-Na^+/K^+-ATPase antibody (Anti-Na+/K+ ATPase α-1, clone C464-6; Millipore, Billerica, MA) and 3 washes in PBS. Sections were then incubated at room temperature with 1:2000 diluted Alexa Fluor 488–conjugated goat antimouse IgG (Invitrogen Corporation) and washed 3 times. They were subsequently washed with PBS in the dark, mounted on glass slides with antifading mounting medium containing 4′,6-diamidino-2-phenylindole (DAPI) (VECTASHIELD; Vector Laboratories, Burlingame, CA) and inspected with a fluorescence microscope (Olympus, Tokyo, Japan).

Transmission Electron Microscopy

For light and transmission electron microscopy, excised corneas, which had first been perfused in situ for 5 to 10 minutes with 4% paraformaldehyde as was done for the immunohistochemistry preparation, were fixed in 2.5% glutaraldehyde and 2% paraformaldehyde in 0.1 M Sorensen buffer, pH 7.2 to 7.4, for 2 to 3 hours at room temperature. After several washes in the buffer and postfixation with 1% osmium tetroxide, they were dehydrated and embedded in Araldite resin. Semithin sections (1 μm thick) were stained with toluidine blue for inspection at the light microscope level, whereas ultrathin sections (~90 nm thick) were collected on uncoated copper grids for study by transmission electron microscopy. Contrasting of ultrathin sections was with phosphotungstic acid and aqueous uranyl acetate (1 and 12 minutes, respectively), followed by Reynolds lead citrate (5 minutes) with washes in between. Stained sections were examined in a JEOL 1010 transmission electron microscope (JEOL, Tokyo, Japan), equipped with a Gatan ORIUS SC1000 CCD camera.

RESULTS

Slit-Lamp Microscopy

Slit-lamp examinations of the 8 operated eyes revealed that the corneas were clear in both the nDSAEK and the DSAEK groups at postoperative day 7 (Fig. 1). In the nDSAEK group, 1 lamellar graft had become dislocated the day after surgery, but it readhered to the center of the cornea after the injection of air into the anterior chamber. Slit-lamp examination revealed that graft adhesion was good in both groups. However, after nDSAEK, folds appeared and became progressively more noticeable in number and size at the graft edge in all 4 cases (Fig. 2).

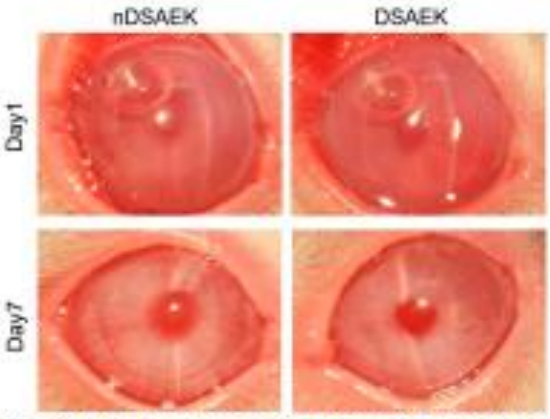

FIGURE 1. Slit-lamp photographs 1 and 7 days after surgery, indicating cloudiness at 1 day with a return to clarity by 7 days after both DSAEK and nDSAEK.

Immunohistochemistry

Histological sections of corneas healing after DSAEK indicated a well-adhered graft with a thin and fairly indistinct stroma-to-stroma interface (Fig. 3). Histology of post-nDSAEK tissue, in contrast, showed the clear retention of residual Descemet membrane and endothelium at the surgical interface, sandwiched between host stroma and graft stroma (Fig. 3). The recipient corneal endothelial cells retained in the cornea after nDSAEK were also identified on histochemistry by the nuclear stain, DAPI, which revealed a line of positive cells at the junction between the host and graft tissues 14 days after surgery (Fig. 4). Immunohistochemistry, moreover, suggested that the sandwiched host endothelial cells retained a lot of cellular function because they were positive for Na^+/K^+-ATPase protein (Fig. 4).

Transmission Electron Microscopy

The lamellar graft in nDSAEK adhered well to the residual endothelium/Descemet layer; nevertheless, at the electron microscopic level, distinct phenotypic and morphological changes in the endothelial cells and Descemet membrane were evident (Fig. 5A, B). Notably, the endothelial cells often appeared to extend cell processes into the adjacent grafted stroma, resulting in partial compartmentalization of the matrix, or to engulf loose strands on the irregular surface of grafted stroma, which might include some phagocytic activity (Figs. 5A, B). Duplication of Descemet membrane was also seen, with the membrane present at the apical and basal sides of the host endothelium (Fig. 6A). Residual endothelial cells also sometimes became detached from the host Descemet membrane, with a layer of stromal tissue that resembled fibrotic tissue lying between the cells and Descemet membrane (Fig. 6B). In these areas of graft–host interface, portions of duplicated, or split and invaded, Descemet membrane could also often be seen in close association with the detached host endothelium (Fig. 6B).

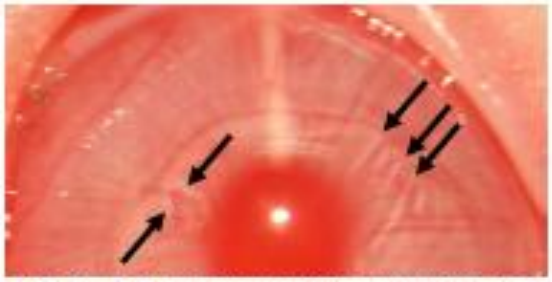

FIGURE 2. A slit-lamp photograph of a representative cornea in the nDSAEK group, 7 days after surgery. The folds seen at the edge of the graft (arrows) are typical of all 4 nDSAEK surgeries and increased in number and size throughout the observation period.

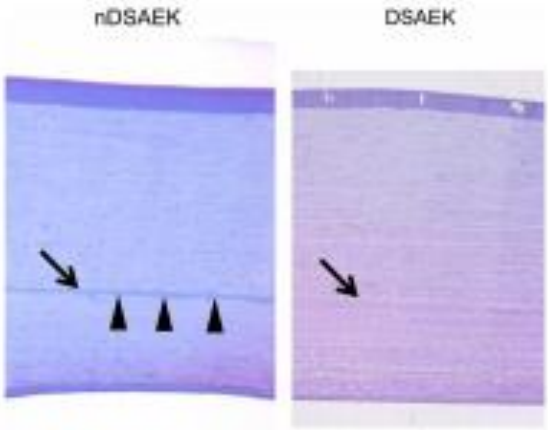

FIGURE 3. Light micrographs of DSAEK and nDSAEK corneas 7 days after surgery taken from semithin sections of resin-embedded tissue stained with 1% toluidine blue. The graft–host interface is indicated by an arrow, with the host Descemet membrane and endothelium clearly visible in nDSAEK sections (arrowheads). Bar = 50 μm.

DISCUSSION

nDSAEK is a contemporary modification of the gamut of endothelial keratoplasties, and although clinical outcomes are promising, there is a dearth of fundamental knowledge about the postoperative fate of the residual endothelium and Descemet membrane. This knowledge is important because it is suspected that the good adherence of the graft interface after DSAEK—where the host endothelium and Descemet membrane are removed—is, much like after laser in situ keratomileusis, a result of direct stroma-to-stroma contact, and we hypothesize that the retained endothelial cells and Descemet membrane might have some effect on this adhesion.

Our investigations reveal that, 2 weeks after nDSAEK, endothelial cells persist at the boundary between host and graft and also express Na^+/K^+-ATPase protein. Often, these

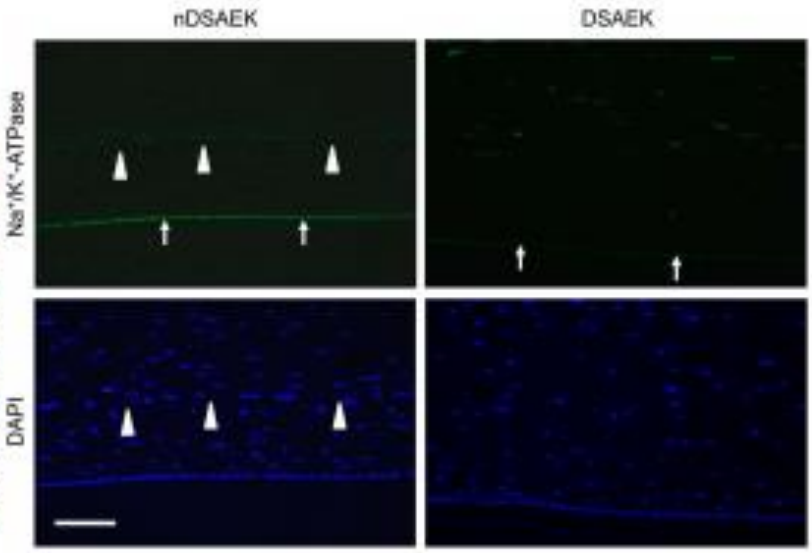

FIGURE 4. Function-related protein expression in the cornea in nDSAEK and DSAEK, 14 days after surgery. Some unexplained focal positivity was seen throughout the stroma in all corneas studied, and in DSAEK and nDSAEK corneas, a single layer of immunolabeled donor endothelial cells were observed with Na^+/K^+-ATPase (arrows). The graft–host interface was not identifiable by immunohistochemistry in DSAEK corneas, but in nDSAEK corneas, the retained monolayer of host corneal endothelial cells expressed Na^+/K^+-ATPase. These were also stained with the nuclear stain, DAPI, which formed a discontinuous line at the graft–host interface (arrowheads). Bar = 100 μm.

cells are closely apposed to the residual host Descemet membrane and form a monolayer not unlike that in a healthy endothelium. On occasion, however, the endothelial cells assume an abnormal phenotype, with cell processes extending into the graft stroma or engulfing loose strands of the dissected stromal matrix. Deposition of fibrotic tissue between the host endothelium and residual Descemet membrane was also found, and we speculate that phenotypic changes in the host endothelium represent the early stages of cellular transformation under stress[8,9] or some phagocytic activity of the endothelial cells. In the normal adult cornea, the endothelium lays down collagen type IV at its distal surface, which constitutes the posterior nonbanded portion of Descemet membrane. It might be the case that the endothelium deposits collagen type IV at its proximal surface also, only for this to be removed by the fluid dynamics of the aqueous humor. If this is so, it might explain the presence of duplicated basement membrane–like material adjacent to the proximal side of the host endothelium.

Immunohistochemistry indicates that retained endothelial cells 2 weeks after nDSAEK display a partial endothelial phenotype as evidenced by Na^+/K^+-ATPase protein expression. This leads us to consider the potential metabolic response of the sandwiched endothelial cells and the likelihood of any pump function. The corneal stroma will swell rapidly if bathed in an aqueous medium,[10] a phenomenon that

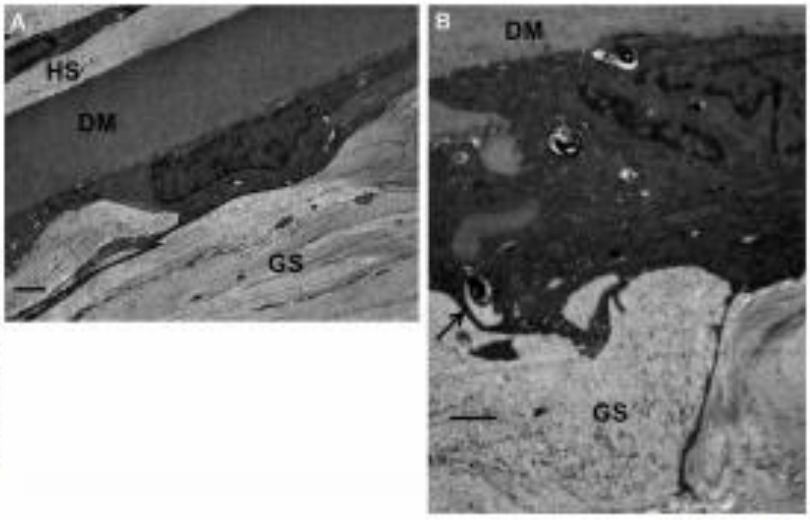

FIGURE 5. A, An electron micrograph of residual host Descemet membrane (DM) and a well-adhered endothelium after nDSAEK. Bar = 2.5 μm. B, An electron micrograph of residual host DM and endothelium (arrow) after nDSAEK. Bar = 500 nm. Endothelial cells appear to extend into graft stroma or engulf loose connective tissue strands on the surface of the transplanted tissue. GS, graft stroma; HS, host stroma.

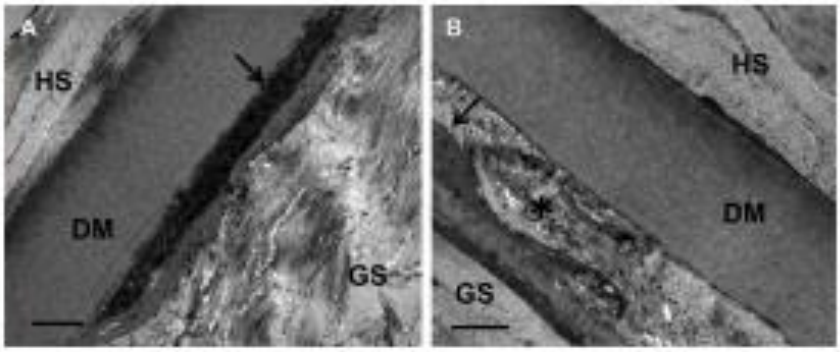

FIGURE 6. A, An electron micrograph of residual host Descemet membrane (DM) and a well-adhered endothelium (arrow) sandwiched between host stroma (HS) and graft stroma (GS) after nDSAEK. Bar = 2 μm. B, An electron micrograph of residual host DM and endothelium sandwiched between HS and GS after nDSAEK. The endothelium (arrow) has become detached from DM, and a fibrotic stromal matrix (indicated by an asterisk) exists between the endothelium and DM. Bar = 2 μm.

is due predominantly to the presence of collagen-bound sulfated proteoglycans[11] and chloride anions that are electrostatically associated with the matrix in a transient manner.[12,13] This swelling tendency is neutralized in the physiologically normal cornea by the continuous removal of bicarbonate ions from the corneal stroma by the metabolically active endothelial pump.[14] The presence of a monolayer of residual host endothelial cells after nDSAEK, aligned with immunohistochemical evidence of Na^+/K^+-ATPase protein expression, prompts us to consider the likelihood of a dual bicarbonate pump in these corneas, with functionality in both the new grafted endothelium and the trapped host endothelium. Physiological reasoning and a consideration of most of the key aspects of endothelial metabolism indicate no reason why the sandwiched endothelium in the early stages after nDSAEK could not function as an active bicarbonate pump. However, we are reminded of a series of experiments (S. A. Hodson, PhD, personal communication, August 2011), which indicated that endothelial pump function examined in vitro was stopped when the circulation of fluid bathing the apical face of the endothelium was temporarily ceased, only to start up again once fluid circulation was resumed. This was attributed to the nonremoval and consequent build up of lactic acid near the endothelium, something that would likely occur in the graft stroma adjacent to the residual endothelium in nDSAEK. Based on this reasoning, aligned to the longer term morphological changes and transformation of the trapped endothelial cells in nDSAEK, we suspect little if any functionality in the retained host endothelium.

nDSAEK is a useful surgery that can lead to favorable clinical outcomes, as has been reported by other investigators. It appears that in the early postoperative period, in rabbits at least, healing is accompanied by the close apposition between graft stroma and the apical surface of host endothelial cells that retain some pump function. We also note that the series of phenomena reported here may not be restricted to nDSAEK but might occur in DSAEK too at the corneal periphery if the lateral extent of the graft material overlaps a smaller debrided area.

ACKNOWLEDGMENT

The authors are indebted to Professor Stuart A. Hodson for his helpful discussions.

REFERENCES

1. Mellen GR, Lander F, Rietveld FJ. Transplantation of Descemet's membrane carrying viable endothelium through a small scleral incision. *Cornea*. 2002;21:415–418.
2. Terry MA, Ousley PJ. Deep lamellar endothelial keratoplasty in the first United States patients: early clinical results. *Cornea*. 2001;20:239–243.
3. Price FW Jr, Price MO. Descemet's stripping with endothelial keratoplasty in 50 eyes: a refractive neutral corneal transplant. *J Refract Surg*. 2005;21:339–345.
4. Mellen GRJ, Ong TS, Vervoort B, et al. Descemet membrane endothelial keratoplasty (DMEK). *Cornea*. 2006;25:987–990.
5. Kobayashi A, Yokogawa H, Sugiyama K. Non-Descemet stripping automated endothelial keratoplasty for endothelial dysfunction secondary to argon laser iridotomy. *Am J Ophthalmol*. 2008;146:543–549.
6. Kobayashi A, Yokogawa H, Sugiyama K. In vivo laser confocal microscopy after non-Descemet's stripping automated endothelial keratoplasty. *Ophthalmology*. 2009;116:1306–1313.
7. Mellen GR, Eggink FA, Lander F, et al. A surgical technique for posterior lamellar keratoplasty. *Cornea*. 1998;17:618–626.
8. Naumann GO, Schlotzer-Schrehardt U. Keratopathy in pseudoexfoliation syndrome as a cause of corneal endothelial decompensation: a clinicopathologic study. *Ophthalmology*. 2000;107:1115–1124.
9. Kawaguchi R, Saika S, Wakayama M, et al. Extracellular matrix components in a case of retrocorneal membrane associated with syphilitic interstitial keratitis. *Cornea*. 2001;20:100–103.
10. Elliott GF, Hodson SA. Cornea, and the swelling of polyelectrolyte gels of biological interest. *Rep Prog Phys*. 1998;61:1325–1365.
11. Quantock AJ, Young RD, Akama TO. Structural and biochemical aspects of keratan sulphate in the cornea. *Cell Mol Life Sci*. 2010;67:891–906.
12. Elliott GF. Measurements of the electric charge and ion-binding of the protein filaments in intact muscle and cornea, with implications for filament assembly. *Biophys J*. 1980;32:95–97.
13. Hodson S, Kaila D, Hammond S, et al. Transient chloride binding as a contributory factor to corneal stromal swelling in the ox. *J Physiol*. 1992;450:89–103.
14. Hodson S, Miller F. The bicarbonate ion pump in the endothelium which regulates the hydration of rabbit cornea. *J Physiol*. 1976;263:563–577.